UNIVERSIDADE DE LISBOA

FACULDADE DE CIÊNCIAS

DEPARTAMENTO DE QUÍMICA E BIOQUÍMICA

CFTR Trafficking and Membrane Anchoring – the role of cAMP signalling

Miguel Gonçalo de Oliveira Jones Ferrão Lobo

Mestrado em Bioquímica

(Especialização em Bioquímica)

Dissertação orientada pelo Professor Doutor Carlos Miguel Farinha

2014

Preface

In the 1990s life used to be simple. The entire family watched Formula 1 on Sunday afternoons and we still didn't know what garbage recycling was. In an interesting analogy, biologists in the 90s thought of protein kinase A (PKA) as the only link between the second messenger cAMP and CFTR (first reported by Cheng et al. in 1991). Our data challenge this linear and somewhat simplistic view unveiling a novel relationship between CFTR and yet another cAMP effector, the exchange protein directly activated by cAMP (EPAC). We propose EPAC as a new player to the CFTR race circuit, a rally that begins in the endoplasmic reticulum, where the protein is translated, and finishes at the plasma membrane (PM), where the channel exerts its function. EPAC is involved in a number of cellular functions such as the regulation of cell-to-cell and cell-matrix adhesion and cytoskeleton rearrangements, processes that affect CFTR regulation. Here we present compelling evidence suggesting that cAMP (here replaced by an analogue that does not activate the PKA pathway) promotes the interaction of EPAC with CFTR with the aid of the protein adaptor NHERF1. The formation of this complex increases the stability of CFTR at the PM.

Using a multidisciplinary approach, we show that EPAC1 (the most abundant of the two EPAC isoforms known) and CFTR co-localize in cystic fibrosis bronchial epithelial cells (CFBE) – reporting this interaction in different airway epithelial cell lines that express endogenous EPAC1, namely A549, CFBE and Calu3. Cyclic AMP promotes EPAC translocation to the PM, in a CFTR-independent manner, as well as its interaction with CFTR. siRNAs or shRNAs against ezrin or NHERF1, proteins involved in the tethering of PKA in the proximity of CFTR, show that the latter (but not the previous) mediates the interaction between EPAC1 and CFTR. However, neither of these scaffolding proteins affects the translocation of EPAC1 to the PM. On the other hand, CFTR biotinylation at the PM shows that EPAC activation decreases CFTR endocytosis and promotes CFTR stabilization at the PM. Transient knockdown of EPAC1 has an opposite effect on CFTR stability. Additionally, EPAC activation does not affect CFTR total protein levels or the CFTR processing efficiency. Finally, the presence of the most common CFTR mutation, F508del, seems to affect levels of endogenous EPAC activation and EPAC-mediated cell adhesion.

In this way, a new link between CFTR regulation and cAMP was established. This novel player on the CFTR race circuit may contribute to a finer and more complex regulation of this channel. Definitely, life has just become more complicated.

Table of Contents

Acknowledgements

First and foremost, I want to express my gratitude to my supervisor Prof. Carlos Farinha, for all the constant support, orientation and opportunities that without him wouldn't have been possible. I really enjoyed to work with him and my time in the lab in Lisbon. I am also grateful to Prof. Margarida Amaral for welcoming me into her group and helping me when needed.

Special thanks are due to the many people in the group which always helped me. Ana Cachaço taught me how to dry my wet shoes during rainy days using a dryer. With Susana I learned how to evaluate the correct amount of butter on a toast. Zé taught me that many women are crazy, as I already thought. Ana Marta was my first bench partner, then replaced by a shorter but equally friendly and happy person, Sara Afonso. With both I learned how to keep my bench perfectly cleaned and organized. Inna, a special friend that probably works for DHL and taught me to 'Do what I say and not what I do'. Without her, I would be more relaxed and with less work to do. Simão, the guy in the lab that uses the same clothes as me. Sara Canato has been proving that human batteries don't run out. Veronica told me that the best way to go on holidays is if I got pregnant. Nikhil, who was my first roommate at an international meeting. Whaaaaatttt?? Ines taught me my first german word…

I also would like to express my gratitude to Prof. Manuela Zaccolo for the opportunity of working with her group in Oxford and also for all the support and constant availability. A really special thanks to Kostas for everything: help related to the lab, opinions regarding the scientific life, share of knowledge, rare meat and tzatziki. Big thanks to Stefania for support and guidance. I am also grateful to Caracoleta, who taught me some Italian words, Oliver (and his BMW), Marcela, Alex, Laura and Claudia.

To my family, muito obrigado por todo o apoio e embalagens de atum XXL.

Abstract

CFTR, Cystic Fibrosis Transmembrane Conductance Regulator, is a chloride channel expressed in the apical membrane of epithelial cells. The malfunction of this protein is responsible for cystic fibrosis, the most common lethal autosomal recessive disease in the Caucasian population. One of the numerous proteins that interacts with CFTR and also regulates the function of this channel through phosphorylation is protein kinase A (PKA). Because PKA activity is cAMP-dependent, this kinase has been recognized as the link between this second messenger and CFTR. However, PKA is not the only cAMP sensor within the cell.

EPAC, an exchange protein directly activated by cAMP, is another cAMP effector, involved in a number of cellular functions such as the regulation of cell-to-cell and cell-matrix adhesion, cytoskeleton rearrangements and cell polarization, processes that affect CFTR regulation and are defective in CF. The aim of this work was to characterize the interaction between CFTR and the most predominant isoform of EPAC, EPAC1, and to evaluate the impact of this cAMP sensor on CFTR biogenesis, trafficking and plasma membrane (PM) anchoring.

Using a multidisciplinary approach, our results show that EPAC1 and CFTR co-localize and co-immunoprecipitate in airway epithelial cells. The second messenger cAMP promotes EPAC1 translocation to the PM and its interaction with CFTR. The adaptor protein NHERF1, but not ezrin, mediates the interaction between EPAC1 and CFTR. Furthermore, EPAC activation does not affect CFTR total protein levels or CFTR processing efficiency but promotes CFTR stabilization at the PM. Additionally, the presence of the most common CFTR mutation, F508del, seems to affect EPAC activity and EPAC-mediated cell adhesion. Thus, this work provided an important characterization of a new CFTR interacting protein that links cAMP to cystic fibrosis modulation in a previously unreported mechanism.

Resumo

A Fibrose Quística (FQ), a doença recessiva autossómica letal mais comum na população caucasiana, é caracterizada por uma grave disfunção da função pulmonar causada pela obstrução das vias respiratórias devido à acumulação de muco e consequentes infecções bacterianas. A FQ é causada por mutações no gene que codifica para uma glicoproteína com 1480 resíduos de aminoácidos, designada CFTR (*Cystic Fibrosis Transmembrane Conductance Regulator*). Esta proteína, presente na membrana apical de células epiteliais, actua como um canal de cloreto. Até à data, foram identificadas cerca de 2000 mutações possíveis causadoras da doença, sendo a mais comum a delecção de três nucleótidos que correspondem ao resíduo de feninalanina na posição 508 da proteína (F508del).

Durante a sua síntese proteica, a proteína CFTR é inserida co-traducionalmente na membrana do retículo endoplasmático, onde adquire a sua conformação nativa, devido à acção de vários chaperones, e passa por um processo de glicosilação inicial. Daqui, é transportada para o Golgi onde os seus resíduos glicídicos são modificados, originando a sua forma madura. Posteriormente, é transportada em vesículas para a membrana plasmática (PM) onde exerce a sua função. Aqui, a proteína CFTR é endocitada sendo depois reciclada de volta para a PM ou enviada para degradação lisossomal. O equilíbrio entre estes processos é crucial para a quantidade de proteína presente na membrana.

Na PM, a proteína CFTR pode estar ancorada a filamentos de actina, o que contribui para a sua estabilidade membranar. A proteína CFTR, através da sua região C-terminal, interage com várias proteínas com um domínio PDZ, nomeadamente a proteína adaptadora NHERF1 (*Na^+/H^+-exchanger regulatory factor isoform 1*), que por sua vez interage com proteínas do citoesqueleto, tal como a ezrina. Desta forma, o complexo CFTR-NHERF1-ezrina-actina contribui para a imobilização e ancoragem da proteína CFTR na PM, prevenindo a sua endocitose. Dessa forma, a ancoragem da CFTR na superfície celular é uma importante via a ser considerada em termos da intervenção terapêutica em doentes com FQ.

Uma vez na PM, a proteína CFTR está envolvida na regulação do transporte transepitelial de iões e água. A abertura do canal CFTR é regulada pela fosforilação catalisada pela proteína cinase A (PKA) em resposta a um aumento local dos níveis de AMP cíclico

(cAMP). A compartimentalização do cAMP depende da integridade do citoesqueleto e é essencial para um aumento da especificidade e eficiência da sinalização deste mensageiro secundário. Uma vez que a actividade da PKA é dependente dos níveis de cAMP, esta cinase tem sido reconhecida como a ligação entre a proteína CFTR e o cAMP. No entanto, a PKA não é o único sensor de cAMP que existe na célula; a proteína EPAC (*exchange protein directly activated by cAMP*) também actua como um efector do cAMP.

A proteína EPAC funciona como um factor de troca de nucleótidos de guanina para a Rap, uma pequena GTPase (enzima que hidrolisa GTP) da família Ras. Esta GTPase está activa quando ligada a GTP e inactiva quando ligada a GDP. Assim, a proteína EPAC promove a activação deste interruptor molecular, já que leva à ligação de GTP. Em resposta ao aumento dos níveis de cAMP, a proteína EPAC transloca do citosol para a PM, onde pode activar a Rap. A interacção com a PM pode ser feita de uma forma dependente de ácido fosfatídico ou através da proteína do citoesqueleto ezrina. Esta informação sugere que a proteína EPAC pode co-localizar, ou até mesmo interactuar, com a proteína CFTR, e, possivelmente, regular a sua função ou estabilidade membranar.

A proteína EPAC está envolvida em várias funções biológicas, principalmente devido às várias localizações sub-celulares que esta proteína pode ter e aos vários parceiros moleculares com que pode interagir. Nomeadamente, está envolvida na regulação da adesão célula-célula ou célula-matriz, organização do citoesqueleto ou polarização celular - processos que afectam a regulação da proteína CFTR, e que estão em geral alterados na FQ. Desta forma, o objectivo deste trabalho consistiu em caracterizar a interacção entre a proteína CFTR e a principal isoforma da proteína EPAC, a EPAC1, e avaliar o impacto deste sensor de cAMP na biogénese, tráfego e ancoragem da CFTR na PM.

O primeiro passo do trabalho consistiu em avaliar se o composto 007-AM de facto actua como um análogo do cAMP específico para a EPAC (e não PKA). Este estudo, bem como outros posteriores, foi realizado em células CFBE (*Cystic Fibrosis Bronchial Epithelial*) de forma a melhor mimetizar os processos que ocorrem no epitélio brônquico de pacientes com FQ. Outras linhas celulares de epitélio respiratório também usadas foram as linhas Calu3 (de glândula submucosa) e A549 (alveolar). A análise por FRET mostrou que o sensor dos níveis de cAMP baseado na estrutura da EPAC sofre grande alteração da

percentagem de FRET, o mesmo não se observando com o sensor da actividade da PKA – o que permitiu evidenciar a selectividade do 007-AM para a EPAC. A activação da proteína EPAC, em resultado do tratamento das células com 007-AM, promove a sua translocação para a PM, em células CFBE, de uma forma independente da proteína CFTR. Além disso, usando um sensor FRET da actividade da EPAC e um ensaio para a actividade da Rap1A (uma das isoformas da Rap), observou-se que células que expressam CFTR WT (*wild-type*) apresentaram um aumento de FRET na PM após tratamento com 007-AM, enquanto células que expressam CFTR F508del tendem a ter níveis mais elevados de Rap1A na forma activa. O tratamento com 007-AM promove também um aumento dos níveis de Rap1A activa em células que expressam CFTR WT mas não nas que expressam CFTR F508del.

Adicionalmente, o tratamento com 007-AM promoveu a adesão celular em células que expressam CFTR WT mas não nas células que expressam CFTR F508del. Isto sugere que, em células que expressam CFTR com esta mutação, a via EPAC-Rap não consegue exercer a sua função e, de forma a ultrapassar esta limitação, a activação endógena da EPAC se encontra aumentada. Consequentemente, uma activação adicional não é detectada, dados os elevados níveis basais de activação.

De seguida, a possível co-localização e interacção entre as proteínas CFTR e EPAC1 foi avaliada. Para isso, recorreu-se a microscopia confocal de fluorescência e a ensaios de co-imunoprecipitação. Observou-se que a EPAC1 co-localiza e interage com CFTR, quer na sua forma WT quer na sua forma mutada. Além disso, a activação da EPAC com 007-AM aumentou a interacção entre CFTR e EPAC1. No entanto, a activação da EPAC1 não afecta a razão de CFTR na forma madura e forma imatura (que permite avaliar a eficiência de processamento da CFTR). Estes dados sugerem que a EPAC não está envolvida na fase inicial da biogénese da CFTR (síntese, folding e processamento inicial).

Observámos também que a depleção de NHERF1 (usando siRNA ou shRNA), mas não de ezrina, impediu a interacção entre a CFTR e a EPAC1 mas sem afectar a localização sub-celular da última. Isto sugere que a interacção entre estas duas proteínas é mediada pela proteína adaptadora NHERF1.

Finalmente, recorreu-se a ensaios de endocitose e biotinilação para avaliar o efeito da EPAC1 na estabilidade da CFTR na PM. Observou-se que a activação da EPAC decresce a quantidade de CFTR que é internalizada ao longo do tempo. Além disso, o tratamento com 007-AM levou a um aumento dos níveis de CFTR na PM enquanto a depleção da EPAC1 usando siRNA diminuiu estes níveis. Adicionalmente, a sobreexpressão de EPAC parece também promover a estabilidade da CFTR. Estas abordagens sugerem que a EPAC1 está envolvida na regulação da estabilidade da CFTR na PM.

Este efeito estabilizador permite também um aumento da quantidade de proteína CFTR F508del madura detectada após o tratamento simultâneo com o corrector de tráfego VX-809 e o agonista 007-AM.

Apesar dos avanços recentes no campo da FQ, ainda existem vários aspectos do tráfego e activação da CFTR por elucidar e parceiros moleculares por identificar. Desta forma, os resultados deste trabalho permitiram identificar uma nova ligação entre a proteína CFTR e a sinalização por cAMP. Este trabalho constitui assim uma importante caracterização de um novo interactor da CFTR, a proteína EPAC1, que liga o cAMP à modulação da FQ, por mecanismos até à data não descritos.

Abbreviations

007	8-(4-Chlorophenylthio)-2'-O-methyladenosine-3',5'-cyclic monophosphate (8-pCPT-2’-O-Me-cAMP)
007-AM	8-(4-Chlorophenylthio)-2'-O-methyladenosine-3',5'-cyclic monophosphate acetoxymethyl ester (8-pCPT-2’-O-Me-cAMP-AM)
A549	Human alveolar epithelial cell line
ABC	ATP-binding cassete
AC	Adenylyl cyclase
AKAP	A-kinase anchoring proteins
AKAR4	A-kinase activity reporter 4
ASL	Airway surface liquid
ATF	Arginine-framed tripeptide
ATP	Adenosine triphosphate
BSA	Bovine serum albumin
CAAX	Cystein-alyphatic-alyphatic-any aminoacid motif
CaCC	Calcium-activated chloride channel
cAMP	Cyclic adenosine monophosphate
Calu-3	Cancer lung 3 cell line
camps	cAMP sensor
CDC25-HD	Cell division cycle 25 homology domain
CF	Cystic fibrosis
CFBE41o- / CFBE	Cystic fibrosis bronchial epithelial cell line
CFP	Cyan fluorescent protein
CFTR	Cystic fibrosis transmembrane conductance regulator
CNB	Cyclic nucleotide–binding domain
COP-II	Coating protein II
C-terminal	Carboxyl-terminal
DAPI	4',6-diamidino-2-phenylindole
DEP	Disheveled, Egl-10, pleckstrin domain
DNA-PK	DNA damage–responsive kinase
DMSO	Dimethylsulfoxide
E3KARP	NHE3 kinase A regulatory protein
EBP50	Ezrin-binding protein

EDEM	ER degradation-enhancing α-mannosidase-like protein
EDTA	Ethylenediaminetetraacetic acid
EMEM	Eagle's minimal essential medium
ENaC	Epithelial sodium channel
EPAC/REPAC	Exchange protein directly activated by cAMP
ER	Endoplasmic reticulum
ERAD	Endoplasmic reticulum-associated protein degradation
ERM	Ezrin/radixin/moesin
ERQC	Endoplasmic reticulum quality control
ESI-09	3-[5-(tert.-Butyl)isoxazol-3-yl]-2-[2-(3-chlorophenyl)hydrazono]-3-oxopropanenitrile
F-actin	Filamentous actin
FBS	Fetal bovine serum
FLIM	Fluorescence lifetime imaging
FRET	Fluorescence resonance energy transfer
Frsk	Forskolin
GAP	GTPase-activating protein
GAPDH	Glyceraldehyde 3-phosphate dehydrogenase
GDP	Guanosine diphosphate
GEF	Guanine nucleotide exchange factor
GFP	Green fluorescent protein
GRASP	Golgi reassembly stacking protein
GST	Glutathione S-transferase
GTP	Guanosine triphosphate
GTPase	Guanosine triphosphate hydrolase
HBSS	Hank's Balanced Salt Solution
HEK	Human embryonic kidney cell line
HRP	Horseradish peroxidase
Hsc70/Hdj2	Heat shock cognate 70kDa protein/human DnaJ homolog 2
Hsp70/Hdj-1	Heat shock protein 70kDa protein/human DnaJ homolog 2
Hsp90	Heat shock protein 90kDa protein
HUVEC	Human umbilical vein endothelial cell line
IBMX	3-isobutyl-1-methylxanthine
I_f	Fluorescence intensity

IP	Immunoprecipitation
IPTG	Isopropyl β-D-1-thiogalactopyranoside
LB	Luria broth
MAP1	Microtubule-associated protein 1
MSD	Membrane-spanning domain
NBD	Nucleotide binding domain
NHERF	Na^+/H^+-Exchanger Regulatory Factor
N-terminal	Amino-terminal
ORCC	Outwardly rectifying chloride channel
P60	Plates with 60mm of diameter
P100	Plates with 100mm of diameter
PAGE	Poliacrylamide gel electrophoresis
PBS	Phosphate buffer saline
PBS-T	Phosphate buffer saline with tween
PCR	Polymerase chain reaction
PDE	Phosphodiesterase
PDE4D3	Phosphodiesterase 4D3
PDZ	Post synaptic density protein (PSD95), Drosophila disc large tumor suppressor (Dlg1), and zonula occludens-1 protein (zo-1)
Pen	Penicilin
PKA	Protein kinase A
PM	Plasma membrane
PP2A	Protein phosphatase-2A
PPase	Protein phosphatase
PVDF	Polivinylidene difluoride
RA	Ras-association domain
RanBP2	Ran-binding protein 2
RBD	Rap-binding domain
RD/R domain	Regulatory domain
REM	Ras exchange motif domain
RFP	Red fluorescent protein
RFU	Relative fluorescence units
RNA	Ribonucleic acid
ROCK	RhoA-activated kinase

ROMK	Renal outer medullary potassium channel
R-ras	Ras-like small GTPase
RT	Room temperature
SBT	Spectral bleed-through
SDS	Sodium dodecylsulphate
SEM	Standard error of the mean value
shRNA	Small hairpin RNA
siRNA	Small interfering RNA
Strep	Streptomycin
TBS	Tris buffer saline
TBS-T	Tris buffer saline with tween
TM	Transmembrane segments
TNF-R1	Tumor Necrosis Factor Receptor 1
Tris	Tris(hydroxymethyl)aminomethane
UGGT	UDPglycoprotein glucosyltransferase
YFP	Yellow fluorescent protein
WB	Western Blot
WCL	Whole cell lysates
WT	Wild-type

Chapter I

Introduction

1. Introduction

1.1 Cystic Fibrosis - Overview

Cystic Fibrosis (CF) is the most common potentially lethal autosomal recessive disorder in Caucasians, affecting about 1 in 2500-6000 newborns. Remarkably, the heterozygote frequency is about 1 in 25 individuals[1]. CF is clinically characterized by chronic lung disease, which is the main cause of morbidity and mortality. Airway obstruction by thick mucus and chronic infection by *Pseudomonas aeruginosa* eventually lead to loss of pulmonary function[2]. Other CF symptoms include pancreatic dysfunction, elevated salt concentration in sweat and male infertility[3].

1.2 The CFTR gene and protein

In 1989, the gene responsible for CF was identified to be located at the long arm of chromosome 7 (7q.31.2) and named Cystic Fibrosis Transmembrane Conductance Regulator (CFTR)[4]. This gene encodes for a cyclic AMP (cAMP)-regulated chloride channel expressed in a number of epithelial tissues. It was found to harbor mutations in all CF patients analyzed, the most common of which being a deletion of three nucleotides encoding for the phenylalanine residue in position 508 in the protein (F508del)[5]. This mutation is present in 90% of CF patients in at least one of their two mutated CFTR alleles.

Gene sequence and direct mutation analysis were turning points in the history of CF and opened new opportunities for molecular and cellular studies in this field. To date, ~2000 CFTR mutations have been described, most of which cause CF[6]. Between these gene defects and the ultimate clinical phenotype of respiratory insufficiency, a series of events that have termed the 'CF pathogenesis cascade', sequentially occurs (*Figure 1.1*)[2]. To better understand the diversity of mechanisms through which single mutations cause CF, CFTR mutants are grouped into functional classes, according to their specific effects upon CFTR biosynthesis and function – and this allows the design of 'mutation-specific therapy'[7]. Class I mutations abolish protein production. Class II mutations result in defective protein processing (F508del mutation belongs to this class). Class III proteins are defective in the regulation of the channel. Class IV mutations are characterized by

defective ion conductance. Class V mutations result in decreased protein synthesis. Class VI mutations decrease CFTR stability at the cell surface[2].

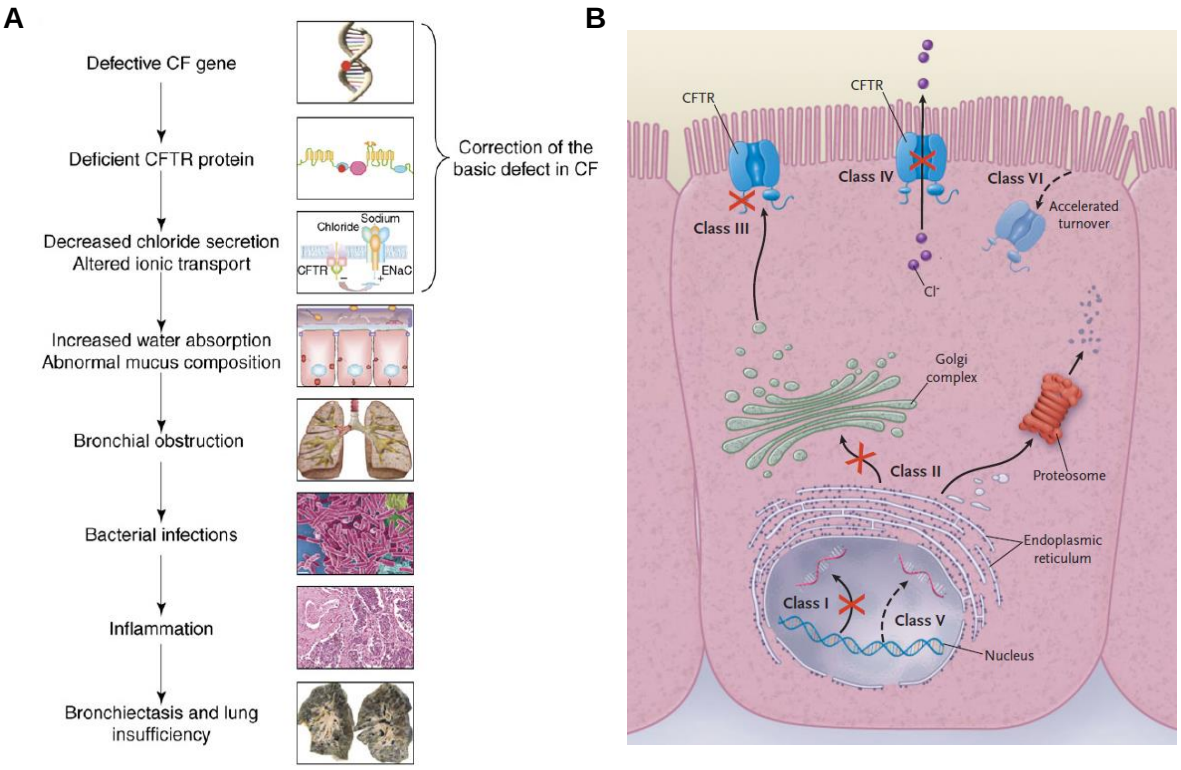

Figure 1.1: Mechanism of CF dysfunction. (a) The CF pathogenesis cascade, from the primary CFTR gene defect to lung deficiency. **(b)** Classes of defects in the CFTR gene include the absence of synthesis (class I); defective protein maturation and premature degradation (class II); altered regulation, such as diminished ATP binding and hydrolysis (class III); defective chloride conductance or channel gating (class IV); reduced amount of CFTR transcripts/protein due to promoter or splicing abnormality (class V); and accelerated turnover from the cell surface (class VI)[2, 3].

Currently, search of new potential therapeutic targets and pharmacological therapies to rescue the molecular defects responsible for CF are the most important topics of disease-related research[2]. In 2012, Kalydeco (developed as VX-770) was approved by the Food and Drugs Administration (USA), and later by the European Medicines Agency, as the first drug targeting the molecular basis of the disease (first mutation-specific therapy). This compound, that corrects the gating defect caused by several mutations on CFTR, has been approved initially for patients carrying the G551D gating mutation[8] and more recently for other Class III/IV mutations. Ongoing clinical trials are exploring a combination of VX-770 with others compounds, namely VX-809, that corrects the trafficking defect of CFTR with other mutations, such as F508del[9]. Thus, approaches aimed at correcting the basic CF defect still hold promise for completely curing the disease.

The CFTR gene directs the synthesis of transcripts of about 6.5kb (after splicing) and encodes for an integral membrane glycoprotein composed of 1480 amino acids[4, 10]. The CFTR protein functions as a chloride channel predominantly expressed at the apical membrane of epithelial cells lining the target organs: lung, pancreas, intestine and sweat gland[2]. As a member of the ATP-binding cassette (ABC) transporter superfamily, CFTR has a symmetrical multi-domain structure, consisting of two membrane spanning domains (MSD1 and MSD2), each composed of six transmembrane segments (TM1-TM12) which form the pore through which anions pass, and two nucleotide-binding domains (NBD1, which harbors F508del mutation, and NBD2)[5]. Both NBDs bind and hydrolyze ATP, regulating the channel opening[11]. CFTR structure also contains a central and highly charged regulatory (R) domain, absent from all other ABC transporters, with multiple phosphorylation consensus sites (*Figure 1.2*)[10, 12]. The phosphorylation status of this domain may regulate the dimerization of the NBDs domains[13]. CFTR C-terminus, well known for accommodating a PSD95, Dlg1, ZO-1 (PDZ)-binding motif, is also involved in several protein interactions[14].

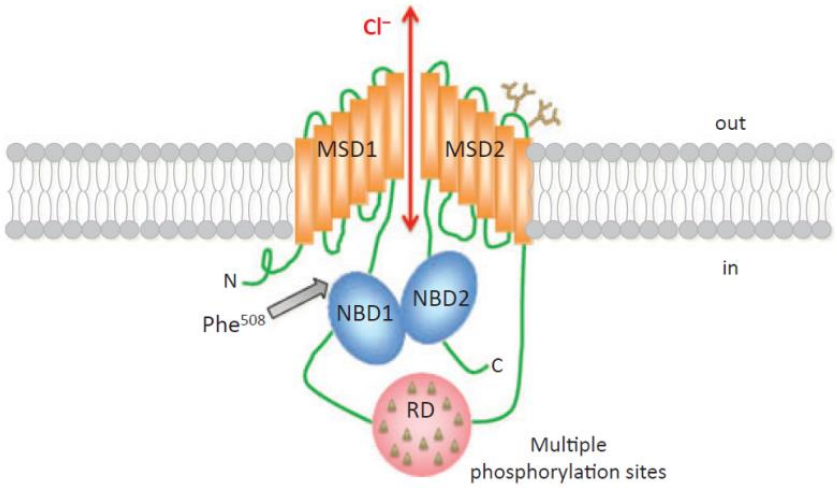

Figure 1.2: CFTR structure at the plasma membrane. MSD, membrane spanning domains; RD, regulatory domain (contains multiple phosphorylation sites); NDB, nucleotide-binding domain (NDB1 harbors the most frequent CF-causing mutation, F508del)[10].

1.3 CFTR folding and trafficking

Although CFTR folding is a highly regulated process, because CFTR is such a large multidomain membrane glycoprotein, proper folding is difficult to achieve. Hereupon, during CFTR biogenesis, only 20-40% of the newly synthesized protein escapes the endoplasmic reticulum (ER) quality control (ERQC), undergo complex glycosylation in the Golgi complex and acquire the native conformation. The remaining protein is tagged for degradation by the ubiquitin-proteasome pathway[15, 16]. Thus, the coordinated folding of CFTR and its individual domains occur through an iterative process in three different cellular compartments: ER membrane and lumen, as well as cytosol[17].

Similarly to what happens with other multidomain glycoproteins, CFTR is co-translationally inserted into the ER membrane and simultaneously N-linked to glycosyl groups. Additionally, as a membrane protein, CFTR follows the general route of the secretory pathway to reach the plasma membrane (PM), i.e. through the Golgi[10].

In this way, while CFTR is being translated in a cytosolic ribosome, an ER targeting motif is recognized by the signal recognition particle, causing it to be targeted to the ER surface and co-translationally inserted into the ER membrane through the Sec61 translocon

complex[17]. While the nascent polypeptide chain is being inserted in the ER membrane, the exposed parts in the cytosol associate with the cytosolic molecular chaperones Hsp90, Hsc70/Hdj-2, and Hsp70/Hdj-1 (with this forming a first checkpoint in the ER quality control (ERQC) for CFTR; *Figure 1.3*)[10, 18]. Immediately after insertion into the ER membrane, the newly synthesized CFTR polypeptide chain emerging into the ER lumen is core-glycosylated at Asn894 and Asn900. CFTR N-glycosylation, which occurs by the addition of a glycoconjugate with 14 osidic residues, plays a pivotal role in its folding, sorting and trafficking[10, 18]. This glycoconjugate is processed by glucosidases generating a glycosylated intermediate recognizable by luminal calnexin and calreticulin chaperones that allow the folding to progress (second checkpoint)[15, 19]. After these two initial ER folding checkpoints, CFTR conformation is assessed at a third checkpoint. This is a retention mechanism that recognizes arginine-framed tripeptide (ATFs) motifs at the ER exit sites. From this point, in the ER, there are two different pathways:

-If the protein didn't attain the proper folding, it is recognized by UDPglycoprotein glucosyltransferase (UGGT), which re-glycosylates CFTR. Hereupon, a new round of chaperone binding, de-glucosylation and proofreading begins. If the protein undergoes too many of these rounds, eventually it becomes subject to the ubiquitination-dependent endoplasmic-reticulum-associated protein degradation (ERAD). After being marked by the ER degradation-enhancing α-mannosidase-like protein (EDEM) for degradation, CFTR is retro-translocated to the cytoplasm and degraded by the ubiquitin-proteasome pathway[10, 15]. Most of the CFTR bearing the F508del mutation, owing to its incorrect folding, is retained and degraded at the ER due to the ERQC system[10];

-If the protein is folded correctly, it proceeds to the secretory pathway. CFTR is released from the ER, loaded into COPII-coated vesicles that traffic to the Golgi, where its glycan moieties undergo further processing. The fully glycosylated CFTR is then incorporated into secretory vesicles and delivered to the apical membrane, exposing its glycans to the extracellular space and exerting its function[10]. More recently, ER stress was reported to induce CFTR trafficking from the ER to the apical membrane through a Golgi-independent GRASP-dependent unconventional secretion pathway[20].

During the maturation process, CFTR undergoes several glycosylation steps, first in the ER and then in the Golgi apparatus. For CFTR, glycosylation at the ER creates the core-glycosylated 135-140kDa (immature) form of the protein (also called band B). From the ER, wild-type (WT) CFTR traffics through the Golgi complex, where it is processed by

multiple Golgi glycosyltransferases and glycosidases, creating the fully 150-160kDa mature form of CFTR (also termed band C)[10, 16].

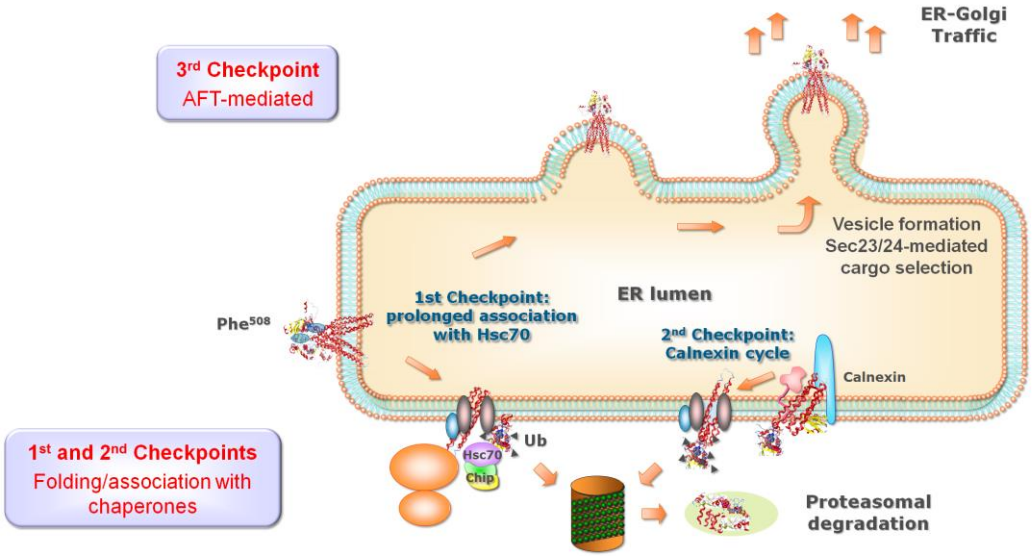

Figure 1.3: Checkpoints for the ER quality control of CFTR. At the first checkpoint, Hsc70 and Hsp70 interact with the cytosolic domains of nascent CFTR to assess its conformation – this is the major mechanism for retaining and discarding F508del-CFTR. At the second checkpoint, WT-CFTR proceeds through the folding pathway through interaction of its N-glycosyl residues with calnexin. After the third checkpoint (retention mechanism that recognizes arginine-framed tripeptide (AFT) motifs), correctly folded CFTR exits the ER, proceeding through the secretory pathway. Ub, ubiquitin[10].

Additionally, after being delivered to the PM, CFTR can be subjected to endocytosis. CFTR is internalized into early endosomes where it can either return to the PM, through Rab11/MyoVb-driven recycling endosomes, or diverted from the recycling pathway into late endosomes, via Rab7, followed by lysosomal degradation[21-23]. As CFTR internalization at the cell surface is a rapid process compared to CFTR biosynthesis and maturation, the recycling of internalized channels is considered to be a key process in maintaining a functional pool of CFTR at the PM[10].

1.4 CFTR anchoring at the plasma membrane

Recycling of internalized CFTR to the PM has been considered to be the main mechanism for sustaining a functional pool of CFTR at the cell surface, albeit some evidence suggest that up to 50% of surface CFTR exists in an immobile pool, tethered to filamentous actin (F-actin), in airway epithelial cells[10, 24]. Because the CFTR C terminus (amino acids residues DTRL) forms a consensus PDZ binding domain (C-terminal X-[S/T]-X-[V/I/L]), it can bind to several proteins that contain these PDZ domains[24, 25]. One of these C-terminus-interactors is the PDZ adaptor protein Na^+/H^+-exchanger regulatory factor isoform-1 (NHERF-1, also known as EBP50, ezrin-binding protein, 50kDa)[26-28]. NHERF-1 anchors CFTR at the PM to the actin cytoskeleton and is also important to target exosome- and endosome associated CFTR to the apical membrane of polarized epithelial cells. The first involves the interaction of CFTR-bound NHERF-1 with the ezrin/radixin/moesin (ERM) family protein ezrin, locking CFTR in an immobile and actin-tethered complex that prevents its endocytosis (*Figure 1.4*)[10, 26]. NHERF1 increases the chloride channel activity of CFTR. It has also been suggested that NHERF1 may induce CFTR dimerization, facilitating CFTR intermolecular interactions, which alter channel conformation and activity. However, the role of PDZ-domain proteins in the formation of CFTR dimers is controversial[26].

NHERF1 role upon CFTR stabilization involves also interaction with small GTPases (guanosine triphosphate hydrolase) of the Rho family. These GTPases, found in all eukaryotic organisms, are divided into three subfamilies, grouped according to their functional and structural similarity to their three founding members, RhoA, Rac1, and Cdc42[10]. The members of the Rho family are key regulators of actin cytoskeleton dynamics, cell polarity and membrane trafficking through their modulation of F-actin remodeling[10, 29, 30]. Consistently, NHERF1 overexpression stimulates the activation of endogenous RhoA and RhoA-activated kinase (ROCK), thus leading to reorganization of the actin cytoskeleton and stabilization of the multiprotein complex F508del-CFTR–NHERF1–ezrin–actin at the apical PM[31]. Therefore, CFTR surface anchoring and retention may be a major target pathway to be considered in CF pharmacotherapy[10].

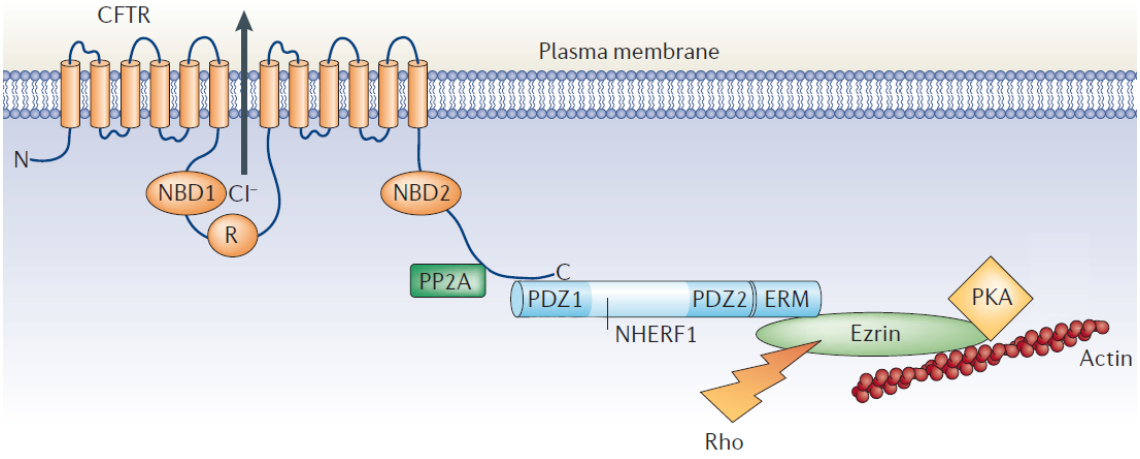

Figure 1.4: CFTR anchoring at the plasma membrane. Several proteins interact directly or indirectly with CFTR, including protein phosphatase-2A (PP2A), Na+/H+ exchanger regulatory factor isoform-1 (NHERF1), protein kinase A (PKA) and ezrin, forming a multiprotein complex that stabilizes CFTR at the plasma membrane. ERM, ezrin, radixin, moesin binding domain; NBD, nucleotide-binding domain; R, regulatory domain[Adapted from 26].

1.5 CFTR function

CFTR functions mainly as a chloride channel, playing a fundamental role in fluid and electrolyte transport across the epithelial cells and regulation of the airway surface liquid composition. However, CFTR function is not restricted to being a chloride channel, being also permeable to other anions, namely bicarbonate, thus providing an important role as a regulator of transmembrane pH gradients[32, 33]. CFTR is also implicated in the control of extracellular reactive oxidative species balance, as a result of glutathione transport[34, 35]. Therefore, because this channel regulates transepithelial salt and water movement, it coordinates epithelial hydration and efficient mucociliary clearance. This is also achieved through the regulation of other PM channels, namely the epithelial sodium channel (ENaC), calcium-activated chloride channels (CaCCs), outwardly rectifying chloride channels (ORCCs) and renal outer medullary potassium channel (ROMK)[36-39]. Contrary to other ABC transporters, CFTR is incapable of actively driving ion transport against a gradient; instead, it functions as a passive channel that allows bidirectional flow of ions[14].

CFTR chloride channel gating is tightly regulated by the balance of kinases and phosphatases activity within the cell and by the cellular levels of ATP and cAMP. The MSDs contribute to the formation of the chloride pore and NBDs bind and hydrolyze ATP to regulate the channel gating. Activation of the cAMP-dependent protein kinase A (PKA) drives the phosphorylation of multiple serine/threonine residues within the R domain, required to channel activation. Finally, protein phosphatases dephosphorylate the R domain and return the channel to its quiescent state (*Figure 1.5*)[12].

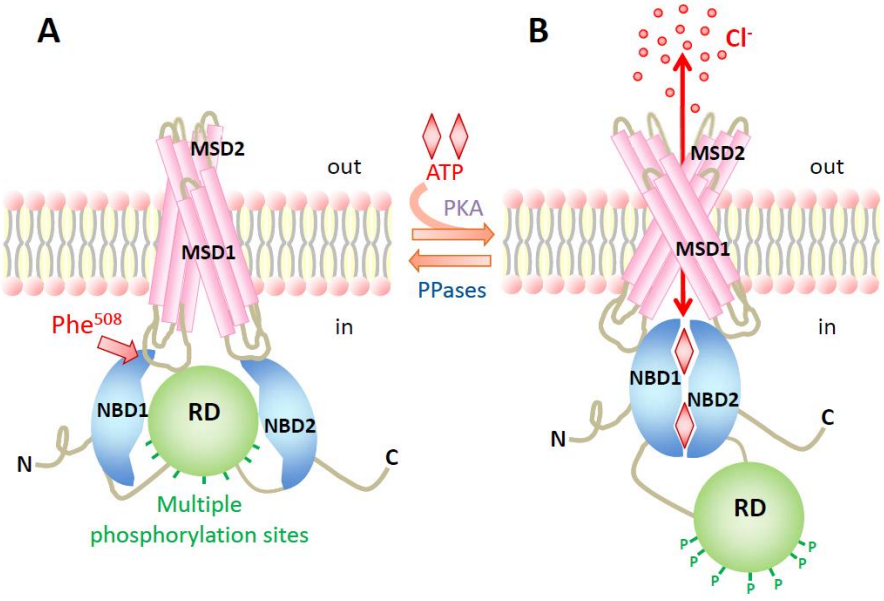

Figure 1.5: Regulation of the CFTR chloride channel opening. Schematic model showing the regulation of CFTR through cAMP-dependent phosphorylation of the R domain (RD) and ATP binding and hydrolysis at the NBDs. In and Out denote the intra- and extracellular sides of the cell membrane. MSD, membrane-spanning domain; NBD, nucleotide-binding domain; P, phosphorylation of the R domain; PKA, protein kinase A; PPase, protein phosphatase[40].

This PKA-mediated activation of CFTR requires integrity of the actin cytoskeleton and compartmentalized cAMP within the cell[41]. It has been reported that the cAMP increase required for PKA-mediated activation of CFTR must be specifically localized near the membrane, in the subcortical compartment[31, 41]. Additionally, this compartmentalization is dependent on the integrity of the subcortical cytoskeleton and on the presence of adenylate cyclases (AC; responsible for the production of cAMP) and A-kinase anchoring proteins (AKAPs), such as ezrin. AKAPs are scaffold proteins, anchoring PKA, phosphatases, phosphodiesterases and other signaling proteins in the vicinity of CFTR. The formation of multiple protein macromolecular complexes in subcellular microdomains increases the specificity and efficiency of signaling towards CFTR, allowing a cAMP-dependent control of chloride efflux[14, 41-44]. Although it is well-established that cAMP plays a crucial role in CFTR regulation, PKA is not the only cAMP sensor within the cell.

1.6 EPAC – Overview

Since the discovery that cAMP activates the phosphorylating enzyme PKA, the cAMP messenger system has been shown to regulate cAMP production by heteromeric guanine nucleotide–binding proteins (G proteins), subsequent binding of cAMP to PKA, and consequent phosphorylation of PKA substrates[45, 46]. cAMP is a second messenger that has a role in many physiological processes ranging from the regulation of heart rhythm, insulin secretion or neurotransmitter release[47, 48]. Initially, PKA was considered to be the essential effector molecule mediating many of these physiological effects initiated by receptors coupled to generation of cAMP[45, 46, 49]. However, PKA has not been clearly linked to all these processes[45]. A database screen conducted to explain the insensitivity of cAMP-induced activation of the small GTPase Rap1 to inhibitors of PKA, in 1998, led to the identification of EPAC, an exchange protein directly activated by cAMP (also known as cAMP-GEF), heralding the age of signal transduction[47, 48, 50]. This approach identified independently two proteins containing a cyclic nucleotide-binding (CNB) domain: EPAC1 and EPAC2 (or RAPGEF3 and 4, respectively). Another protein highly homologous to EPAC with activity toward Rap, known as REPAC (or RAPGEF5), was later identified; however, this protein lacks a cAMP-binding domain[51].

EPAC proteins function as guanine nucleotide exchange factors (GEFs) for both Rap1 and Rap2[51]. Rap is a small Ras-like GTPase that was first identified as a protein that could suppress the oncogenic transformation of cells by Ras. It belongs to the Ras superfamily of small G proteins, specifically to the Rap subfamily, which cycle between an inactive guanosine diphosphate (GDP)-bound state and an active guanosine triphosphate (GTP)-bound state. Thus, small G-proteins function as simple molecular switches with an inactive GDP-bound and active GTP-bound conformation[47, 50, 52]. GEFs catalyze the exchange of GDP for GTP and thereby the activation of the G protein, whereas GTPase-activating proteins (GAPs) enhance GTP hydrolysis. Several other GEFs for Rap, in addition to EPAC, have been identified. These GEFs connect different inputs to Rap activation and are associated to distinct functions of Rap. The most intriguing RapGEF, however, is EPAC, because this GEF represents a novel target for cAMP, independent from the classical target protein PKA[51]. Rap, whose activation by cAMP occurs independently of PKA, is activated by several extracellular stimuli and is involved in an immense diversity of cellular processes such as cell proliferation and adhesion, actin cytoskeleton dynamics, cell polarity, exocytosis, membrane protein recycling and cell differentiation[50, 54-61].

EPAC1 and EPAC2 are present in most tissues, although with different expression levels: EPAC1 is highly abundant in blood vessels, skeletal muscles, central nervous system, kidney, adipose tissue, ovary and uterus; EPAC2 is mostly expressed in the central nervous system, pancreas and adrenal gland[45, 50, 62]. REPAC is strongly expressed in the human brain[63].

1.7 EPAC protein and its activation

EPAC1 and EPAC2 are multidomain proteins that consist of an N-terminal regulatory region and a C-terminal catalytic region (*Figure 1.6a*). The regulatory region has one (EPAC1) or two (EPAC2) CNB domains and a DEP (Dishevelled, Egl-10, and Pleckstrin) domain. The catalytic region harbors the CDC25-homology domain (CDC25-HD) for enzymatically exchange activity, which is stabilized by a Ras exchange motif (REM) domain. There is a Ras-association (RA) domain between these domains. The regulatory region has an autoinhibitory function that is relieved by binding of cAMP (*Figure 1.6b*)[47, 48, 51, 64, 65]. In the inactive conformation, the CNB domains sterically prevent Rap binding to the catalytic site. As already known for EPAC2, an ionic interaction between the C-terminal CNB (CNB-B) domain and the CDC25 domain dynamically stabilizes this conformation. Upon binding of cAMP, a subtle change within the CNB-B domain allows the regulatory region to move away from the catalytic region. This position is stabilized by interactions between cAMP, CNB-B and REM domains[47, 66, 67].

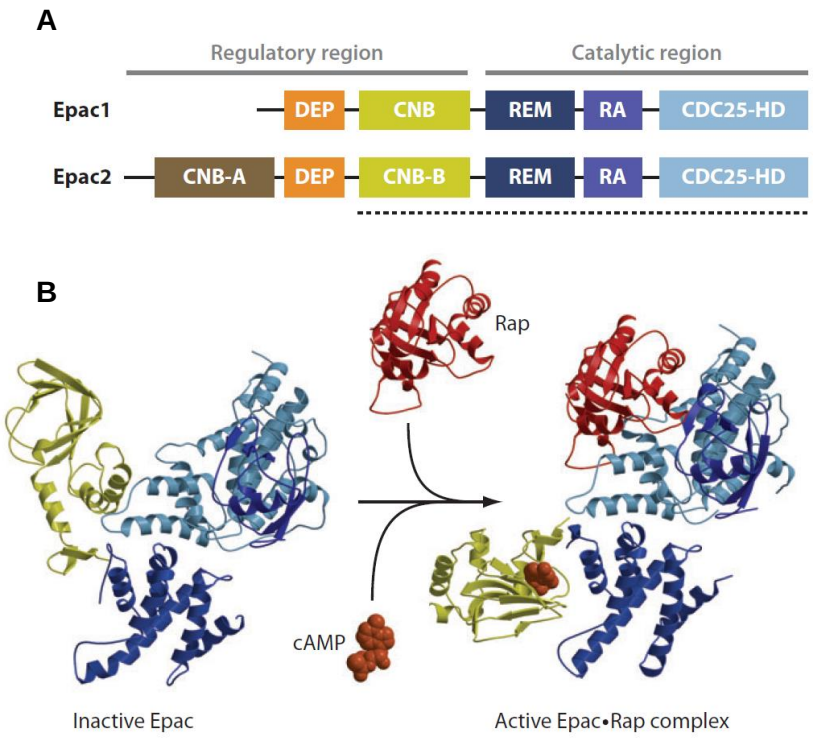

Figure 1.6: Structure of EPAC. (a) Schematic representation of the domain architecture of both EPAC proteins. The regulatory region contains one or two CNB (cyclic nucleotide–binding) domains and a DEP (Disheveled, Egl-10, and Pleckstrin) domain. The catalytical region harbors the CDC25-homology domain (CDC25-HD), the Ras exchange motif (REM) domain and a Ras-association (RA) domain. (b) Crystal structure model of both inactive and active EPAC2. For simplicity, only the catalytic region and the CNB-B domain (indicated with a dotted line in panel a) are shown[47].

Hormonal stimulation of many heterotrimeric G-protein-coupled receptors frequently results in the activation of AC leading to an increase in cAMP levels. cAMP can be then degraded by phosphodiesterases (PDE). In the past, the discovery and analysis of cAMP-mediated events has been greatly facilitated by specific compounds that modulate intracellular cAMP levels. The most commonly used ones are forskolin, a natural compound that directly activates ACs, and a variety of PDE inhibitors, such as 3-isobutyl-1-methylxanthine (IBMX), both added to further enhance cAMP levels[47, 48, 68]. During the development of EPAC-selective analogs of cAMP, it was noticed that EPAC proteins lack the glutamate residue that, in PKA and cAMP-gated ion channels, interacts with the ribose

of cAMP. Taking advantage of this knowledge, 8-pCPT-2'-O-Me-cAMP (also known as 007) was developed as a selective agonist for EPAC, being ten times more efficient than cAMP in activating EPAC1. To increase the relatively low membrane permeability of this compound, an acetoxymethyl (AM)-ester was introduced to mask the negatively charged phosphate group, originating 007-AM. This modification allows exceptional cell permeability being intracellularly removed by esterases to generate 007[47, 69-71]. Despite 007-AM also activating EPAC2, it was reported recently that sulfonylurea selectively activates EPAC2 isoform, but not the closely related EPAC1, further establishing a new class of isoform-selective enzyme activators[48, 72].

1.8 Spatial regulation of EPAC

Although cAMP can rapidly diffuse within the cytosol, it becomes unevenly distributed and concentrated in local microdomains. Thus, cAMP-elevating hormones do not induce homogenous increases of cAMP within the cell. The molecular basis of this cAMP signaling compartmentalization involves its synthesis by membrane-associated AC, subsequent diffusion through the cell and local cAMP degradation by PDEs. As a result, these cAMP mediators generate cAMP gradients within the cell[47, 73]. In addition to cAMP compartmentalization, cAMP effectors are also spatially regulated by binding to scaffolding proteins, as has been previously shown for PKA (*section 1.5*). AKAPs target PKA to distinct subcellular locations and mediate the assembly of large signaling complexes, linking PKA to specific cellular functions. In a similar way, EPAC proteins are spatially regulated by different anchoring mechanisms[47].

In response to the cAMP-induced conformational change, EPAC1 is targeted to the PM. This is essential for the ability of EPAC1 to induce its downstream effectors, like Rap, at the PM[74]. The DEP domain is required for this translocation and it has been shown to tether EPAC1 to phosphatydic acid (PA) at the membrane[75]. EPAC1 is also tethered to the PM by an additional mechanism, through phosphorylated (active) ERM scaffolding proteins[76]. Thus, EPAC1 can be recruited to PM by two different pathways: one is through PA and is cAMP- and DEP-dependent; the other way is through ERM proteins and is cAMP-independent and N-terminal-region-dependent[75, 76]. Radixin has also been reported to bind EPAC1 and PKA simultaneously, bringing these two cAMP sensors together and creating a functional cAMP-sensing compartment for efficient signal transduction[77]. All

these data suggest that EPAC1 might co-localize or even interact with CFTR, which argues for a possible function of this GEF in CFTR function regulation or membrane stability. Additionally, EPAC1 is activated by stimuli that result in increased subcortical cAMP, the same stimuli that induce PKA-mediated activation of CFTR, which further supports this hypothesis.

EPAC2 is targeted to the PM after binding to activated Ras proteins, via its RA domain and independently of its conformational state[78].

Several other subcellular localizations have been reported for EPAC1, some of which link EPAC1 to specific cellular processes (*Figure 1.7*). Nuclear EPAC1 was found to regulate the DNA damage–responsive kinase (DNA-PK) within the nucleus[79]. EPAC1 is also targeted to microtubules, in interphase or mitotic cells, and this interaction is probably required for the role of EPAC in microtubule polymerization. EPAC1 has also been observed in other localizations that may be associated with distinct functions, such as centrosomes, mitochondria, the nuclear pore complex and the apical membrane of renal epithelial cells[47, 52]. The multidomain structure of EPAC indicates that it may have multiple binding partners, and indeed numerous interacting proteins have already been described for both EPAC1 and EPAC2. Alternative splicing may further add another layer of complexity to the spatial regulation of EPAC[47].

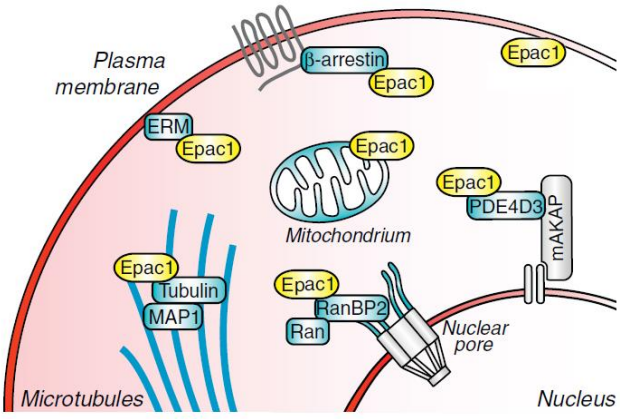

Figure 1.7: Spatial regulation of EPAC1. (a) Spatial regulation of the EPAC1, showing how the diverse EPAC1-interacting proteins (blue) affect the localization of this GEF. ERM, Ezrin, Radixin, Moesin; MAP1, microtubule-associated protein 1; PDE4D3, phosphodiesterase 4D3; RanBP2, Ran-binding protein 2[Adapted from 52].

1.9 Biological functions of EPAC

The major catalytic function of EPAC is the guanine nucleotide exchange of Rap1 and Rap2, with EPAC thus controling the Rap-mediated processes downstream of cAMP. However, several other GEFs or GAPs can regulate Rap activity and Rap1 and Rap2 might not mediate all effects of cAMP-EPAC (*Figure 1.8*). It has been reported that EPAC1 also activates R-ras, a Ras-like small GTPase implicated in the control of integrin-mediated cell adhesion. Undoubtedly, the EPAC-selective cAMP analog 007 has helped to highlight a role for EPAC and Rap in a wide range of biological processes, ranging from exocytosis of insulin in the β-cells of the pancreas to the regulation of calcium currents in cardiomyocytes, permeability of the vascular endothelium, ionic transport across intestinal cells and tissue fibrosis. Most of these processes are also modulated by signaling via the cAMP effector PKA, proving the interconnectivity between both cAMP pathways[47, 48, 80-83]. Indeed, both cAMP targets are often associated with the same biological process, in which they fulfill either opposite or synergistic effects. This dual control may enhance the dynamic range of cAMP signaling, as PKA-mediated events are proposed to occur at much lower cAMP levels than the activation of EPAC[84]. For increased complexity, the spatial localization of EPAC is also a crucial determinant of its function[48]. Thus, it is anticipated that the study of EPAC as a cAMP-signaling mediator is a starting field with a lot more to be discovered, in the same way that cAMP has been a major hit of research since its discovery more than 50 years ago.

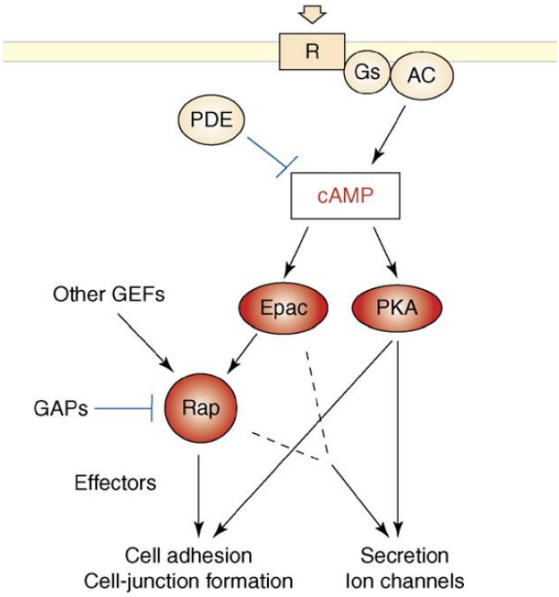

Figure 1.8: Interconnectivity between the EPAC- and PKA-signaling pathway. After stimulation of a receptor (R) coupled to a stimulatory G protein (Gs), adenylate cyclase (AC) is activated, promoting cAMP synthesis and consequent activation of both EPAC and PKA. Both proteins are involved in the regulation of cell adhesion, cell–cell junction formation, secretion and ion channels. Inhibitory G proteins may also inhibit AC activity. PDE, Phosphodiesterase; GEF, guanine-nucleotide-exchange factors; GAP, GTPase-activating protein[48].

Although a potential connection between CFTR and EPAC has never been reported, this cAMP effector is involved, as already mentioned, in the regulation of cell-to-cell and cell-matrix adhesion, cytoskeleton rearrangements and cell polarization, processes that affect CFTR regulation[41, 85, 86]. Thus, more detailed knowledge about a potential relationship between CFTR and EPAC is needed, as EPAC may be a new link between CFTR and cAMP.

1.10 Objectives

Here, we proposed to study the role of a novel cAMP signalling pathway in the regulation of CFTR at the plasma membrane in order to better understand the mechanisms by which the protein is anchored at its cellular location and ultimately how can this be modulated for the benefit of CF patients.

Specifically, the aim of the present work is to study the interaction between CFTR and EPAC1, the predominant isoform of EPAC in cAMP signaling, and to evaluate the impact of this cAMP effector on CFTR biogenesis, trafficking and PM anchoring. In order to achieve this goal, we propose to:

1- Validate 007-AM as a specific cAMP analogue for EPAC in Cystic Fibrosis Bronchial Epithelial cells (CFBE) by fluorescence resonance energy transfer (FRET) and co-immunoprecipitation (co-IP);
2- Validate cAMP-induced translocation of EPAC in CFBE cells by confocal live-cell imaging and cell fractionation;
3- Evaluate co-localization and interaction between CFTR and EPAC1 (and the effect of 007-AM) by confocal live-cell imaging and co-IP;
4- Characterize the molecular linkers involved in the CFTR and EPAC1 interaction and the role of PDZ binding domain on CFTR-EPAC1 interaction;
5- Assess the effect of EPAC1 on CFTR PM stability using endocytosis and biotinylation assays;
6- Assess the dependence of EPAC-induced cell adhesion dependence on the expression of CFTR.

Chapter II

Materials and Methods

2. Materials and Methods

2.1 Molecular Biology

2.1.1 Plasmid vectors and siRNAs

All plasmids and siRNAs (small interfering RNA) used in this work are listed on the following tables (*Table 2.1 and 2.2, respectively*). Maps for all vectors are available in *Appendices Plasmid maps*.

Table 2.1: List of plasmids used and their description.

Plasmid Name	Vector (antibiotic resistance)	Description
pEGFP-EPAC1	pEGFP-C2 (kanamycin)	GFP-EPAC1 fusion protein tagged with GFP at the N-terminus of EPAC1
pEGFP-C2		Destination vector for expression of proteins with a GFP tag at the N-terminus (used as control)
pcDNA3.1-CFTR	pcDNA3.1 (ampicillin)	WT or ΔTRL (1478-1480) CFTR
pmCherry-C2-CFTR-FLAG	pmCherry-C1 (kanamycin)	mCherry- CFTR fusion protein with the mCherry tag at the N-terminus containing a FLAG at the forth extracellular loop of WT- or F508del- CFTR
Raichu-Rap1	pCAGGS (ampicillin)	FRET sensor (EYFP-ECFP) that responds to EPAC activity[87] (*section 2.4*)
AKAR4	pcDNA3.1+ (ampicillin)	FRET sensor (EYFP-ECFP) that responds to PKA activity[88] (*section 2.4*)
camps	pcDNA3 (ampicillin)	FRET sensor (EYFP-ECFP) that responds to cAMP levels[89] (*section 2.4*)

Table 2.2: List of siRNA used.

siRNA Name	Brand (Reference)
Silencer® Select Negative Control No. 2 siRNA	Life Technologies (4390846)
Silencer® Select siRNA RAPGEF3	Life Technologies (4392420)
siGENOME SMART pool non-targeting siRNA	Thermo Scientific (D-001206-13)
siGENOME SMART pool human EZR	Thermo Scientific (EG:7430)
siGENOME SMART pool human SLC9A3R1	Thermo Scientific (EG:9368)

2.1.2 Transformation of competent bacteria

The bacterial strains used for cloning and DNA amplification were: One Shot TOP10 (Invitrogen) or 2); XL1-Blue competent cells (Stratagene). Preparation of competent bacteria was done in-house according to the technique described by Hanrahan[90].
Bacteria were transformed by incubating a 200µL aliquot of competent bacteria with DNA (at least, 100ng of ligation products or 5ng of purified plasmids) for 30 min in ice. Afterwards, the mixture was submitted to heat-shock (90 sec at 42ºC), incubated 2 min on ice followed by incubation in LB media without antibiotic for 45 min at 37ºC at 220rpm, in order to allow antibiotic resistance to be expressed. After pelleting the bacteria (3000g for 5 min), the supernatant was discarded and the pellet was resuspended in the remaining medium. This suspension was then plated into LB-agar supplemented with appropriate concentration of the selected antibiotic and plates were incubated overnight at 37ºC.
Transformed bacterial colonies were then grown in LB medium supplemented with the appropriate antibiotic and plasmid DNA was extracted. Clones were stored in liquid LB medium supplemented with 15% (w/v) glycerol (Sigma-Aldrich) at -20ºC.

2.1.3 DNA extraction and quantification

Plasmid DNA was purified, at small or large scale, with QIAGENMiniprep kit (QIAGEN) or QIAGENMaxiprep kit (QIAGEN), respectively, accordingly with manufacturer's guidelines.
DNA concentration was determined by measurement of the absorbance at 260nm using a Nanodrop 2000 spectrophotometer (Thermo Scientific) and its purity was evaluated by assessment of the A_{260}/A_{280} ratio. Only DNA with a ratio above 1.8 was considered pure enough for further use.

2.1.4 Mutagenesis

The TRL deletion was performed on pcDNA3.1-WT-CFTR using the KOD Hot Start DNA Polymerase (Novagene) with a pair of complementary custom designed mutagenic primers (Thermo Electron Corporation): delTRL_FW (forward primer, sequence 5'-GAAGAGGTGCAAGATTAGAGAGCAGCATAAATG-3') and delTRL_REV (reverse primer, sequence 5'-CATTTATGCTGCTCTCTAATCTTGCACCTCTTC-3'). Primers were designed with the software BioEdit (http://www.mbio.ncsu.edu/bioedit/bioedit.html). The PCR program used for the mutagenesis reaction is displayed in the following table.

Table 2.3: PCR program for the mutagenesis reaction.

Temperature (ºC)	Time	Number of cycles
95	2min	18
95	20s	
47	20seg	
70	5min	

After confirming the DNA amplification by agarose gel electrophoresis, the PCR products were incubated for 1h with DpnI (Invitrogen), a restriction enzyme that specifically hydrolyzes methylated and semi-methylated DNA, thus degrading the non-amplified template DNA. After bacteria transformation (*section 2.1.2*) and DNA extraction (*section 2.1.3*), the presence of the mutation was confirmed by DNA sequencing (*section 2.1.5*).

2.1.5 DNA sequencing

The sequencing reactions were outsourced to StabVida. Primers used for CFTR and EPAC plasmids are listed below (*Table 2.4*). All sequencing primers were obtained through StabVida. The resulting sequences were analyzed using the BioEdit software by comparison with a reference sequence.

Table 2.4: Primers used for sequencing.

Primers		
For CFTR plasmids		**5' – 3'**
AC1L	Reverse	GAAACCAAGTCCACAGAAGGC
CMV	Forward	CGCAAATGGGCGGTAGGCGTG
Ex5F		CTCCTTTCCAACAACCTGAAC
B3R		AATGTAACAGCCTTCTGGGAG
C2R		AGCAGTATACAAAGATGCTG
D1R		GACAACAGCATCCACACGAA
E1R		AGATTCTCCAAAGATATAGC
Ex18F		AACTCCAGCATAGATGTGG
Ex22F		AGCAGTTGATGTGCTTGGC
For EPAC plasmid		**5' – 3'**
CMV	Forward	CGCAAATGGGCGGTAGGCGTG
EGFP		CATGGTCCTGCTGGAGTTCGTG
RapGEF3a1		TACGCATTCCTCTACCGTAAG
RapGEF3b2		AGCCGAAGCTGCATTTCTG
RapGEF3b3		AAGGAAGTAGTTCTGCCTGG
RapGEF3	Reverse	AGATTCCCACAACTTGGCTC

2.2 Cell Culture

Cells were cultured in the appropriate medium in plastic flasks or plates, in an incubator with a humidified atmosphere of 5% CO_2 at 37ºC. For cell detachment from the plastic surface, cells were washed with in PBS and then incubated with trypsin (Life Technologies). Cell lines were stored frozen at -80ºC or in liquid nitrogen in 40% (v/v) of the appropriated cell medium, 50% (v/v) FBS and 10% (v/v) DMSO (Sigma-Aldrich). To minimize cell damage, freezing was performed in a way that allows a cooling speed around 1ºC/min. After thawing, cells were washed and seeded with the indicated medium for each cell line (see below). To eradicate/prevent mycoplasma contamination, cells were treated occasionally with Myco4 (AppliChem). To assess cell contamination, a PCR test for Mycoplasma was performed.

2.2.1 Cell types

2.2.1.1 CFBE cells

Cystic Fibrosis Bronchial Epithelial (CFBE41o-) cells[91], from now on simply referred as CFBE, stably overexpressing either WT- or F508del-CFTR[92] or without expressing CFTR (parental CFBE) were cultured in Eagle's minimal essential medium (EMEM; Life Technologies) supplemented with 10% fetal bovine serum (FBS; Life Technologies), 2mM L-glutamine (Invitrogen). When appropriate/needed, medium was also supplemented with an antibiotic mixture of penicillin (Pen; 100U/mL; Life Technologies) and streptomycin (Strep; 100µg/mL; Life Technologies) and with puromycin (2.5µg/mL; Life Technologies).

2.2.1.2 Calu3 cells

Non-transduced Calu3[93] cells (Calu3-WT) or expressing a control (Calu3 shControl), Ezrin (Calu3 shEzrin) or NHERF1 shRNA (Calu3 shNHERF1) were generated in this work (*section 2.2.4*) and used for further analysis. Cells were cultured in DMEM-F12 (Lonza) media supplemented with 10% FBS and with or without puromycin (5µg/mL).

2.2.1.3 A549 cells

A549 cells overexpressing mCherry-WT- or mCherry-F508del-CFTR[94] under control of a tet-on promoter were cultured in DMEM (Lonza) media supplemented with 10% FBS and puromycin (2.5µg/mL). CFTR expression was induced with 10 µg/mL of doxycycline and 1mM of sodium butyrate for 24h.

2.2.1.4 HEK293 cells

Human Embryonic Kidney (HEK293) cells[95] were cultured in DMEM media supplemented with 10% FBS.

2.2.3 Transfections

Cells were transiently transfected with plasmid DNA or siRNA (*section 2.1.1*) using Lipofectamine2000 (Life Technologies), a cationic liposome formulation that forms DNA complexes able to fuse with cell membrane, according to the manufacture's guidelines[96].
Usually, for one 6 well-plate, 750µL of OptiMEM (Life Technologies) were mixed with 36µL of Lipofectamine and other 750µL of OptiMEM were mixed with 12µg of plasmid DNA or 1µL of 20µM siRNA and incubated at RT (room temperature) for 5min. After that, the second mixture was added to the first one and incubated 30min at RT. 250µL of this final mixture was added to each well with 60-90% confluent cultured cells.
Medium was changed after 6h and all experiments were done 24 to 48h after transfection.

2.2.4 Lentivirus infection

2.2.4.1 Lentivirus production

HEK293 cells were transiently transfected with a mixture of the packaging (pCMV-dR8.74psPAX2), envelop (pMD2.G) and hairpin-pLKO.1 vector (Empty vector control, SHC001; NHERF1, SHCLND SLC9A3R1; Ezrin, SHCLND EZR; Sigma-Aldrich) plasmids using X-tremeGENE9 DNA transfection reagent (LifeScience), according to the manufacturer's guidelines, and incubated at 37ºC. Because lentivirus start to appear in the media supernatant ~22h post-transfection, 18h after incubation at 37ºC, the transfection reagent medium was removed and replaced with high-BSA growth media (DMEM supplemented with 10%iFBS (inactivated FBS), 1.1g/100mL BSA (Bovine serum albumin) and 1x Pen/Strep). The next day, the media was harvested and stored at -20ºC. The cells were incubated again with high-BSA growth media and the medium was harvested one last time 24h later.

2.2.4.2 Production of a stable cell line

After washing 70% confluent Calu3-WT cells with Hank's Balanced Salt Solution (HBSS; Life Technologies), EMEM medium supplemented with 10% (v/v) FBS, polybrene (8µg/mL) and 5-20% (v/v) lentivirus-containing medium (*section 2.2.4.1*) was added to the cells. After centrifugation (2200rpm) at 37ºC for 30min, the cell plates were incubated at 37ºC for 24h. The medium was then replaced by EMEM supplemented with 10% (v/v) FBS and puromycin (5µg/mL), which allows the selection of cells that were efficiently infected. This medium change was repeated for, at least, 5 consecutive days.

2.3 Biochemical Analysis

2.3.1 Cell lysis and total protein quantification

For protein extraction, cells were washed 3 times with cold PBS and lysed with sample buffer (1.5% (w/v) SDS; 5% (v/v) glycerol; 0.01% (w/v) bromophenol blue; 0.05mM dithiotreitol; 0.095M Tris pH 6.8). DNA was sheared by enzymatic action of 5-25U/mL of benzonase (Sigma-Aldrich) in the presence of $MgCl_2$ 2.5mM.
Total protein quantification was performed using Bradford method. 1mL of Bradford reagent (Sigma Aldrich) was added to 2µL or 5µL of sample. A standard curve was performed by adding 1mL of Bradford solution to increasing concentrations of BSA (Sigma Aldrich) standards. Afterwards, the absorbance was measure at 595nm and data analysis was performed.

2.3.2 Western blot

Protein extracts were separated by SDS-polyacrylamide gel electrophoresis (PAGE) on 7.5, 8, 10 or 12.5%T (w/v) separating and 4%T stacking gels at 100-150 V. Subsequently, proteins were transfered onto *Immobilon* polivinylidene difluoride (PVDF) membranes (Millipore) at 400 mA for 1.5h. After blocking with 5 % (w/v) skimmed milk in phosphate-buffered saline (PBS: NaCl 137mM; KCl 2.7mM; KH_2PO4 1.5mM; Na_2HPO4 6.5mM, pH 7.4) containing 0.1% (v/v)-Tween (PBS-T) or Tris-buffered saline with 0.5% Tween 20 (TBS-T; Alfa Aesar) for 1h at RT, membranes were incubated overnight with primary antibodies (*Table 2.5*) at 4ºC. After three 10 min washes with PBS-T/TBS-T, the membranes were incubated 1h at RT with horseradish peroxidase-conjugated secondary antibody (see antibodies on Table 2.5) and washed as above. All antibodies were diluted in blocking solution. Chemiluminescent detection was performed using: Chemidoc XRS+ analyser (BioRad) and the signal was developed with the ImmunStar Western C Chemiluminescence kit (BioRad) or using Compact X4 Automatic Processor (Xograph) and the signal was developed using ECL Western Blotting Substrate (Thermo Scientific). The quantification of band volume was performed using the Image Lab software (BioRad) or ImageJ (http://imagej.nih.gov/ij/). In order to re-incubate with another primary antibody, the membranes were washed at least 5 times for 10 min with PBS-T or TBS-T, or washed 1h with PLUS Western Blot Stripping Buffer (46430, Thermo Scientific). After this washing step, the membranes were blocked again for 1h at RT.

Table 2.5: List of primary and secondary antibodies used.

Antibody	Antigen	Reference (Brand)	Application (Dilution)
Primary	α-tubulin	T5168 (Sigma Aldrich)	WB (1:2000)
	β-tubulin	sc-9104 (Santa Cruz Biotechnology)	WB (1:1000)
	Calnexin	610523 (BD Biosciences)	WB (1:1000)
	CFTR (NBD2)	596 (Cystic Fibrosis Foundation)	WB (1:3000), IP (1:1000)
	EPAC1	ARP52140_P050 (Aviva Systems Biology)	WB (1:1000), IP (1:1000)
	Ezrin	610602 (BD Biosciences)	WB (1:1000)
	GAPDH	sc-166574 (Santa Cruz Biotechnology)	WB (1:1000)
	GFP	sc-9996 (Santa Cruz Biotechnology)	WB (1:1000)
	NHERF1	611160 (BD Biosciences)	WB (1:1000)
	Rap1A	sc-1482 (Santa Cruz Biotechnology)	WB (1:200)
	TNF-R1	Sc-8436 (Santa Cruz Biotechnology)	WB (1:1000)
Secundary	Mouse IgG, HRP-conjugated	W4018 (Promega)/1703516 (BioRad)	WB (1:3000)
	Rabbit IgG, HRP-conjugated	W4028 (Promega)/ 1706515 (BioRad)	WB (1:3000)

2.3.3 Immunoprecipitation

Cells were grown in P60/P100 plates until confluence was reached and then lysed with 0.5/1mL PD buffer (50mM Tris-HCl, 0.1M NaCl, 1% (v/v) NP40 (Roche), 10% (v/v) glycerol, pH 7.5 supplemented with a 1x Complete protease inhibitor cocktail (Roche) at 4ºC and collected with a cell scraper. After that, cell membranes and debris were pelleted by centrifugation at 10,000rpm for 5min at 4ºC and the supernatant was pre-cleared through incubation at 4 ºC for 2h with 40µL of Protein-G agarose beads (Invitrogen). The beads were pelleted by centrifugation for 1min at 10,000rpm followed by overnight incubation of the supernatant with the appropriate antibody (see antibodies on Table 2.5) at 4ºC. For mCherry pull-down, anti-RFP antibody-linked beads (RFP-Trap_A sta-20; Chromotek) or untagged beads (bab-20; Chromotek), as a control, were used. In this case,

no pre-clearing step was performed. The beads were pelleted by centrifugation for 1min at 10,000rpm, washed 3x with wash buffer (Tris-HCl 0.1M, NaCl 0.3M, Triton X-100 1% (v/v), pH 7.5) followed by elution with 1x sample buffer and spin-down. For certain samples, a 5 min incubation at 90ºC was performed. The immunoprecipitate was loaded and separated on SDS-PAGE gels and analyzed by Western Blot (*section 2.3.2*).

2.3.4 Rap1A activity assay

The active fraction of Rap was purified using a pull-down assay, as described[97]. This assay exploits the selective interaction of the Rap-binding domain (RBD) of RalGDS with the active, GTP-bound form of Rap. This domain was expressed tagged with glutathione S-transferase (GST), which strongly binds to glutathione-coupled agarose beads. These beads allow to selectively pull-down active Rap from cell extracts (*Figure 2.1*).

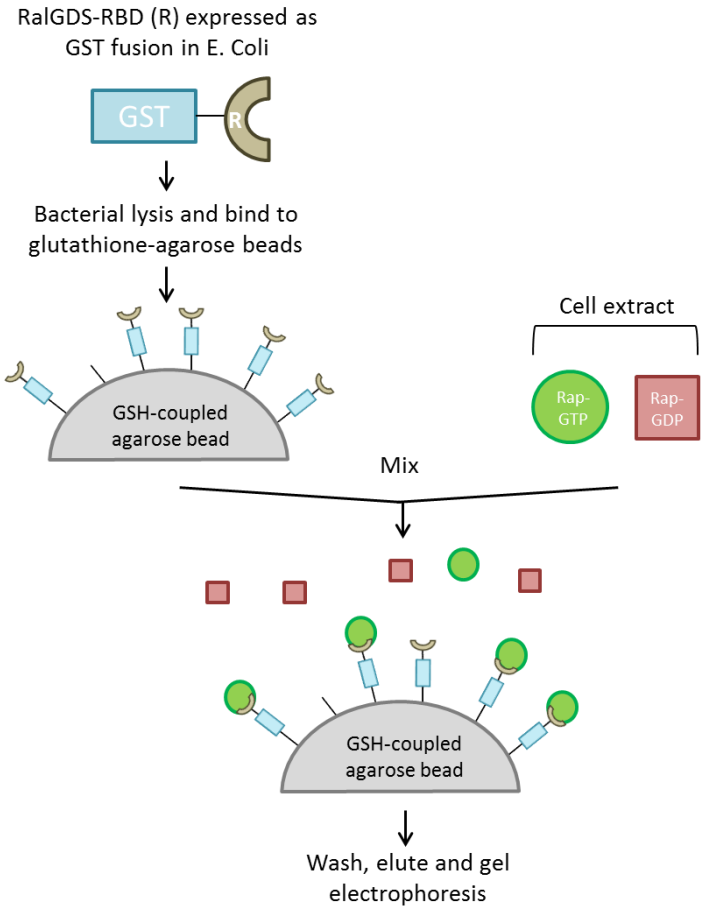

Figure 2.1: Schematic representation of the Rap1A activity assay.

For the beads preparation, bacteria transformed with pGEX-RalGDS-RBDGST (a kind gift from Dr.David Altschuler, University of Pittsburgh School of Medicine) were grown in LB medium. After reaching an OD600 of 0.6, the expression of RalGDS-RBD-GST fusion protein was induced with IPTG 1mM (Isopropyl β-D-1-thiogalactopyranoside; NZYTech) for 4h, followed by a centrifugation to collect the bacteria. These were resuspended in PBS containing 1x Complete protease inhibitor cocktail (Roche) and sonicated 10x 10 cycles of 0.7s. Proteins were solubilized with 1% (v/v) Triton X-100 (GE Healthcare) for 30min at 4ºC, centrifuged 10min at 10000 g and incubated with glutathione agarose beads (Thermo Scientific) for 1-2 hours at 4ºC. Finally, the beads were diluted 1:1 in PBS and a 50% slurry was added 1:1 to glycerol and stored at - 20ºC.
The expression of the recombinant protein, after induction with IPTG, was monitored by running aliquots of bacterial lysates (taken before and after the addition of IPTG) in a SDS-PAGE gel. The gel staining with Coomassie Blue showed a robust expression after adding IPTG (*Figure 2 Appendices*). GST-RalGDS-RBD-coupled beads were also confirmed in a SDS-PAGE, confirming that the protein was effectively captured (*Figure 4 Appendices*).

For the pull-down assay, cells were lysed on ice in Rap1A lysis buffer (25mM Tris-HCl, 1% (v/v) NP-40, 5mM MgCl2, 150mM NaCl, 0.1mM DTT, 5% (v/v) glycerol, Complete protease inhibitor cocktail, pH 7.5) for 15min. Lysates were centrifuged 10,000g for 10min at 4ºC and the supernatant was incubated with glutathione agarose beads coupled to GST-RalGDS for 2 hour at 4ºC. For Western Blot analysis, beads were washed and resuspended in 1x sample buffer for Western Blot analysis.

2.3.5 Biotinylation assay

Cells were grown in P100 plates until confluence was reached and incubated at 4ºC with NHS S-S Biotin buffer (0,1mg biotin (Pierce)/1 mL PBS with 1mM $MgCl_2$, 0.1mM $CaCl_2$, pH 8.2) for 30 min. Cells were lysed with 1.5mL of BL buffer (25mM HEPES, 1% (v/v) Triton X-100, 10% (v/v) glycerol, supplemented with a 1x Complete protease inhibitor cocktail (Roche), pH 8.2) and collected with a cell scraper. Cell membranes and debris were pelleted by centrifugation at 10,000rpm for 10min at 4ºC and, after pre-clearing, the supernatant was incubated at 4ºC overnight with streptavidin beads. The beads were

pelleted, washed 1x with BL buffer and 2x with PBS and the samples were then analyzed by Western Blot.

2.3.6 Endocytosis assay

Cells were grown in P100 plates until confluence was reached and incubated at 4ºC with NHS S-S Biotin buffer (0,1mg biotin (Pierce)/1 mL PBS 1mM $MgCl_2$ 0.1mM $CaCl_2$ pH 8.2) for 30min. Endocytosis was promoted by placing the cells at 37 and terminated by returning them to 4ºC. Cells were incubated 5 times with GSH solution (75mM NaCl, 1mM $MgCl_2$, 0.1mM $CaCl_2$, 50mM GSH (Sigma), 80mM NaOH, 10% fetal bovine serum, pH 8.6) for 15min at 4ºC, lysed with 1.5mL of BL buffer (25mM HEPES, 1% (v/v) Triton X-100, 10% (v/v) glycerol, supplemented with a 1x Complete protease inhibitor cocktail (Roche), pH 8.2) and collected with a cell scraper. Cell membranes and debris were pelleted by centrifugation at 10,000rpm for 10min at 4ºC and, after pre-clearing, the supernatant was incubated at 4ºC overnight with streptavidin beads. The beads were pelleted, washed 1x with BL buffer and 2x with PBS and the samples were then analyzed by Western Blot.

2.3.7 Cell fractionation

Cells were grown in P100 plates until 75% confluence was reached, washed 2x with PBS, lysed with 0.5 mL of fractionation buffer (205mM sucrose, 20mM HEPES, 10mM KCl, 1.5mM $MgCl_2$, 1mM EDTA, 1mM EGTA, 1mM DTT, supplemented with a 1x Complete protease inhibitor cocktail (Roche), pH 7.4) and collected with a cell scraper at 4ºC. Cell lysate was incubated in a rocker at 4ºC for 30min and centrifuged at 720g for 5min at 4ºC. Supernatant was transferred to a new tube. Pellet was washed with 0.5mL of fractionation buffer and centrifuged again at 720g for 10min at 4ºC. Pellet was resuspended in nuclear buffer (fractionation buffer with 10% (v/v) glycerol and 0.1% (v/v) SDS added) – this is the membrane fraction (includes plasma membrane and other intracellular membranes). The supernatant was ultracentrifuged at 100,000g at 4ºC for 1h. The new supernatant is the cytosolic fraction and the pellet was discarded. All samples were analyzed by Western Blot.

2.4 Live cell imaging

2.4.1 Measurements of cAMP levels and PKA or EPAC activity by fluorescence resonance energy transfer (FRET)

Sensitized emission FRET measurements were performed as already described[41, 98]. For this purpose, the fluorescence emission of the acceptor that results from the radiation-free energy transfer of an excited donor molecule is measured. For these experiments, cAMP sensor (camps), AKAR4 (A-kinase activity reporter 4) or Raichu-Rap1 FRET sensors were used.

- In camps, which is a EPAC-based FRET sensor, the cyclic nucleotide–binding domain of EPAC is sandwiched by yellow fluorescent protein (YFP) and cyan fluorescent protein (CFP)[89, 99-101]. The binding of cAMP generates a conformational change, moving apart the two fluorophores, thereby decreasing FRET between these two.
Changes in cAMP concentration using camps were monitored by measuring YFP (545 nm)/CFP (480 nm) fluorescence emission values upon excitation of the transfected cells at 430 nm (*Figure 2.2*).

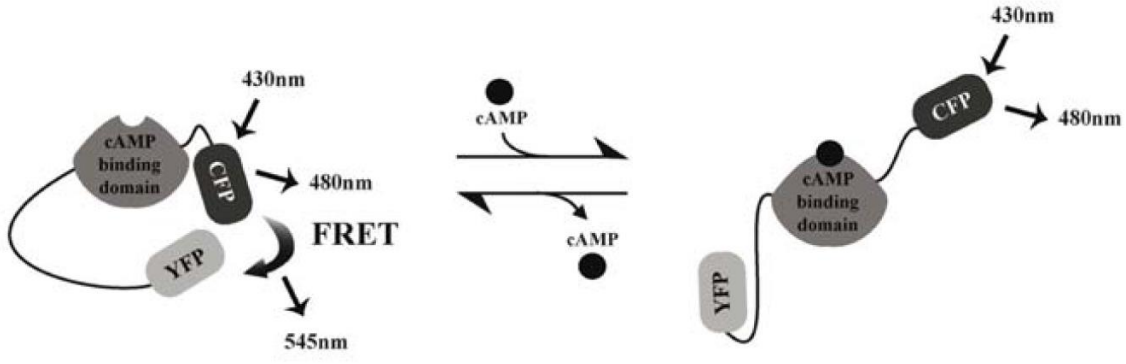

Figure 2.2: Schematic representation of camps bound or not to cAMP. The binding of cAMP to the cyclic nucleotide–binding domain induces a conformational change that abolishes FRET between YFP and CFP[101].

- In AKAR4, a PKA substrate sequence is inserted between the cerulean and venus FRET pair[100, 102]. The phosphorylation of this sensor generates a conformational change, which promotes the approaching of these two fluorophores and the increase of FRET signal. PKA-mediated phosphorylation using AKAR4 was monitored by measuring venus (545 nm)/cerulean (480 nm) fluorescence emission values upon excitation of the transfected cells at 430 nm (the principle is illustrated for the equivalent AKAR1 in *Figure 2.3*).

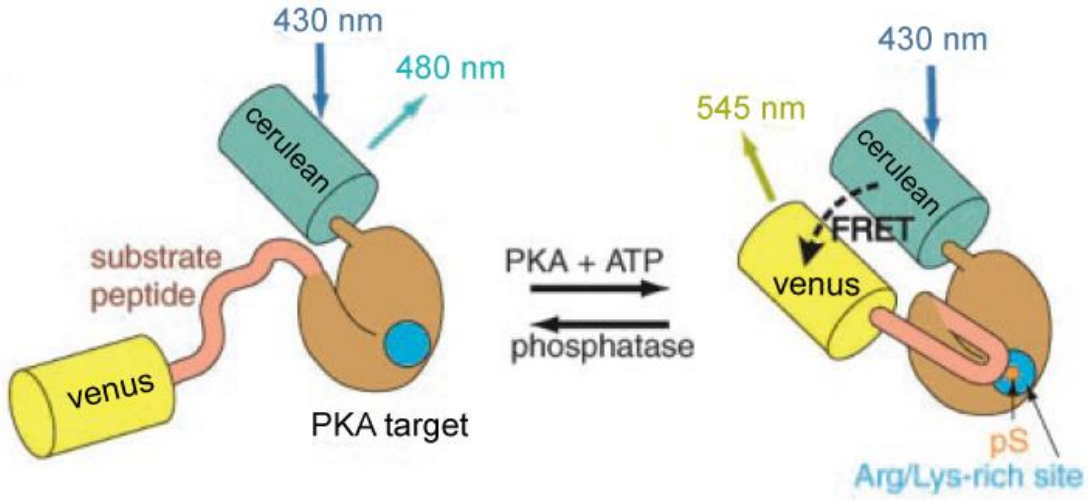

Figure 2.3: Schematic representation of AKAR4 phosphorylated or not phosphorylated. The phosphorylation of the domain with a PKA phosphorylation site induces a conformational change that allows FRET between venus and cerulean[Adapted from 88].

- There are so far no genetically encodable probes for EPAC activation that are able to measure the percentage of endogenous active EPAC. However, since the major output of EPAC activation is Rap activation, Raichu-Rap FRET sensor of Rap activity was used as an indirect reporter of EPAC activation. In this FRET sensor, the Rap1 sequence is between YFP and CFP fluorophores[87]. The binding of GTP to this FRET sensor, promoted by EPAC, generates a conformational change, thereby increasing FRET between the two fluorophores.

EPAC-mediated Rap activation (exchange of GDP by GTP) using the Raichu-Rap FRET sensor was monitored by measuring YFP (545 nm)/CFP (480 nm) fluorescence emission values upon excitation of the transfected cells at 430 nm (*Figure 2.4*).

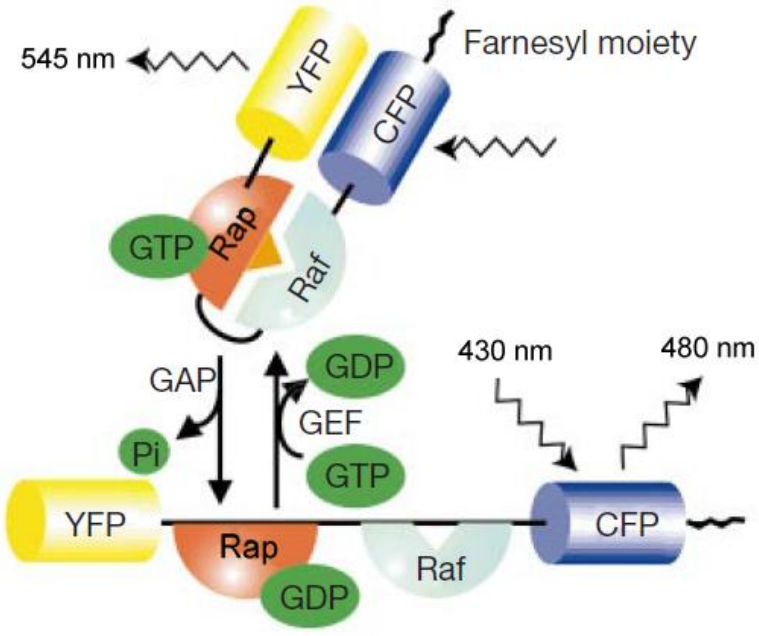

Figure 2.4: Schematic representation of Raichu-Rap bound to GDP or GTP. GTP binding, promoted by EPAC, induces a conformational change that allows FRET between YFP and CFP[Adapted from 87].

FRET imaging experiments were performed 24-48 hours after transfection. Cells were maintained at RT or at ~34ºC in Dulbecco's Phosphate-Buffered Saline (DPBS; Life Technologies) and imaged on an inverted microscope (Olympus IX81) using a PlanApoN, 60X, NA 1.42 oil immersion objective, 0.17/FN 26.5 (Olympus, UK). The microscope was equipped with an ORCA-AG CCD camera (C4772-80- 12AG, Hamamatsu Photonics, UK), White and 505nm light-emitting diode (LED; Cairn Research) and a beam-splitter optical device (Dual-view simultaneous imaging system, DV2 mag biosystem, Photometrics, ET-04-EM). The FRET filter settings used throughout were: CFP excitation filter ET436/20x, dichroic mirror 455DCLP (all from Chroma Technology) in the microscope filter cube; dichroic mirror 505DCLP, YFP emission filter 545nm, CFP emission filter 480nm (Chroma Technology) in the beam splitter. Images were acquired using MetaFluor or MetaMorph software (Molecular Devices) and processed using ImageJ. FRET changes were measured as changes in the background-subtracted 545/480 nm fluorescence emission intensity on excitation at 430 nm and expressed as R/R0, where R is the ratio at time t and R0 is the ratio at time = 0 s. Values are expressed as the mean ± SEM.

2.4.2 Translocation of EPAC1 and co-localization studies

Fluorescence imaging was performed 24-48 hours after co-transfection of CFBE or Calu3 cells with plasmids encoding for GFP-EPAC1 and mCherry-FLAG-CFTR. Cells were maintained at RT in Dulbecco's PBS (DPBS; Life Technologies) and imaged on an Fluoview FV1000 microscope, which is an inverted IX81 confocal system (Olympus), using a 60X, NA 1.35 oil immersion UPlanSApo objective (Olympus). The microscope was equipped with a Becker and Hickl FLIM system and with fluorescence filters suitable for UV and green or red dyes. Images were acquired using FluoView viewer software (FV10-ASW software, Olympus) and processed using ImageJ. This confocal fluorescence microscope was used to assess the intracellular localization of EPAC1 and CFTR in live cells in the absence or presence of 007-AM. The localization of these two proteins was monitored and the extent of overlap between the two was quantified using Pearson's correlation coefficient (ImageJ, JACoP plugin)[103-106]. Briefly, this coefficient describes the correlation of the intensity distribution between two channels. Since no threshold needs to be defined, no human factor can be introduced during image analysis. This is the main reason why Pearson's coefficient was used instead of others coefficients to estimate co-localization, such as Manders coefficient or other overlap coefficients. The overlap between the images of both proteins was performed using ImageJ software. For fluorescence pixel intensity quantification in a specific region of interest (for example, plasma membrane), MetaFluor software (Molecular Devices) was used.

2.5 Functional Analysis

2.5.1 Adhesion assay

The adhesion assay was performed as previously described[107]. 96-well plates were coated overnight with fibronectin coating solution (LHC basal medium (Life Technologies), 0.1mg/mL BSA (Life Technologies), 29µg/mL bovine collagen I (BD Laboratories, 40231) and 10µg/mL human fibronectin (BD Laboratories)). CFBE WT- and F508del-CFTR were grown on P100 plates until they reach 80/90% of confluence. At this point, cells were incubated with 1µM 007-AM or 5µM ESI-09, an EPAC specific inhibitor (or DMSO as a control) and after 2 hours were trypsinized. CFBE cells were resuspended in EMEM supplemented with 1µM 007-AM/5µM ESI-09 (or the same volume of DMSO as a control) and 0.2 µg/mL of Hoechst 33342 (nucleic acid stain; Life Technologies, H1399) and seeded into a fibronectin pre-coated 96 well-plate at a density of $5x10^4$ cells per well. Cells were allowed to attach for 30, 60 or 180min and then non-adherent and loosely attached cells were removed by washing the wells 3x with 100 µL aliquots of PBS while gently shaking the plate. Washes were performed in order to avoid directly affecting the cell adhesion. After the final wash, 200µL of EMEM was added to each well. Fluorescence intensity (I_f) at 465nm was measured using a plate reader (Tecan Infinite F200 PRO) before and after the washing step. The results are expressed as a percentage of adherent cells (ratio between I_f after washes/ I_f before washes). For each 96-well plate, a standard curve was made to ensure that there was a linear relationship between I_f and number of cells (*Figure 5 Appendices*).

2.6 Statistical Analysis

Data are presented as a mean standard error of the mean (SEM), as indicated in figure legends. Data were analyzed using student's t-test, with $p<0.05$ accepted as the level of statistical significance.

Chapter III

Results

3. Results

3.1 Effect of 007-AM treatment on EPAC1

The main aim of this work was to assess if EPAC1 and CFTR interact and the influence of this cAMP-effector on CFTR biogenesis, trafficking, and PM anchoring. This will allow an improved knowledge regarding the relationship between this channel and EPAC1. To answer this question, we proposed to use epithelial cells from the respiratory tract. CFBE cells were originally isolated from the bronchial epithelium of CF patients and immortalized. This cell line (called parental CFBE) has no endogenous expression of CFTR and was later transduced with either WT- or F508del-CFTR. These variants allow the study of pathways related to CF. Additionally, Calu3 or A549 cells were also used because, being lung adenocarcinoma cells, they are also considered as a good model to study features of the airway cells.

The first step was to evaluate the effect of 007-AM, an EPAC specific agonist, on EPAC tertiary structure, sub-cellular localization and activity. To prove the selectivity of 007-AM to EPAC, a FRET approach (sensitized emission FRET) was chosen using two different cAMP-sensors: one based on EPAC (camps) and the other based on a PKA substrate (AKAR4) (*described in section 2.4.1*). Hereupon, both sensors should respond to a forskolin (Frsk) treatment while only camps should respond to a 007-AM treatment. We chose to use a final concentration of 1µM 007-AM because it has been already reported to promote maximum activation of EPAC in A431 and HUVECs cells, being the concentration mostly used in the literature[76, 108-110]. After doing a Frsk standard curve for both sensors, a range of Frsk concentrations between 10 and 25µM was chosen (*Figure 1 Appendices*). Thus, cells were initially treated with 1µM 007-AM followed by increasing concentrations of Frsk until saturating conditions (*Figure 3.1*).

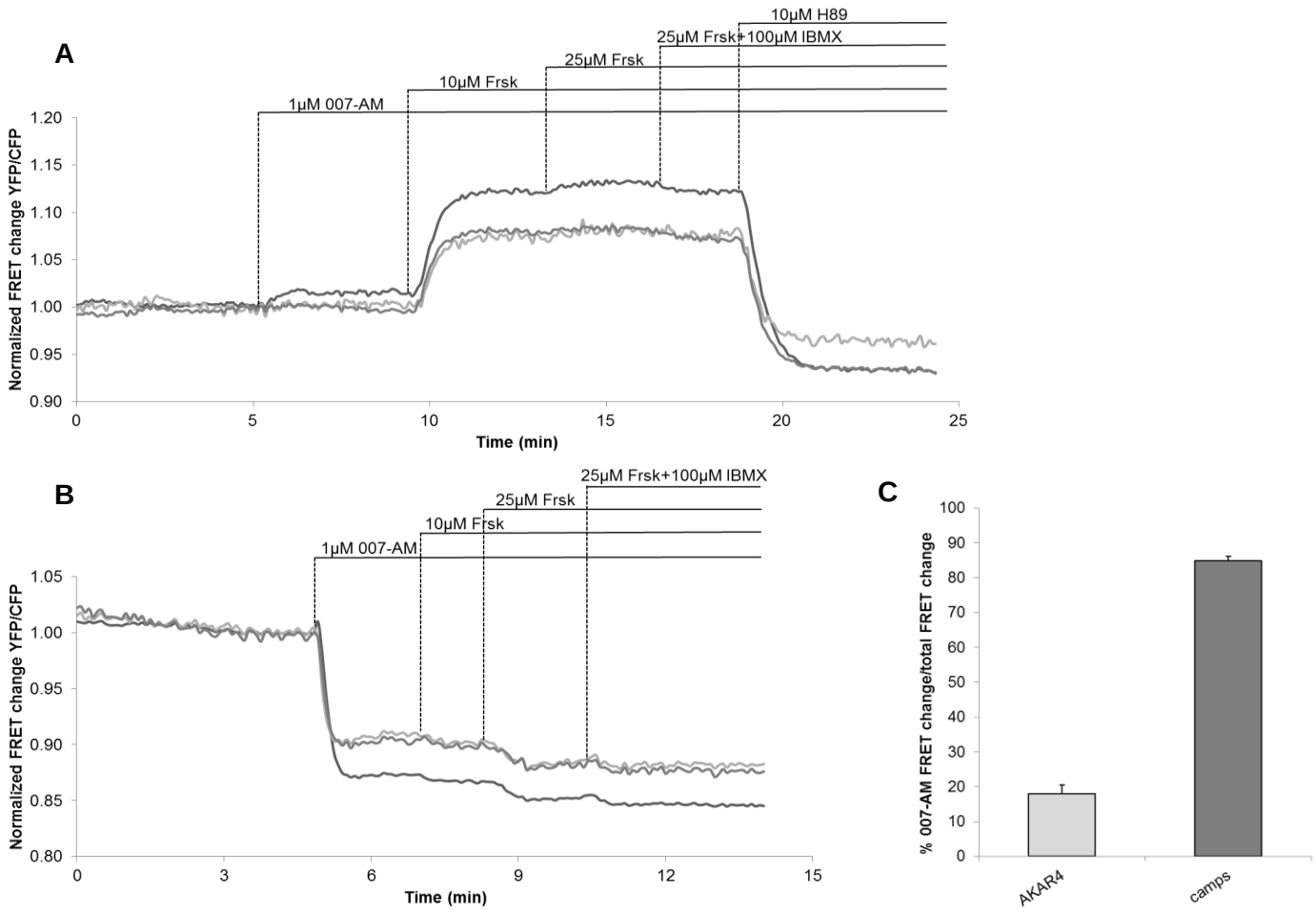

Figure 3.1: FRET analysis of cAMP levels and PKA activity in CFBE cells. Analysis of the (A) PKA activity-sensor AKAR4 and the (B) cAMP-sensor based on EPAC (camps) upon stimulation with 1 µM 007-AM followed by increasing concentrations of Frsk. 25uM Frsk + 100uMIBMX represents a saturation condition where adenylate cyclases are fully activated and PDEs are inhibited, leading to higher levels of cAMP. H89, a selective PKA inhibitor, was used to show that the FRET change is due to a change in PKA activity. FRET change is the normalized 545nm/408nm value calculated at each acquisition time point. The three lanes of each plot represent 3 different and independent cells. (C) Summary of all experiments performed in A and B, showing the percentage of 007-AM-induced FRET change compared to the maximum FRET change for both sensors. Data represent means ± SEM. n = 30/19 (AKAR4/camps).

As expected, 007-AM induced a high percentage of FRET change for camps while only a small FRET change was observed for AKAR4. To decreased this minor effect of 007-AM on PKA, a lower concentration of this compound should have been used. Nevertheless, this result indicates that 007-AM is an EPAC specific agonist in CFBE cells. However, we must have in consideration that AKAR4 measures PKA activity while camps, although it is an EPAC-based FRET sensor, measures cAMP levels or EPAC conformational change and not endogenous EPAC activity. This will be assessed later (*Figure 3.3*).

After confirming the effect of 007-AM on PKA and EPAC activation, the effect of this cAMP analogue on EPAC1 localization was assessed by fluorescence confocal microscopy. For this, CFBE parental cells or stably expressing WT- or F508del-CFTR were transfected with GFP-EPAC1. HEK293 cells were used as a control because EPAC1 translocation to the PM after 007-AM treatment has been already reported in these cells[76, 108, 109] (*Figure 3.2*). To complement these results, a Western Blot was performed after cell fractionation to assess the sub-cellular localization of endogenous EPAC1.

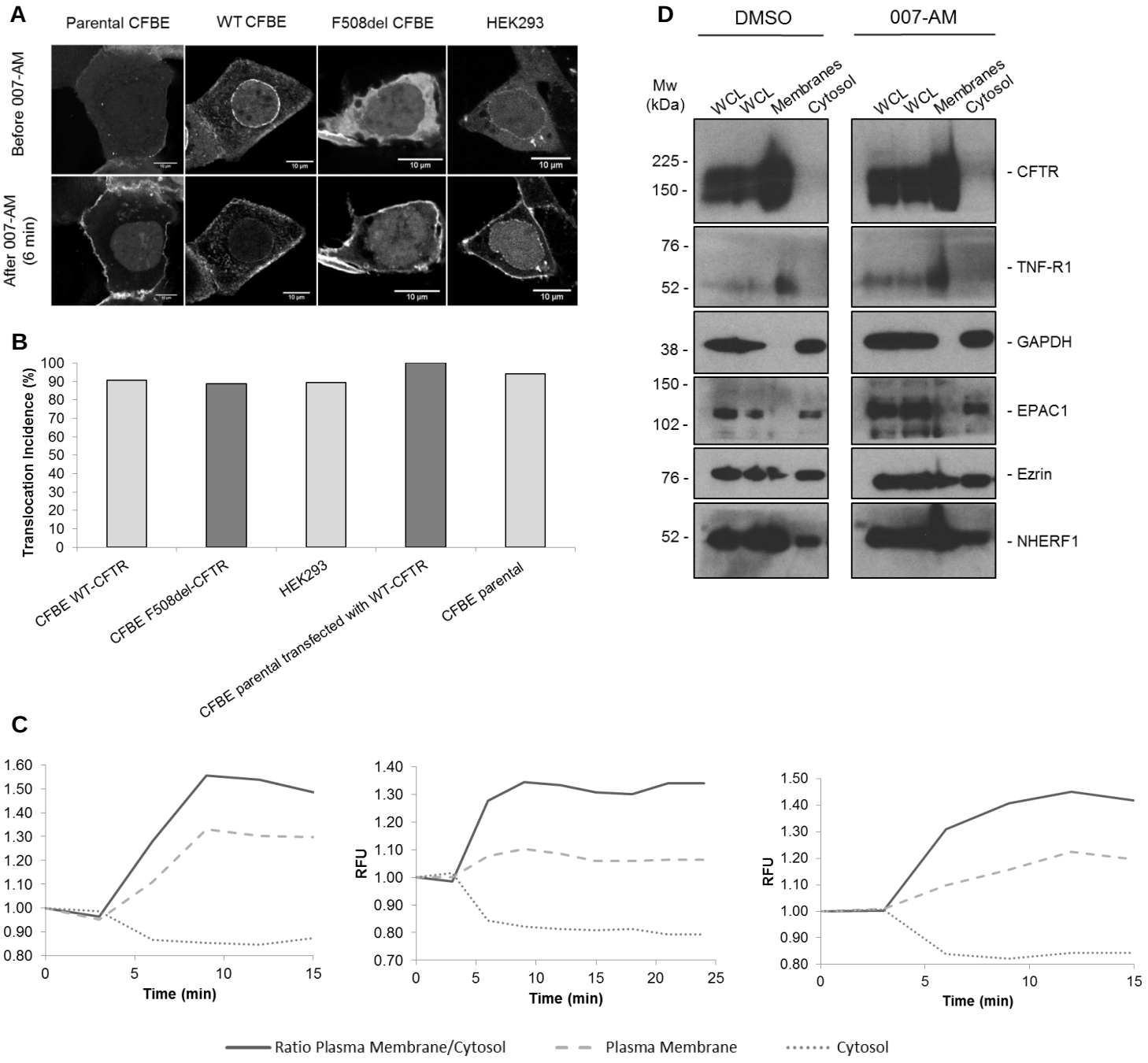

Figure 3.2: Analysis of EPAC1 localization after treatment with 007-AM in CFBE cells. (A) Confocal live cell imaging analysis of GFP-EPAC1 in CFBE and HEK293 cells. For each cell, only images before and 6 minutes after addition of 1µM 007-AM are shown. Scale bars, 10 µm. (B) The bar graph shows the percentage of cells showing translocation of EPAC1 to the PM upon 007-AM stimulation[according to 75]. n=11-40. (C) The graphs show an illustrative fluorescence pixel intensity of GFP-EPAC1 at the PM versus cytosol during stimulation with 1µM 007-AM relative to pre-stimulus levels, calculated as described in *Materials and Methods*. Images were acquired every 3 min.

As shown by live cell imaging, EPAC1, that is mainly localized in the cytosol and around the nucleus under basal conditions, translocates to the PM after being activated with 007-AM, in CFBE and HEK293 cells. This translocation occurs within the first 3 min of incubation with this cAMP analogue and it is independent of CFTR (*Figure 3.2A*). The Western Blot analysis after cell fractionation confirmed the translocation phenomenon for endogenous EPAC1, in CFBE cells. Additionally, the cellular distribution of EPAC1 suggests that this protein and CFTR may co-localize or even interact with each other, mainly under 007-AM treatment.

Although we have already shown that 007-AM induces a conformation change on camps and possibly the activation of endogenous EPAC, we don't know yet if this analogue can induce the activation of one of the downstream effectors of EPAC, Rap, as a result of endogenous EPAC activation. To assess this question, CFBE cells were transfected with Raichu-Rap FRET sensor, a reporter of EPAC activity (*described in section 2.4.1*). Additionally, a pull-down based Rap activity assay (*described in section 2.3.4*) was also performed, with two objectives: to confirm that 007-AM promotes the activation of EPAC and to see if there is any difference in the levels of active EPAC in cells expressing WT- or F508del-CFTR (*Figure 3.3*).

Figure 3.2 (continuation): 007-AM was added after the acquisition at minute 3. RFU, Relative Fluorescence Units. CFBE Parental – left plot; CFBE WT-CFTR – middle plot; CFBE F508del-CFTR – right plot. (D) Western Blot showing the presence of endogenous EPAC1 in the membrane fraction after 30 min incubation with 1µM 007-AM (or DMSO as control) in CFBE cells. CFTR and TNF-R1 (Tumor Necrosis Factor Receptor 1) were used as PM markers; GAPDH (Glyceraldehyde 3-phosphate dehydrogenase) was used as a cytosol marker. Whole cell lysates (WCL) were analyzed as controls.

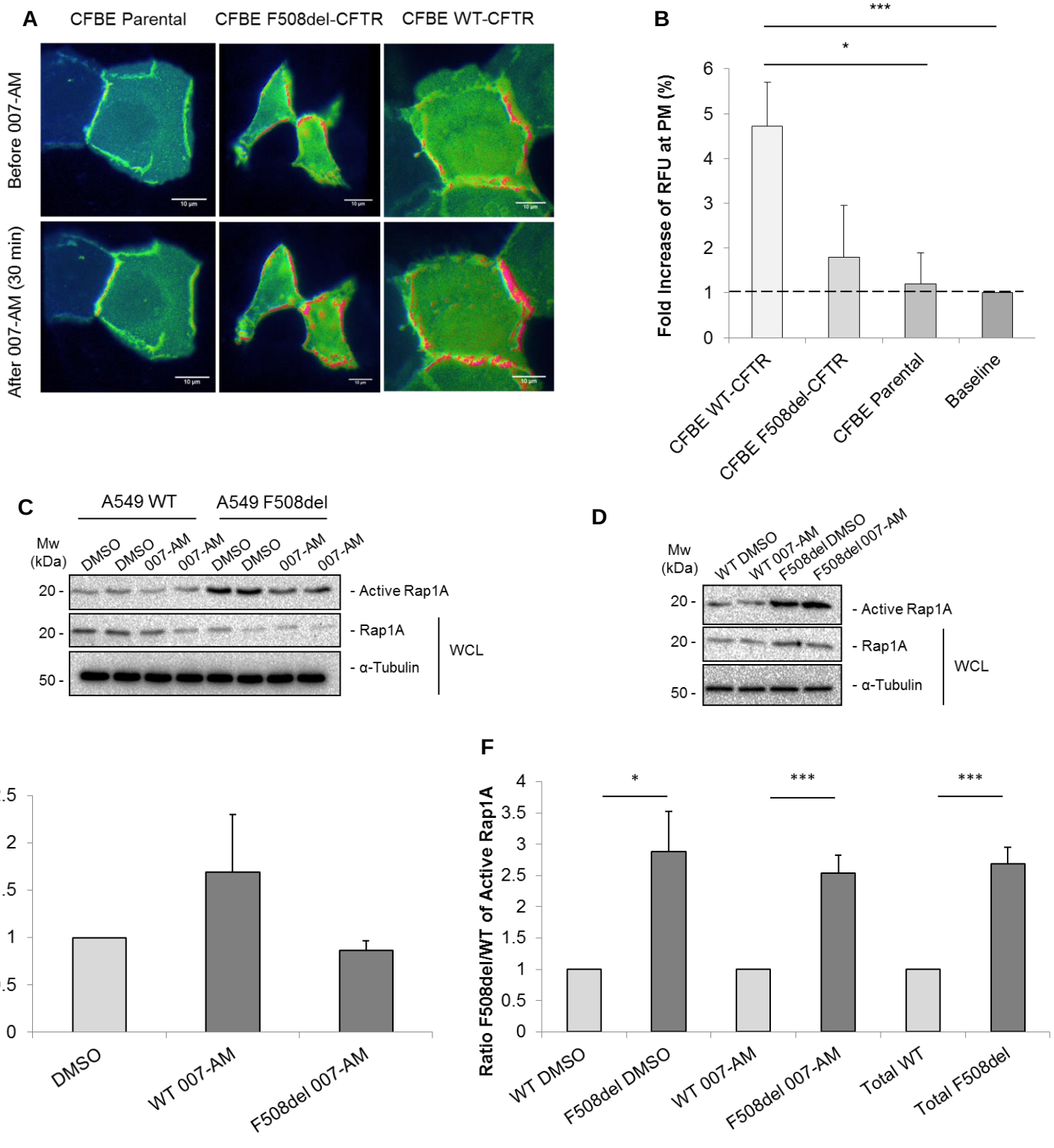
A
CFBE Parental
CFBE F508del-CFTR
CFBE WT-CFTR
Before 007-AM
After 007-AM (30 min)
B
***
*
Fold Increase of RFU at PM (%)
CFBE WT-CFTR
CFBE F508del-CFTR
CFBE Parental
Baseline
C
A549 WT
A549 F508del
Mw (kDa)
DMSO
007-AM
- Active Rap1A
- Rap1A
- α-Tubulin
WCL
D
WT DMSO
WT 007-AM
F508del DMSO
F508del 007-AM
E
Fold Increase active Rap1A
DMSO
WT 007-AM
F508del 007-AM
F
Ratio F508del/WT of Active Rap1A
WT DMSO
F508del DMSO
WT 007-AM
F508del 007-AM
Total WT
Total F508del

The most evident result of *Figure 3.3A* is the fact that there is a higher FRET change at the PM for all cell lines. Theoretically, FRET changes are insensible to the concentration of FRET sensor at a certain region[111]. Thus, this may lead us to conclude that EPAC is mostly active at the PM. However, due to experimental artifacts like spectral overlap between donor and acceptor fluorophores (spectral bleed-through; SBT) this is not what we observe. SBT may refer to: part of the donor emission spectrum that overlaps with acceptor emission (donor SBT); part of the acceptor absorption spectrum that is excited by the donor wavelength (acceptor SBT)[111]. First of all, the PM localization of this FRET sensor can be explained by the fact that this sensor contains the full length of Rap, which has already been reported to localize at the PM due to CAAX motifs at their carboxyl termini that provide sites for lipid modification[112-114]. Thus, higher concentration of Raichu-Rap at the PM may explain the higher FRET signal in this sub-cellular location. However, we can conclude that EPAC is active near the PM but not more active when compared to other cell compartments. To answer this question, it would be useful to use a Raichu-Rap FRET sensor without the PM-target domain (with cytosol localization). FLIM (Fluorescence lifetime imaging), a FRET method based on the fact that molecules doing FRET have shorter fluorescence lifetimes, could have been used because it is not affected by changes in probe concentration. However, this technique was not available at the time.

Figure 3.3: Analysis of EPAC1 activation after treatment with 007-AM. (A) Analysis of Raichu-Rap FRET sensor upon stimulation of CFBE cells with 1µM 007-AM. Intensity-modulated pseudo-color images are shown here. For each cell, only images before and 30 minutes after addition of 007-AM are shown. Scale bars, 10 µm. (B) Summary of all experiments performed in A, showing the fold increase in RFU of the FRET signal at the PM (as a percentage) 30 min after the addition of 007-AM relative to pre-stimulus levels. 'Baseline' represents the value obtained if 007-AM does not induce a FRET change at the PM. Data represent means ± SEM. n = 24-45. (C, D) Western Blot showing the effect of 007-AM treatment upon the fraction of active Rap1A, in A549 or CFBE cells (C and D, respectively). Cells were incubated with 1µM 007-AM for 2h (or DMSO as control). (E) Quantification of fold increase of active Rap1A after treatment with 007-AM for A549 cells expressing WT- or F508del-CFTR. Amount of active Rap1A was normalized to the amount of total Rap1A and shown as fold change relatively to DMSO incubated cells. (F) Quantification of the ratio between active Rap1A in inducible A549 cells expressing F508del-CFTR versus cells expressing WT-CFTR. Data represent means ± SEM. n=3-4. **P*<0.05; ****P*<0.005.

Surprisingly, only CFBE cells stably expressing WT-CFTR show a FRET fold increase at the PM after treatment with 007-AM significantly different from the baseline (*Figure 3.3B*). Moreover, A549 or CFBE cells expressing F508del-CFTR tend to have higher levels of active Rap1A relative to cells expressing WT-CFTR (*Figure 3.3 C, D and F*). 007-AM treatment also seems to induce an increase of active Rap1A in A549 cells expressing WT-CFTR but not in cells expressing F508del-CFTR (*Figure 3.3E*). One possible explanation to these observations is that cells expressing F508del-CFTR (or even cells that do not express CFTR at all) have higher levels of active EPAC (or active EPAC is closer to Rap1A). As a consequence, Rap activation cannot be increased so easily in these cells as in cells expressing WT-CFTR because they already have higher endogenous levels of active Rap.

3.2 Co-localization and interaction between CFTR and EPAC1

To assess the co-localization between CFTR and EPAC1, confocal fluorescence microscopy was used. Hereupon, CFBE parental cells were co-transfected with mCherry-CFTR (WT or F508del) and GFP-EPAC1 and live cell imaging was performed (*Figure 3.4*).

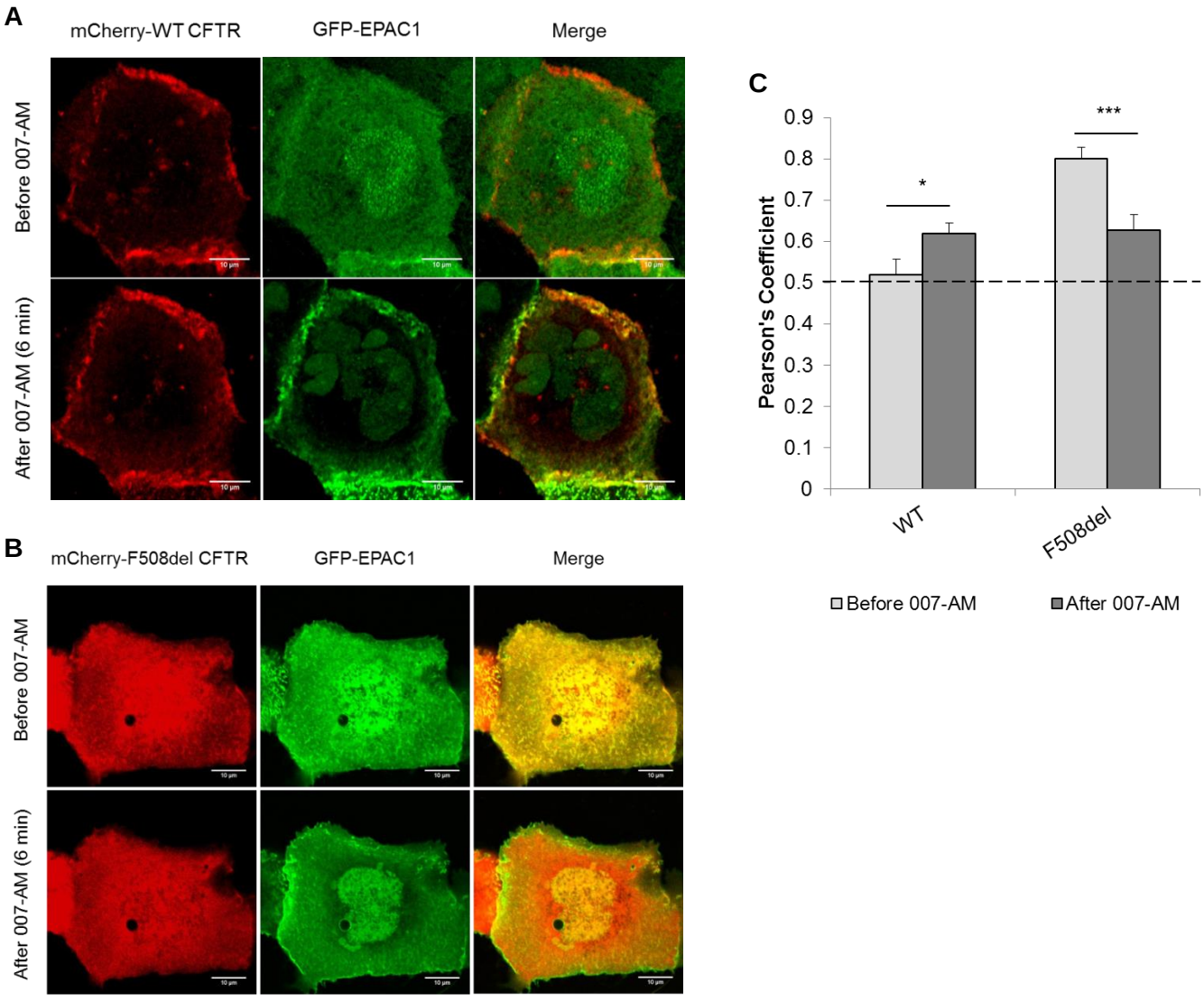

Figure 3.4: Analysis of CFTR and EPAC1 co-localization after treatment with 007-AM in CFBE cells. Confocal live-cell imaging analysis of (A) mCherry-WT-CFTR or (B) mCherry-F508del-CFTR and GFP-EPAC1 in CFBE cells. For each cell, only images before and 6 min after addition of 1µM 007-AM are shown. Scale bars, 10 µm. (C) The bar graph shows the Pearson's Coefficient analysis from A and B. Any value above the dotted line is considered to be significant for co-localization[106]. Data represent means ± SEM. n=9/18 (WT-CFTR/F508del-CFTR). **P*<0.05; ****P*<0.005.

As expected, WT-CFTR localizes at the PM while F508del-CFTR has a dispersed distribution within the cell. EPAC1 localizes in the cytosol, under pre-stimulus conditions, translocating to the PM after being activated with 007-AM, in CFBE cells overexpressing either WT- or F508del-CFTR. Thus, treatment with this cAMP analogue increases co-localization between CFTR and EPAC1 (as assessed by Pearson's Coefficient) in CFBE cells overexpressing WT-CFTR while it decreases this co-localization in CFBE cells overexpressing F508del-CFTR. For all conditions, there is a significant degree of co-localization between CFTR and EPAC1. However, we must not confuse co-localization with physical interaction between proteins – co-localizing proteins may even be nowhere near each other. To prove that mCherry-CFTR and GFP-EPAC1 are close enough to interact, a photobleaching FRET approach (based on the fact that donor emission intensity will increase after acceptor photobleaching) was used because these fluorophores were already reported as a FRET pair[115]. However, no FRET was observed between these proteins (data not shown). One possible explanation is that the fluorophores are in opposite sides in this CFTR-EPAC1 complex, too far to allow energy transfer between them. It can also be explained by the method itself because for acceptor bleaching we need a strong and stable donor but not too bright in order to see any difference after photobleaching the acceptor. Other alternatives would be FLIM or sensitized emission FRET. However, this technique was not available at the time. Therefore, to evaluate the likely interaction between these two proteins, co-immunoprecipitation experiments were performed in CFBE and A549 cells (*Figure 3.5*).

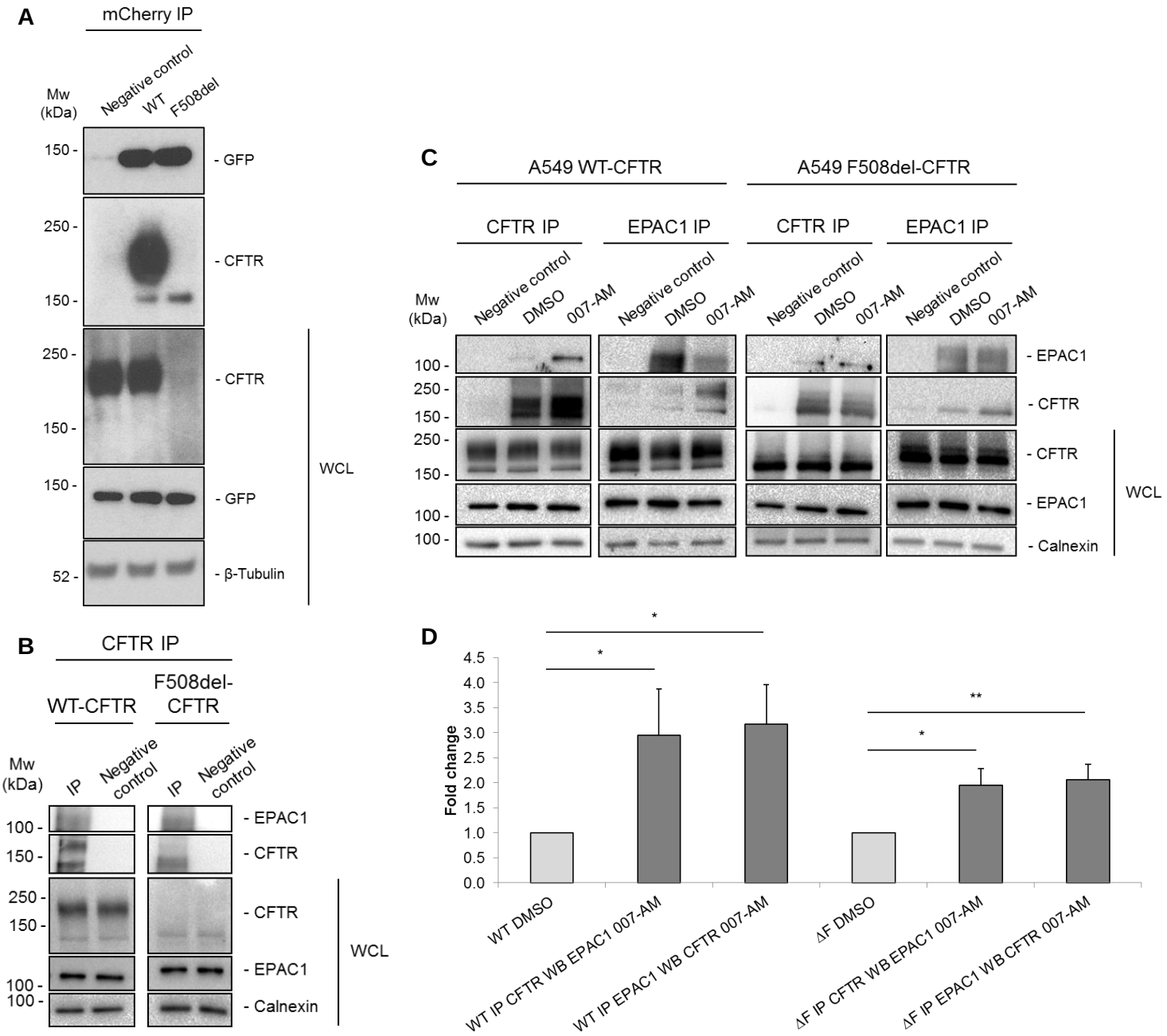

Figure 3.5: Co-immunoprecipitation of CFTR and EPAC1. (A) Co-IP between GFP-EPAC1 and mCherry-WT-CFTR in transfected CFBE parental cells. Pull-down with beads only (without conjugated antibody) was used as a negative control. (B) Co-IP between CFTR and endogenous EPAC1 in CFBE cells stably expressing WT- or F508del-CFTR. (C) Co-IP between CFTR and endogenous EPAC1 in A549 cells overexpressing WT- or F508del-CFTR. Cells were treated with 1μM 007-AM for 2h (or DMSO as control). (D) Quantification of CFTR-EPAC1 interaction fold increase after treatment with 007-AM in A549 cells overexpressing WT- or F508del-CFTR. Amount of precipitated CFTR or EPAC1 was normalized to the amount of immunoprecipitated EPAC1 or CFTR, respectively, and shown as fold change relatively to DMSO incubated cells. Data represent means ± SEM. n=3-5. **P*<0.05; ***P*<0.01.

It was observed that GFP-EPAC1 co-immunoprecipitate with mCherry-WT-CFTR under basal conditions, suggesting that although the degree of co-localization under these conditions was near 0.5, these proteins can still interact with each other. To confirm this result, the same experiment was performed but this time using A549 or CFBE cells expressing WT- or F508del-CFTR. Besides showing that EPAC1 co-immunoprecipitates with WT-CFTR, the same result was observed for F508del-CFTR. This may indicate that EPAC1 can interact with CFTR even if this chloride channel is not at the PM, in early stages of CFTR trafficking. Additionally, incubation with 007-AM seems to promote the interaction between CFTR (WT or F508del) and EPAC1. This suggests that this interaction is promoted when EPAC1 is active. Based on these experiments we cannot conclude if the CFTR is only interacting with active EPAC1. Although an interaction between these proteins is still observed in the absence of 007-AM treatment, we do not know if endogenous levels of cAMP are enough to activate EPAC1 and promote its interaction with CFTR. Nevertheless, it seems that active EPAC1 interacts more easily with CFTR than inactive EPAC1. After being activated, EPAC1 translocates from the cytosol and perinuclear region to the PM vicinity which may facilitate the interaction with CFTR, mainly with WT-CFTR. This may explain the trend that 007-AM promotes more easily the interaction between EPAC1 and WT-CFTR compared to F508del-CFTR. From these experiments, we can also observe that EPAC activation does not affect total protein levels of CFTR and EPAC1, in cells expressing WT- or F508del-CFTR. The band C/band B ratio, indicative of the proportion of CFTR that has been correctly processed, is not affected by 1μM 007-AM 2h treatment. It was also observed that 007-AM treatment does not affect the levels of total CFTR or the band C/band B ratio, relative to DMSO treatment, for 15min, 1, 2, 4, 6, 24 and 48 h incubation period in CFBE cells stably expressing WT- or F508del-CFTR (*data not shown*).

Based on these results, we proposed that CFTR and EPAC1 may interact through a scaffold protein, like Ezrin or NHERF1, the later binding to CFTR PDZ binding domain. This was suggested mainly due to the fact that co-immunoprecipitation between EPAC1 and CFTR was only detected in A549cells when EPAC1 was pulled-down. Although CFTR is a high molecular weight protein, an intermediate protein between EPAC1 and CFTR would help to explain this result, as EPAC has a lower molecular weight when compared to CFTR. In order to test this hypothesis, we used three different approaches: transient transfection of CFBE cells with siRNAs (*Figure 3.6*); Calu3 cells with stable knockdowns

using shRNAs (*Figure 3.7*); generation of a CFTR variant lacking the PDZ binding domain (ΔTRL CFTR) (*Figure 3.8*). Then, co-immunoprecipitation assay was once again used.

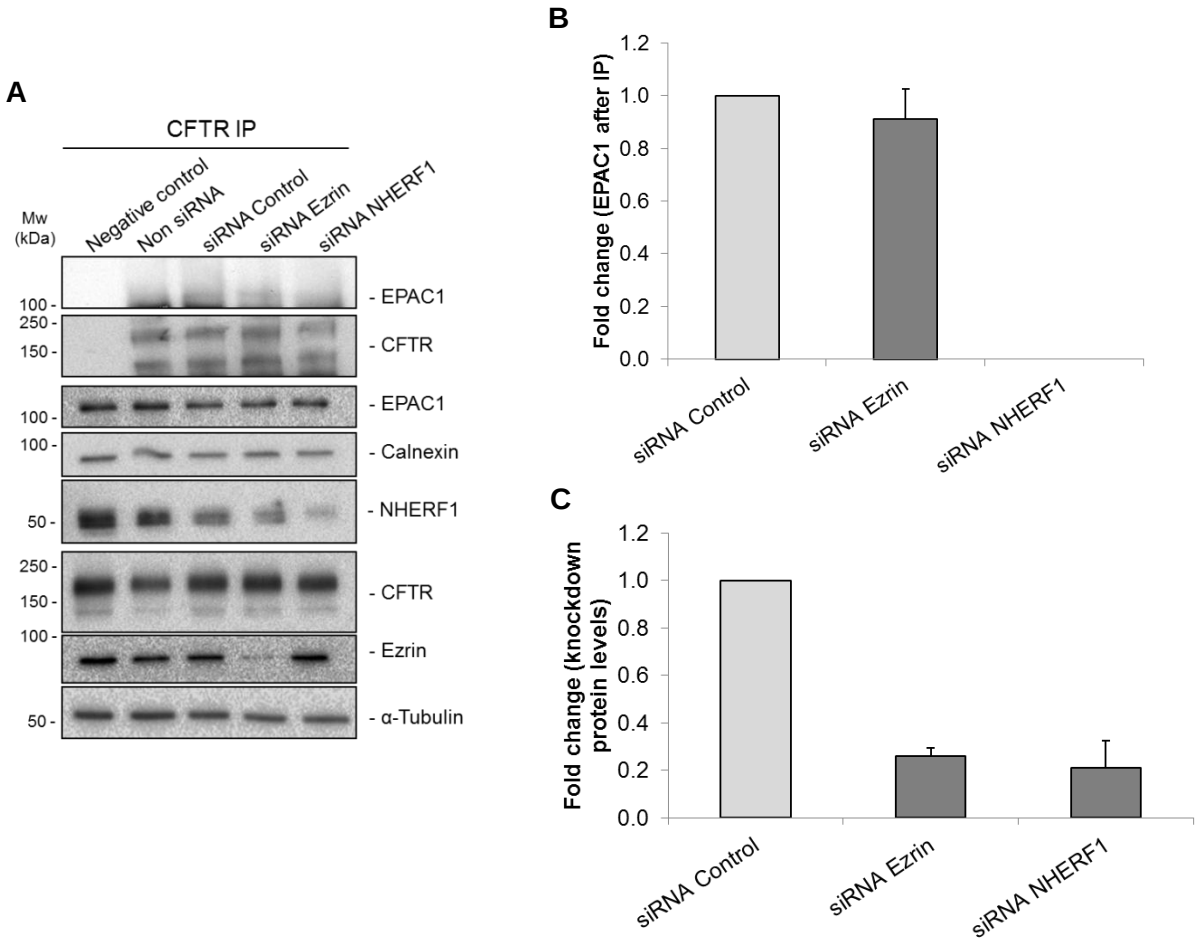

Figure 3.6: Co-immunoprecipitation of CFTR and EPAC1 in CFBE cells transiently transfected with siRNA against ezrin or NHERF1. (A) Co-IP between WT-CFTR and endogenous EPAC1 in CFBE cells stably expressing WT-CFTR. Non-targeting siRNA was used as siRNA control. (B) Amount of precipitated EPAC1 was normalized to the amount of immunoprecipitated CFTR, respectively, and shown as fold change relatively to siRNA control transfected cells. (C) Knockdown efficiency. Quantification of the amount of total Ezrin/NHERF1 under transfection with siRNA (siRNA Ezrin and siRNA NHERF1, respectively), normalized to the amount of α-Tubulin/Calnexin and shown as fold change relatively to siRNA control transfected cells. Data represent means ± SEM. n=3.

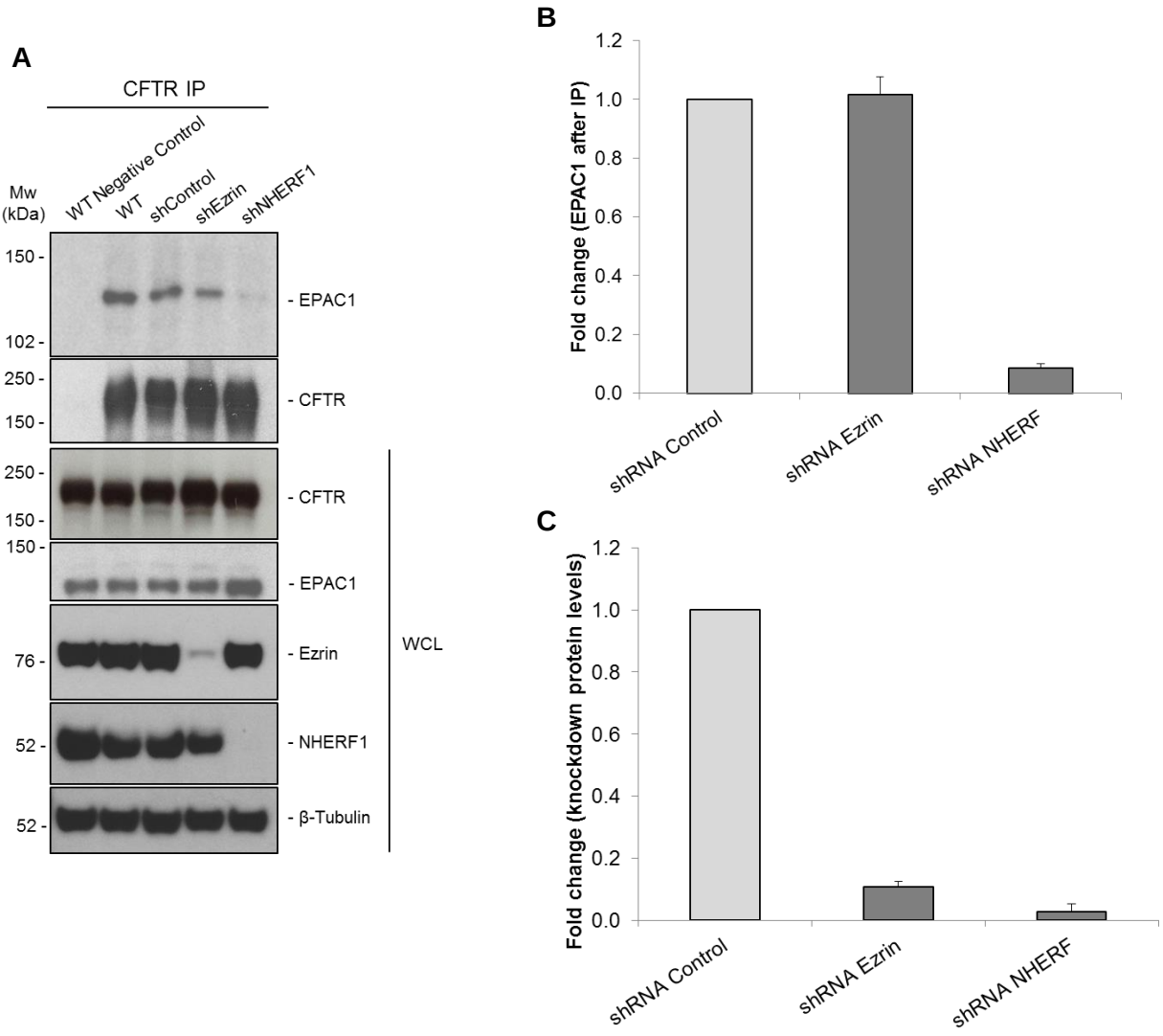

Figure 3.7: Co-immunoprecipitation of CFTR and EPAC1 in Calu3 cells stably transfected with shRNA against ezrin or NHERF1. (A) Co-IP between endogenous WT-CFTR and EPAC1 in Calu3 cells stably transfected with shRNAs. Empty vector control without coding for any shRNA was used as shRNA control. (B) Amount of precipitated EPAC1 was normalized to the amount of immunoprecipitated CFTR, respectively, and shown as fold change relatively to shRNA control transfected cells. (C) Knockdown efficiency. Quantification of the amount of Ezrin or NHERF1 under transfection with shRNA (shEzrin or shNHERF1, respectively) relative to the amount of these proteins when shControl was used. Data represent means ± SEM. n=3.

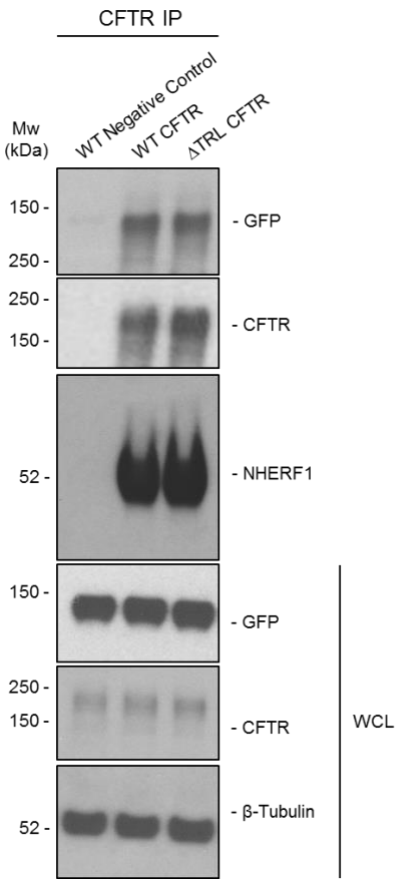

Figure 3.8: Co-immunoprecipitation of GFP-EPAC1 and WT- or ΔTRL-CFTR in CFBE cells. Co-IP between GFP-EPAC1 and WT- or ΔTRL-CFTR in co-transfected CFBE parental cells. Co-IP between CFTR and NHERF1 was also performed to validate CFTR bearing the ΔTRL mutation.

As observed in *Figure 3.6* and *Figure 3.7*, NHERF1, but not Ezrin, knockdown, seems to abolish the interaction between EPAC1 and CFTR. Additionally, in *Figure 3.7*, co-IP between endogenous EPAC1 and endogenous CFTR was performed in Calu3 cells, confirming the interaction between CFTR and EPAC1 (*as previously shown in Figure 3.5*).

It has been already reported that deletion of the TRL residues (1478-1480) in CFTR abolishes the interaction with the scaffolding protein NHERF1[27, 43]. Thus, this mutation should also prevent CFTR-EPAC1 interaction if it is NHERF1-mediated. However, this was not observed. To confirm that ΔTRL-CFTR does not interact with NHERF1, this protein was also detected by Western Blot after CFTR pull-down. As seen in *Figure 3.8*, this mutation did not affect CFTR-NHERF1 interaction. Although ΔTRL-CFTR plasmid was sequenced after being generated to confirm the presence of this mutation, perhaps some mutations occurred during DNA amplification processes. Thus, ΔTRL-CFTR plasmid needs to be re-sequenced to confirm the presence of this mutation. Nevertheless, these three independent experiments that were performed seem to suggest that NHERF1, but not ezrin, mediates EPAC1-CFTR interaction. However, another possible hypothesis is

that NHERF1 may disrupt the sub-cellular localization of EPAC1, thus preventing its interaction with other proteins such as CFTR. To test this idea, fluorescence live-cell imaging was performed in Calu3 cells transfected with GFP-EPAC1 (*Figure 3.9*).

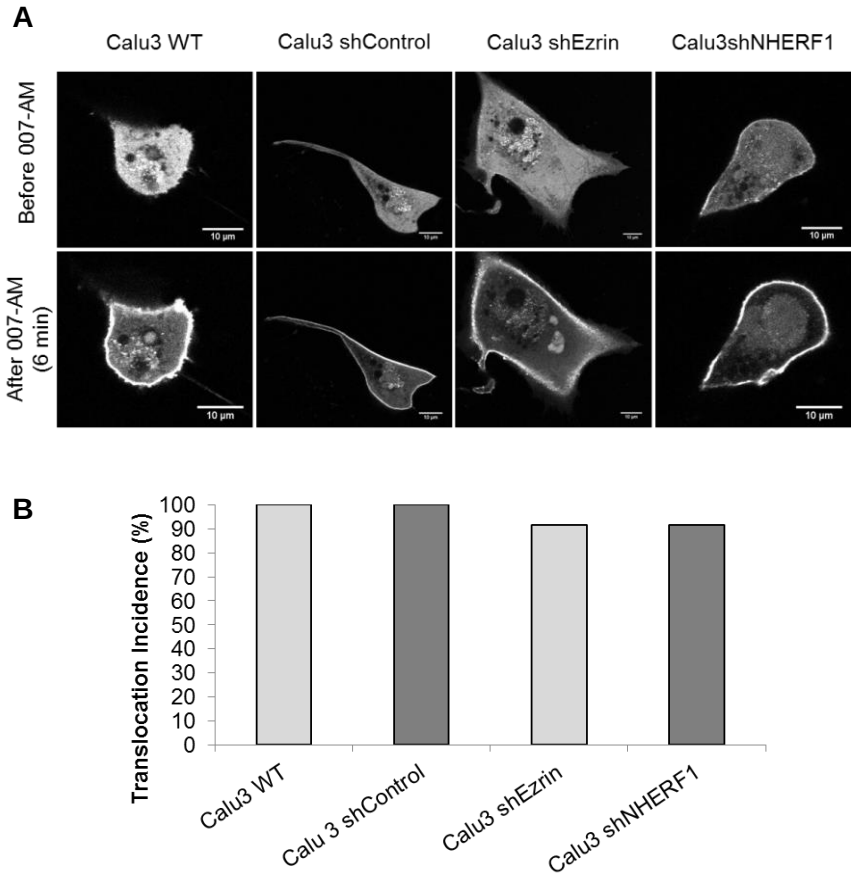

Figure 3.9: Analysis of EPAC1 localization after treatment with 007-AM in Calu3 cells. (A) Confocal live cell imaging analysis of GFP-EPAC1 in Calu3 cells. For each cell, only images before and 6 minutes after addition of 1µM 007-AM are shown. Scale bars, 10 µm. (B) The bar graph shows the percentage of cells showing translocation of EPAC1 to the PM upon 007-AM stimulation[according to 75]. n=9-15.

EPAC1 sub-cellular localization or even its translocation to the PM after 007-AM treatment does not seem to be affected by ezrin or NHERF1 knockdown. This result was already anticipated because it has been already reported that cAMP regulates the binding of EPAC1 directly to phosphatidic acid at the PM[108]. Nevertheless, this observation is in agreement with the hypothesis that EPAC1-CFTR interaction is mediated by NHERF1.

3.3 Effect of EPAC1 on CFTR stability

The next step was to evaluate the effect of EPAC activation/inhibition or EPAC1 knockdown upon the stability of CFTR at the PM. To assess these, cell surface biotinylation and an endocytosis assay for CFTR were performed (*Figure 3.10*).

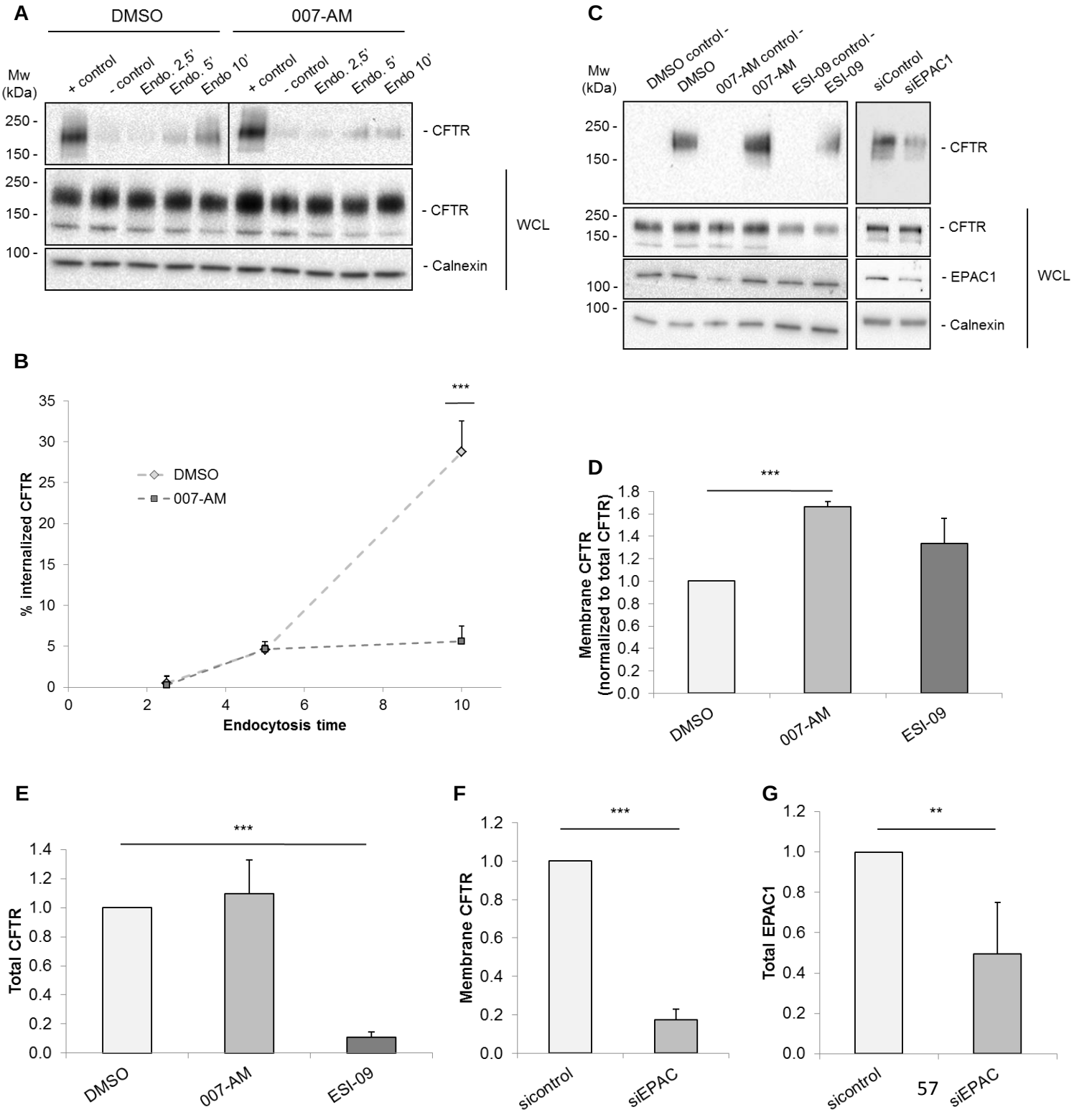

Figure 3.10: CFTR surface expression and endocytosis under EPAC activation. (A) CFBE cells expressing WT-CFTR treated with 1μM 007-AM for 2h (or DMSO as control) were subjected to cell surface protein biotinylation, followed by incubation at 37ºC (during 2.5, 5 or 10 minutes). After that, cells were treated with a GSH solution and, following cell lysis, the obtained extracts were subjected to a streptavidin pull-down (*described in section 2.3.6)*. Samples not treated with GSH were considered as a positive control. Samples not incubated at 37ºC were considered as a negative control. (B) Quantification of the percentage of internalized CFTR. From the amount of endocyted CFTR, - control was subtracted followed by a normalization to the + control. Data represent means ± SEM. n=3. (C) CFBE cells expressing WT-CFTR treated with 1μM 007-AM or 5μM ESI-09 for 2h (or DMSO as control) were subjected to cell surface protein biotinylation. ESI-09 has been reported as a EPAC specific inhibitor. Samples not treated with biotin were considered as a negative control. Additionally, CFBE cells expressing WT-CFTR were also transfected with siRNAs. Non-targeting siRNA was used as siRNA control. (D, F) Quantification of the amount of CFTR at the PM. Amount of CFTR at the PM was normalized to the amount of total CFTR and shown as fold change relatively to DMSO or siRNA control treated cells. Data represent means ± SEM. n=3. (E) Quantification of the amount of total CFTR normalized to the amount of Calnexin and shown as fold change relatively to DMSO incubated cells. Data represent means ± SEM. n=6. (G) Knockdown efficiency. Quantification of the amount of total EPAC1 normalized to the amount of Calnexin shown as fold change relatively to siRNA control. Data represent means ± SEM. n=3. ***P*<0.01; ****P*<0.005.

The endocytosis assay showed that EPAC activation promotes CFTR stability at the PM, decreasing the percentage of internalized CFTR over time (*Figure 3.10A and B*). In agreement with this result, activation of EPAC increased CFTR-PM steady-state levels (*Figure 3.10C*). Additionally, incubation of CFBE cells with ESI-09, an EPAC specific inhibitor[116, 117], seems to decrease PM levels of CFTR, which would complement the previous results. However, when normalized to total CFTR, there is no significant difference between DMSO and ESI-09 treatment because this EPAC inhibitor also decreased the levels of total CFTR. This effect is CFTR-specific as total levels of EPAC1 or calnexin were not affected by this inhibitor. However, it has been already suggested that ESI-09 may act as general protein denaturing agent and does not act on EPAC selectively[118] – an observation that does not explain the absence of effect upon EPAC1 or calnexin levels. However, as CFTR is a large membrane protein that needs scaffolding proteins to be stable at the PM, it may be more affected by this compound than EPAC1 or Calnexin, which are not membrane and probably more stable proteins. Nonetheless,

EPAC1 knockdown using siRNAs decreased the levels of PM CFTR, which is in agreement with the previous experiments (*Figure 3.10C, F and G*). This approach allowed for discrimination between EPAC1 and EPAC2 and confirmed that EPAC-effect on CFTR stability is probably mediated by EPAC1; however, this result does not exclude the involvement of EPAC2 on CFTR regulation. So, all the results from this set of experiments suggest that EPAC1 promotes CFTR stability at the PM.

Nonetheless, the observed effect may result from promotion of CFTR traffic towards the PM or from CFTR increased stability at the PM (decreased endocytosis and/or reduced recycling). Therefore, we used an alternative approach to evaluate the effect of EPAC1 upon CFTR stability. This time, we wondered if EPAC1 overexpression could promote newly synthetized-CFTR stability. For this, CFBE Parental cells were transiently co-transfected with mCherry-WT-CFTR and GFP or GFP-EPAC1 and the levels of CFTR were assessed by WB at specific time points after incubation with cycloheximide (*Figure 3.11*).

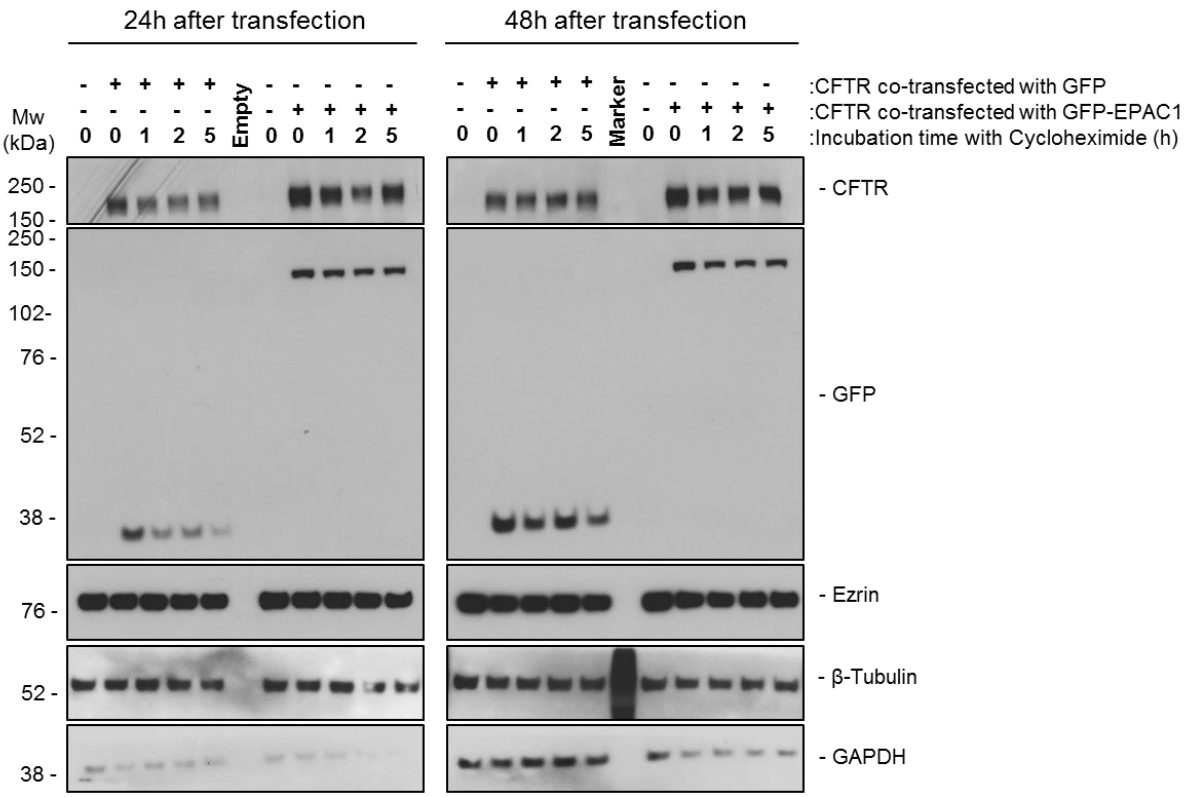

Figure 3.11: Effect of EPAC upon CFTR stability. CFBE Parental cells transiently co-transfected with mCherry-WT-CFTR and GFP or GFP-EPAC1 were treated with 10µg/mL of cycloheximide for 1, 2 or 5h, 24 or 48 h after transfection. Cycloheximide was used as an inhibitor of protein biosynthesis. Cells not transfected with GFP or GFP-EPAC1 were also not transfected with mCherry-WT-CFTR. Because the amount of CFTR used to transfect cells for each condition is of extremely importance, all transfection solutions were prepared starting from the same solution to avoid human error.

Interestingly, GFP-EPAC1 overexpression seems to promote CFTR stability relative to GFP overexpression. This new data complements the previous results, strengthening the hypothesis that EPAC1 may promote CFTR stability at and before reaching the PM. Although we cannot drain any conclusion from this single experiment, overall, EPAC1 appear to effect CFTR stability. Surprisingly, results from quantitative PCR (*data not shown*) seem to indicate lower amount of CFTR transcripts in cells incubated with 007-AM (relative to DMSO). Because this compound does not affect the total protein levels of CFTR, this result may also suggest that EPAC1 activation promotes CFTR stability.

Additionally, we wondered if VX-809-induced rescue of F508del-CFTR can be improved by EPAC activation. To answer this question, a Western Blot methodology was used (*Figure 3.12*).

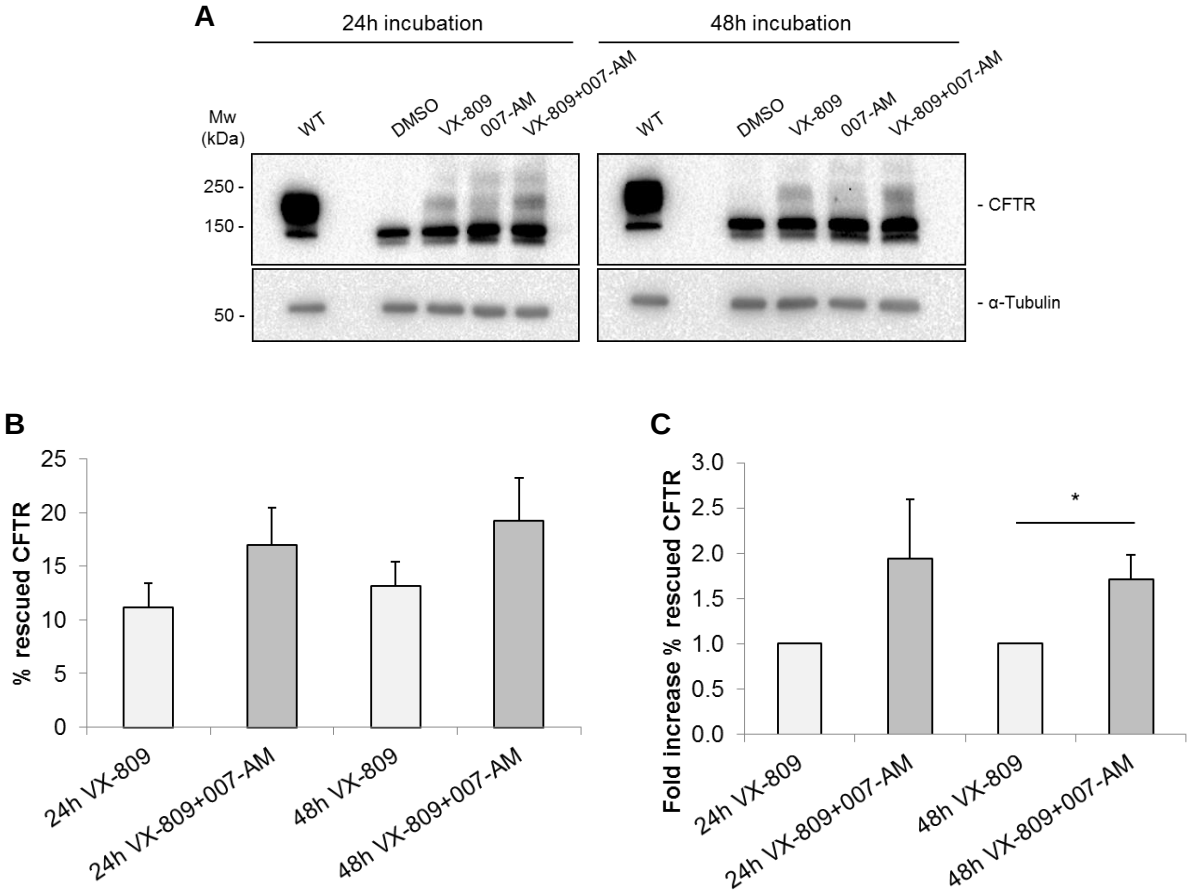

Figure 3.12: Effect of 007-AM upon F508del-CFTR rescue. (A) CFBE cells expressing F508del-CFTR were treated with 1µM 007-AM, 3µM VX-809 (a compound that corrects the trafficking defect of F508del-CFTR; Selleckchem) or both (DMSO was used as a negative control) for 24 or 48h. (B) Quantification of the percentage of rescued CFTR. The amount of band C was normalized to the total amount of CFTR (band C + band B). This ratio obtained was normalized to the WT ratio and the result was express as a percentage. (C) The values obtain from C are shown as a fold increase relatively to VX-809 treated cells. Data represent means ± SEM. n=8-10. **P*<0.05.

The combined effect of VX-809 and 007-AM tends to improve F508del-CFTR rescue relative to VX-809 treatment – suggesting that targeting of CFTR membrane stability through EPAC activation may be an approach to use in combinatorial treatment with the corrector.

3.4 Effect of CFTR upon EPAC-induced cell adhesion

The last goal was to evaluate the effect of CFTR on EPAC-promoted biological function. One of the major biological roles of EPAC is the regulation of cell to cell or cell to matrix adhesion[47]. Thus, we performed a cell adhesion assay to evaluate if the presence of F508del-CFTR could affect this process in comparison to WT-CFTR (*Figure 3.13*).

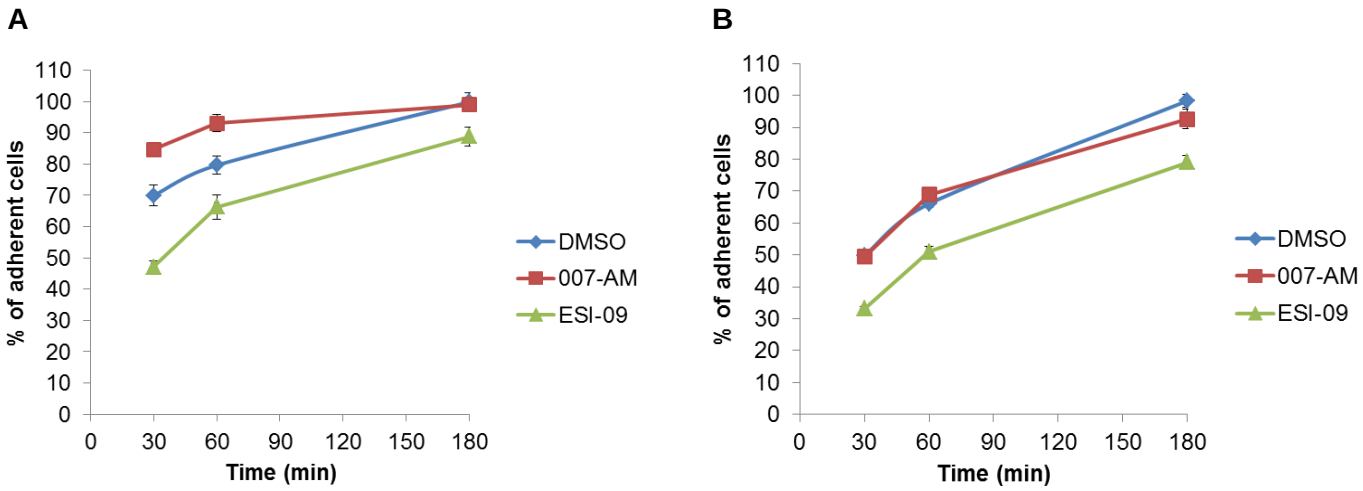

Figure 3.13: Effect of CFTR upon EPAC-induced cell adhesion. CFBE cells expressing (A) WT- or (B) F508del-CFTR were treated with 1µM 007-AM or 5µM ESI-09 (DMSO was used as a control) for 2h. Cells were allowed to attach to a coated surface for 30, 60 or 180 minutes (*described in section 2.5.1*). The results are expressed as percentage of cells that attached to the surface (ratio between I_f after washing/ I_f before washing) over time. Data represent means ± SEM. n=20-30.

As expected, the more time cells had to attach to the surface, higher the percentage of adherent cells. Moreover, CFBE cells expressing F508del-CFTR seem to attach badly to the plate surface comparing to CFBE cells expressing WT-CFTR. Additionally, ESI-09 treatment decreases the percentage of cells that attached to the surface.

The most interesting result was the fact that 007-AM seems to promote cell adhesion in CFBE cells expressing WT-CFTR but not in CFBE cells expressing F508del-CFTR. This suggests that lower amounts of CFTR at the PM somehow abolish the activation of EPAC downstream effectors and consequent promotion of cell adhesion.

Chapter IV

Discussion and Perspectives

4. Discussion and Perspectives

Ion transport through CFTR is stimulated when cAMP levels in the subcortical compartment increase leading to PKA activation, thus triggering CFTR phosphorylation and channel opening. However, PKA is not the only cAMP sensor within the cell. EPAC, an exchange protein directly activated by cAMP, is another more recently discovered cAMP effector[47, 48, 50].

EPAC proteins are mainly known for their function as guanine nucleotide exchange factor for Rap, a small Ras-like GTPase[51]. It has been reported that EPAC is involved in the regulation of cell-to-cell and cell-matrix adhesion, cytoskeleton rearrangements and cell polarization[47, 48, 82, 119]. Interestingly, all these processes are involved in CFTR regulation. Moreover, since cytoskeleton proteins have an important role in tethering CFTR to the plasma membrane, this is a process in which EPAC can affect CFTR steady-state membrane levels. Moreover, Rap signaling has a known role in E-cadherin recycling via Rab11-positive vesicles and CFTR recycling also requires Rab11-containing vesicles[23]. Since CFTR recycling regulates the amount of protein at the plasma membrane, EPAC via Rap may also regulate this process. Additionally, EPAC1, an EPAC isoform, shifts to the plasma membrane in response to a cAMP-induced conformational change[74]. EPAC1 is activated by stimuli that result in increased subcortical cAMP, the same stimuli that induce PKA-mediated activation of CFTR. This makes plausible that activation of both CFTR and EPAC might be spatially and temporally coincident. All this data supports the hypothesis that EPAC1 has a potential effect on CFTR trafficking and PM anchoring. However, the possible connection between these proteins has never been studied.

Thus, this work was based on the hypothesis that EPAC1, the only EPAC isoform whose conformation and translocation are cAMP-dependent, could be a new link between this second messenger and CFTR regulation. Therefore, the aim of the present work was to study the interaction between CFTR and EPAC1 and to evaluate the impact of this cAMP effector on CFTR biogenesis, trafficking and PM anchoring.

4.1 Effect of 007-AM treatment on EPAC1

The first objective was to evaluate the effect of the compound 007-AM treatment on EPAC tertiary structure, sub-cellular localization and activity. This allows confirmation of this compound as an EPAC specific agonist. This and the following studies were performed mainly in CFBE cells to better mimic the processes that occur in the bronchial epithelium of CF patients with F508del mutation. Adenocarcinoma cells, such as Calu3 and A549 cells, were also used, as they are also good cell models to study the airways.

FRET analysis of cAMP levels and PKA activity, using camp or AKAR4 FRET sensors, respectively, showed a high percentage of FRET change for camps compared to the small FRET change observed for AKAR4, after adding 007-AM. This confirmed 007-AM as an EPAC specific agonist and validated the concentration of this compound used for this work (1µM). EPAC1 translocation to the plasma membrane after 007-AM treatment was observed in CFBE cells and found to be independent of CFTR, as assessed by confocal fluorescence microscopy. This was already expected since EPAC translocates to the PM by a phosphatydic acid- or ERM proteins-dependent way[75, 76]. However, this does not exclude a possible interaction between EPAC1 and CFTR. Instead, EPAC1 cellular distribution suggests that this protein and CFTR may co-localize or even interact with each other, mainly under 007-AM treatment as EPAC1 is relocated to the PM.

Additionally, activity of endogenous EPAC was studied using Raichu-Rap FRET sensor and a pull-down based Rap activity assay. Interestingly, only cells expressing WT-CFTR showed a FRET fold increase at the PM after treatment with 007-AM, while cells expressing F508del-CFTR tend to have higher levels of active Rap1A. 007-AM treatment also leads to an increase the levels of active Rap1A in cells expressing WT-CFTR but not in cells expressing F508del-CFTR. One possible explanation for these observations is that cells expressing F508del-CFTR (and probably cells that do not express CFTR) have higher levels of active EPAC or alternatively active EPAC is closer to Rap1A. Consequently, Rap activation cannot be increased so easily in these cells as in cells expressing WT-CFTR, since they already have higher endogenous levels of active Rap. This may suggest that EPAC-Rap pathway is not able somehow to exert its function and, in order to try to compensate and overcome this situation, a negative feedback loop promotes EPAC activation in cells expressing F508del-CFTR.

Following this idea, it would be interesting to follow this pathway and see if there are any proteins or even transcription factors downstream EPAC differentially regulated/expressed in cells expressing WT- or F508del-CFTR. Ideally, a protein whose regulation is affected by the presence of CFTR at the PM would be identified.

4.2 Co-localization and interaction between CFTR and EPAC1

EPAC1 co-localizes with both WT- or F508del-CFTR, in CFBE cells without stimulus or under 007-AM treatment. Additionally, these proteins co-immunoprecipitate in CFBE, A549 and Calu3 cells. The fact that EPAC1 interaction is also detected with F508del-CFTR suggests that this interaction may occur at the early stages of CFTR trafficking, when this chloride channel is not at the PM. However, it remains to be further clarified at which phase of CFTR trafficking these proteins interact. Co-IP after cell fractionation was performed but the output was inconclusive. Moreover, EPAC activation promotes CFTR-EPAC1 interaction, which suggests that this interaction is promoted when EPAC1 is active. However, it remains to be elucidated if inactive EPAC1 can interact with CFTR. Although without 007-AM treatment co-IP between these proteins is achieved, endogenous levels of cAMP may be enough to activate EPAC and promote its interaction with CFTR – even if EPAC1 is not clearly at the PM under basal conditions in CFBE or Calu3 cells, as detected by confocal fluorescence microscopy. To address this question, the same experiments could have been performed in the presence of indomethacin (depleting endogenous cAMP levels). Nevertheless, it seems that active EPAC1 interacts more easily with CFTR than inactive EPAC1.

This increased interaction under EPAC activation may result from different molecular events:

- EPAC1 suffers a conformational change;
- EPAC1 translocates to the PM;
- EPAC1 becomes catalytically active (or combination of several options).

This question can be assessed by using EPAC1 mutants without the DEP domain (required for cAMP-induced translocation of EPAC1), mutated in the CNB (cyclic nucleotide–binding) domain (to prevent cAMP-induced conformation change) or catalytically dead mutants (mutated in the catalytic region).

After being activated, EPAC1 translocates from the cytosol and perinuclear region to the PM vicinity, which may facilitate the interaction with CFTR, mainly with WT-CFTR. This may explain why 007-AM promote more easily the interaction between EPAC1 and WT-CFTR compared to EPAC1 and F508del-CFTR. Moreover, EPAC activation does not affect the band C/band B ratio, indicative of the proportion of CFTR that has been correctly processed, suggesting that EPAC is not involved in the early stages of CFTR biogenesis, such as folding and processing of this chloride channel.

On the other hand, NHERF1, but not ezrin, knockdown (through siRNA or shRNA transfection) prevented CFTR-EPAC1 interaction without disrupting EPAC1 sub-cellular localization. Thus, EPAC1 may interact with CFTR through the NHERF1 mediator. This is somehow expected as NHERF1 is a protein adapter highly expressed in epithelial tissues with the ability to bring together membrane and non-membrane proteins to regulate cell metabolism and growth[120]. However, to confirm this result, co-IP between EPAC1 and ΔTRL-CFTR needs to be redone after confirming the sequence of this plasmid. Additionally, the role of the structurally related protein E3KARP (NHE3 kinase A regulatory protein or NHERF2) in CFTR-EPAC1 interaction remains to be clarified, since both NHERFs have already been reported to interact with CFTR[120]. This could be done using the same approach used for NHERF1. Based on our results, it is likely that EPAC1 physically interacts with NHERF1, although EPAC1-NHERF1 interaction has not been shown yet. This needs to be assessed in the near future.

Both NHERF1 and NHERF2 have two PDZ domains and both bind to CFTR[27, 121]. It has also been suggested that ezrin can positively regulate the cooperative binding of NHERF to C-terminus of CFTR. As a result of ezrin binding, a specific ternary complex $(CFTR)_2$-NHERF-Ezrin of 2:1:1 stoichiometry is formed, in which two CFTR molecules are anchored to NHERF[122]. Moreover, it would also be interesting to see which NHERF1 domain is involved in EPAC1-CFTR interaction. This could be tested using GST fusion proteins, with each PDZ domain of NHERF1, immobilized on glutathione-agarose beads, as has been already reported[121], or using NHERF1 mutated in its PDZ domains. Nevertheless, one possibility is that NHERF1 interacts simultaneously with CFTR and EPAC1, through its PDZ domains, and with ezrin through its carboxyl terminus (the later may also tether PKA). The generation of a macromolecular complex also involving cytoskeleton proteins may play a key role in fine-tuning the regulation of CFTR stability and function, as has been suggested[123].

EPAC1 or EPAC2 (UniProtKB accession numbers O95398 and Q8WZA2, respectively) do not contain a PDZ domain within their sequence, supporting the need of an adaptor protein between CFTR and EPAC1, since EPAC probably cannot bind directly to CFTR C-terminus[124]. Nevertheless, several hits were identified for both EPACs accordingly to the consensus sequence of the PDZ binding domain (C-terminal X-[S/T]-X-[V/I/L])[24], as assessed by ScanProsite tool[125]. However, a more stringent consensus sequence of PDZ binding domain has been published: [S/T]-[R/Y]-L-COOH for NHERF PDZ1 domain and S-[S/T]-W-L-COOH for NHERF PDZ2 domain[25]. Using PDZ1 consensus sequence, we identified 3/2 hits for EPAC1/EPAC2, while using PDZ2 consensus sequence no hit was identified (*Table 4.1*). Interestingly, only EPAC1 has a putative PDZ1 binding domain (residues SRL) at its C-terminus. To validate these hypotheses, EPAC mutants could be generated and tested by co-IP with CFTR. Nonetheless, this is in agreement with the previous hypothesis of a macromolecular complex involving CFTR, NHERF1, Ezrin, PKA and EPAC1.

Without ezrin, the PDZ2 domain of NHERF is inhibited. Binding of ezrin to NHERF promotes a conformational change exposing the PDZ2 domain[126]. If binding of EPAC1 to NHERF was PDZ2 mediated, ezrin knockdown would abolish this interaction - however, this is not what we observe. Thus, this suggests that the interaction between EPAC1 and NHERF may be mediated by PDZ1 domain (*Figure 4.1*).

Table 4.1: Hits for PDZ1 consensus sequence on EPAC1 and EPAC2 sequences.

Proteins (length)	Residues	Position
EPAC1 (923)	TRL	501-503
	SRL	767-769
	SRL	915-917
EPAC2 (1011)	TRL	36-38
	SRL	876-878

4.3 Effect of EPAC1 on CFTR stability

The endocytosis assay showed that EPAC activation promotes CFTR stability at the PM, decreasing the amount of internalized CFTR over time. Moreover, 007-AM treatment increased CFTR-PM steady-state levels while EPAC1 knockdown by siRNA decreased these levels. This approach allowed for discrimination between EPAC1 and EPAC2 and confirmed that EPAC-effect on CFTR stability is probably mediated by EPAC1. However, this result does not exclude the involvement of EPAC2 on CFTR regulation. To assess this question, an EPAC2 specific inhibitor, such as ESI-05 or ESI-07, could be used for the biotinylation or endocytosis assay[118, 127]. Nevertheless, interaction of EPAC1 with CFTR promotes the stability of this chloride channel at the PM.

GFP-EPAC1 overexpression seems to promote CFTR stability relative to GFP overexpression. Additionally, combined effect of VX-809 and 007-AM tends to improve F508del-CFTR rescue relative to VX-809 treatment. Altogether, these results enforce the hypothesis that EPAC1 promotes CFTR stability at and before reaching the PM, and also suggest that modulation of the EPAC pathway may be followed as an additional strategy for the functional correction of F508del-CFTR.

Results from quantitative PCR show a reduced amount of CFTR transcripts in cells incubated with 007-AM (relative to DMSO). Because this compound does not affect the total protein levels of CFTR, this result may also suggest that EPAC1 activation promotes CFTR stability. However, we do not know yet if this is a result of an EPAC1 downstream effector or of EPAC1 protein itself. To test this, a catalytically dead EPAC1 mutant can be used. It would be also interesting to use a pulse-chase approach to evaluate the impact of EPAC1 on CFTR trafficking to the PM.

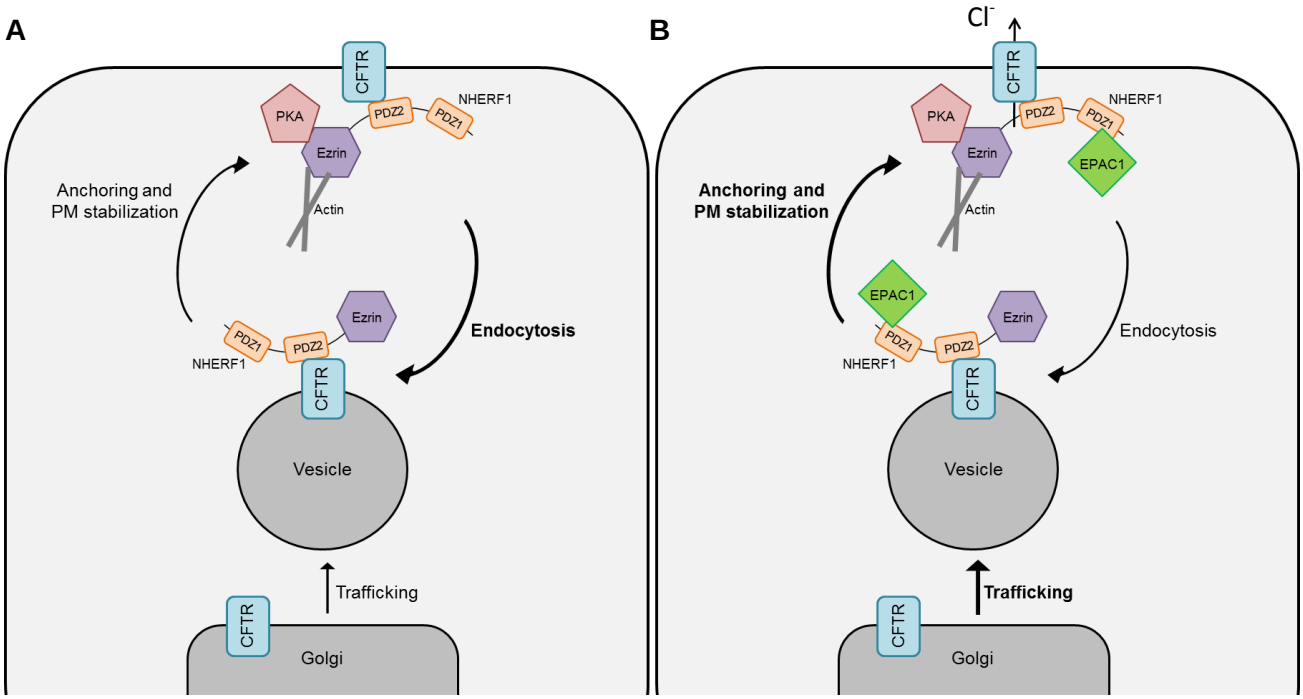

Figure 4.1: Model of CFTR-EPAC1 interaction. Binding of CFTR to NHERF1 anchors the channel (via Ezrin) to the actin cytoskeleton. In cells with low levels of cAMP (A), EPAC1 is inactive and its interaction with CFTR is not promoted. In cells with high levels of cAMP (B), both PKA and EPAC1 are active, promoting the opening of the channel and stabilizing CFTR at the PM, respectively. PDZ - PSD95, Dlg1, ZO-1 binding motif.

4.4 Effect of CFTR upon EPAC-induced cell adhesion

The cell adhesion assay showed that CFBE cells expressing F508del-CFTR seem to attach less to the plate surface comparing to CFBE cells expressing WT-CFTR. Moreover 007-AM promotes cell adhesion in CFBE cells expressing WT-CFTR but not in CFBE cells expressing F508del-CFTR. This suggests that lower amounts of CFTR at the PM somehow abolish the activation of EPAC downstream effectors and consequent promotion of cell adhesion. However, the mechanism or pathway responsible for this observation is still unknown. Nevertheless, this result corroborates the hypothesis (*section 4.1*) that, in cells expressing F508del-CFTR, EPAC-Rap pathway is not able to exert its function and, in order to try to compensate and overcome this problem, a negative feedback loop promotes EPAC activation. It would be of major interest to perform more experiments to confirm and understand how CFTR can affect EPAC, as these results suggest.

Despite the recent advances in the CF field, there are still major aspects of its traffic/activation which remain to be solved and key intervenients in these processes which remain unidentified. The present work unveiled a new relationship between CFTR and the cAMP effector EPAC1.

In summary, here we confirmed 007-AM as an EPAC specific agonist that induces a conformational change and translocation of EPAC1 to the PM. Unexpectedly, cells expressing F508del-CFTR seem to have higher levels of active EPAC and Rap1A. On the other hand, EPAC1 and CFTR co-localize and physically interact through the protein adaptor NHERF1. Finally, EPAC activation promotes this interaction and CFTR stability. Thus, this work constitutes an important characterization of a new CFTR interacting protein that links cAMP signaling to Cystic Fibrosis modulation in a previously unreported mechanism.

4.5 Future Perspectives

The results obtained suggest a deeper characterization of the cross-talk between CFTR and EPAC. To better understand the mechanism underneath this relationship, the regulatory pathways already known for both proteins and common points need to be further studied, in order to establish new experimental procedures that will also help to clarify some of the results observed.

Besides all the future studies already suggested (*section 3 and 4*), several experiments remain to be performed. It would be interesting to evaluate if EPAC2 also interacts with CFTR and to study the impact of EPAC2 on CFTR stability, using the same approaches that have been used. For this, siRNA against EPAC2, specific inhibitors (such as ESI-05) or activators (such as sulfonylurea) would be of great interest.

To reinforce that all the results observed are a result of the impact of EPAC on CFTR stability, a PKA specific agonist can be also used as a control.

Cell polarization is characterized by a selective distribution of membrane proteins among the apical and basolateral sides – CFTR trafficking to the PM is dependent on the cell polarization state[85, 86]. Thus, confocal fluorescence microscopy and co-IP assays to evaluate EPAC1 and CFTR co-localization or physical interaction could be performed in polarized CFBE cells or even in freshly isolated bronchial/tracheal/nasal epithelial primary cells. This more biological relevant model would add a new layer of complexity since this relationship may also be dependent on cellular polarization.

It has been shown that EPAC is involved in cAMP-stimulated Cl^- secretion but not through CFTR[128]. Nonetheless, it would be interesting to complement our results to evaluate the impact of EPAC on CFTR function using electrophysiological approaches such as iodide efflux assays, Ussing chamber or Patch Clamp experiments.

Additionally, generation of new cell systems with inducible EPAC1 and EPAC2 expression would allow a more detailed characterization of EPAC impact on CFTR stability and function.

Finally, electron microscopy combined with fluorescence microscopy using EPAC tagged with APEX (a tag based on Horseradish peroxidase) and a fluorophore could be used to better evaluate EPAC localization before and after 007-AM stimulus in polarized cells[129].

References

1. Collins FS. Cystic fibrosis: molecular biology and therapeutic implications. *Science*. 1992 May 8; 256(5058):774-9.
2. Amaral MD, Kunzelmann K. Molecular targeting of CFTR as a therapeutic approach to cystic fibrosis. *Trends Pharmacol Sci*. 2007 Jul; 28(7):334-41.
3. Rowe SM, Miller S, Sorscher EJ. Cystic fibrosis. *N Engl J Med*. 2005 May 12; 352(19):1992-2001.
4. Riordan JR, Rommens JM, Kerem B, Alon N, Rozmahel R, Grzelczak Z, Zielenski J, Lok S, Plavsic N, Chou JL, et al. Identification of the cystic fibrosis gene: cloning and characterization of complementary DNA. *Science*. 1989 Sep 8; 245(4922):1066-73.
5. Zielenski J. Genotype and phenotype in cystic fibrosis. *Respiration*. 2000; 67(2):117-33.
6. "Cystic Fibrosis Mutation Database." Available: http://www.genet.sickkids.on.ca/app
7. Kerem E. Pharmacological induction of CFTR function in patients with cystic fibrosis: mutation-specific therapy. *Pediatr Pulmonol*. 2005 Sep; 40(3):183-96.
8. Mall MA, Hartl D. CFTR: cystic fibrosis and beyond. *Eur Respir J*. 2014 Jun 12.
9. "Cystic Fibrosis Foundation: Drug Development Pipeline." Available: http://www.cff.org/research/drugdevelopmentpipeline/.
10. Farinha CM1, Matos P, Amaral MD. Control of cystic fibrosis transmembrane conductance regulator membrane trafficking: not just from the endoplasmic reticulum to the Golgi. *FEBS J*. 2013 Sep; 280(18):4396-406.
11. Hwang TC, Sheppard DN. Gating of the CFTR Cl- channel by ATP-driven nucleotide-binding domain dimerisation. *J Physiol*. 2009 May 15; 587(Pt 10):2151-61.
12. Sheppard DN, Welsh MJ. Structure and function of the CFTR chloride channel. *Physiol Rev*. 1999 Jan; 79(1 Suppl):S23-45.
13. Bozoky Z, Krzeminski M, Chong PA, Forman-Kay JD. Structural changes of CFTR R region upon phosphorylation: a plastic platform for intramolecular and intermolecular interactions. *FEBS J*. 2013 Sep; 280(18):4407-16.
14. Kunzelmann K, Mehta A. CFTR: a hub for kinases and crosstalk of cAMP and Ca2+. *FEBS J*. 2013 Sep; 280(18):4417-29.
15. Lukacs GL, Verkman AS. CFTR: folding, misfolding and correcting the ΔF508 conformational defect. *Trends Mol Med*. 2012 Feb; 18(2):81-91.
16. Kopito RR. Biosynthesis and degradation of CFTR. *Physiol Rev*. 1999 Jan; 79(1 Suppl):S167-73.
17. Kim SJ, Skach WR. Mechanisms of CFTR Folding at the Endoplasmic Reticulum. *Front Pharmacol*. 2012 Dec 13; 3:201.
18. Amaral MD. CFTR and chaperones: processing and degradation. *J Mol Neurosci*. 2004; 23(1-2):41-8.

19. Glozman R, Okiyoneda T, Mulvihill CM, Rini JM, Barriere H, Lukacs GL. N-glycans are direct determinants of CFTR folding and stability in secretory and endocytic membrane traffic. *J Cell Biol*. 2009 Mar 23; 184(6):847-62.
20. Gee HY, Noh SH, Tang BL, Kim KH, Lee MG. Rescue of ΔF508-CFTR trafficking via a GRASP-dependent unconventional secretion pathway. *Cell*. 2011 Sep 2; 146(5):746-60.
21. Swiatecka-Urban A, Talebian L, Kanno E, Moreau-Marquis S, Coutermarsh B, Hansen K, Karlson KH, Barnaby R, Cheney RE, Langford GM, Fukuda M, Stanton BA. Myosin Vb is required for trafficking of the cystic fibrosis transmembrane conductance regulator in Rab11a-specific apical recycling endosomes in polarized human airway epithelial cells. *J Biol Chem*. 2007 Aug 10; 282(32):23725-36.
22. Gentzsch M, Chang XB, Cui L, Wu Y, Ozols VV, Choudhury A, Pagano RE, Riordan JR. Endocytic trafficking routes of wild type and DeltaF508 cystic fibrosis transmembrane conductance regulator. *Mol Biol Cell*. 2004 Jun; 15(6):2684-96.
23. Ameen N, Silvis M, Bradbury NA. Endocytic trafficking of CFTR in health and disease. *J Cyst Fibros*. 2007 Jan; 6(1):1-14.
24. Haggie PM, Kim JK, Lukacs GL, Verkman AS. Tracking of quantum dot-labeled CFTR shows near immobilization by C-terminal PDZ interactions. *Mol Biol Cell*. 2006 Dec; 17(12):4937-45.
25. Wang S, Raab RW, Schatz PJ, Guggino WB, Li M. Peptide binding consensus of the NHE-RF-PDZ1 domain matches the C-terminal sequence of cystic fibrosis transmembrane conductance regulator (CFTR). *FEBS Lett*. 1998 May 1; 427(1):103-8.
26. Guggino WB, Stanton BA. New insights into cystic fibrosis: molecular switches that regulate CFTR. *Nat Rev Mol Cell Biol*. 2006 Jun; 7(6):426-36.
27. Short DB, Trotter KW, Reczek D, Kreda SM, Bretscher A, Boucher RC, Stutts MJ, Milgram SL. An apical PDZ protein anchors the cystic fibrosis transmembrane conductance regulator to the cytoskeleton. *J Biol Chem*. 1998 Jul 31; 273(31):19797-801.
28. Hall RA, Ostedgaard LS, Premont RT, Blitzer JT, Rahman N, Welsh MJ, Lefkowitz RJ. A C-terminal motif found in the beta2-adrenergic receptor, P2Y1 receptor and cystic fibrosis transmembrane conductance regulator determines binding to the Na+/H+ exchanger regulatory factor family of PDZ proteins. *Proc Natl Acad Sci U S A*. 1998 Jul 21; 95(15):8496-501.
29. Ridley AJ. Rho GTPases and actin dynamics in membrane protrusions and vesicle trafficking. *Trends Cell Biol*. 2006 Oct; 16(10):522-9.
30. Moniz S, Sousa M, Moraes BJ, Mendes AI, Palma M, Barreto C, Fragata JI, Amaral MD, Matos P. HGF stimulation of Rac1 signaling enhances pharmacological correction of the most prevalent cystic fibrosis mutant F508del-CFTR. *ACS Chem Biol*. 2013 Feb 15; 8(2):432-42.

31. Favia M, Guerra L, Fanelli T, Cardone RA, Monterisi S, Di Sole F, Castellani S, Chen M, Seidler U, Reshkin SJ, Conese M, Casavola V. Na+/H+ exchanger regulatory factor 1 overexpression-dependent increase of cytoskeleton organization is fundamental in the rescue of F508del cystic fibrosis transmembrane conductance regulator in human airway CFBE41o- cells. *Mol Biol Cell*. 2010 Jan 1; 21(1):73-86.
32. Hug MJ, Tamada T, Bridges RJ. CFTR and bicarbonate secretion by [correction of to] epithelial cells. *News Physiol Sci*. 2003 Feb; 18:38-42.
33. Kim D, Steward MC. The role of CFTR in bicarbonate secretion by pancreatic duct and airway epithelia. *J Med Invest*. 2009; 56 Suppl:336-42.
34. Hudson VM. Rethinking cystic fibrosis pathology: the critical role of abnormal reduced glutathione (GSH) transport caused by CFTR mutation. *Free Radic Biol Med*. 2001 Jun 15; 30(12):1440-61.
35. Kogan I, Ramjeesingh M, Li C, Kidd JF, Wang Y, Leslie EM, Cole SP, Bear CE. CFTR directly mediates nucleotide-regulated glutathione flux. *EMBO J*. 2003 May 1; 22(9):1981-9.
36. Schreiber R, Nitschke R, Greger R, Kunzelmann K. The cystic fibrosis transmembrane conductance regulator activates aquaporin 3 in airway epithelial cells. *J Biol Chem*. 1999 Apr 23; 274(17):11811-6.
37. Reddy MM, Light MJ, Quinton PM. Activation of the epithelial Na+ channel (ENaC) requires CFTR Cl- channel function. *Nature*. 1999 Nov 18; 402(6759):301-4.
38. Kunzelmann K, Schreiber R. CFTR, a regulator of channels. *J Membr Biol*. 1999 Mar 1; 168(1):1-8.
39. Kunzelmann K, Mall M, Briel M, Hipper A, Nitschke R, Ricken S, Greger R. The cystic fibrosis transmembrane conductance regulator attenuates the endogenous Ca2+ activated Cl- conductance of Xenopus oocytes. *Pflugers Arch*. 1997 Dec; 435(1):178-81.
40. Amaral MD, Farinha CM. Novel therapeutic approaches addressing the basic defect in cystic fibrosis. *Hospital Pharmacy Europe*. 2013; pp. 55–57.
41. Monterisi S, Favia M, Guerra L, Cardone RA, Marzulli D, Reshkin SJ, Casavola V, Zaccolo M. CFTR regulation in human airway epithelial cells requires integrity of the actin cytoskeleton and compartmentalized cAMP and PKA activity. *J Cell Sci*. 2012 Mar 1; 125(Pt 5):1106-17.
42. Sun F, Hug MJ, Lewarchik CM, Yun CH, Bradbury NA, Frizzell RA. E3KARP mediates the association of ezrin and protein kinase A with the cystic fibrosis transmembrane conductance regulator in airway cells. *J Biol Chem*. 2000 Sep 22; 275(38):29539-46.
43. Moyer BD, Duhaime M, Shaw C, Denton J, Reynolds D, Karlson KH, Pfeiffer J, Wang S, Mickle JE, Milewski M, Cutting GR, Guggino WB, Li M, Stanton BA. The PDZ-interacting domain of cystic fibrosis transmembrane conductance regulator is required for functional expression in the apical plasma membrane. *J Biol Chem*. 2000 Sep 1; 275(35):27069-74.

44. Pawson T, Nash P. Assembly of cell regulatory systems through protein interaction domains. *Science*. 2003 Apr 18; 300(5618):445-52.
45. Kawasaki H, Springett GM, Mochizuki N, Toki S, Nakaya M, Matsuda M, Housman DE, Graybiel AM. A family of cAMP-binding proteins that directly activate Rap1. *Science*. 1998 Dec 18; 282(5397):2275-9.
46. Walsh DA, Perkins JP, Krebs EG. An adenosine 3',5'-monophosphate-dependant protein kinase from rabbit skeletal muscle. *J Biol Chem*. 1968 Jul 10; 243(13):3763-5.
47. Gloerich M, Bos JL. Epac: defining a new mechanism for cAMP action. *Annu Rev Pharmacol Toxicol*. 2010; 50:355-75.
48. Bos JL. Epac proteins: multi-purpose cAMP targets. *Trends Biochem Sci*. 2006 Dec; 31(12):680-6.
49. Taylor SS. cAMP-dependent protein kinase. Model for an enzyme family. *J Biol Chem*. 1989 May 25; 264(15):8443-6.
50. de Rooij J, Zwartkruis FJ, Verheijen MH, Cool RH, Nijman SM, Wittinghofer A, Bos JL. Epac is a Rap1 guanine-nucleotide-exchange factor directly activated by cyclic AMP. Nature. 1998 Dec 3;396(6710):474-7.
51. de Rooij J, Rehmann H, van Triest M, Cool RH, Wittinghofer A, Bos JL. Mechanism of regulation of the Epac family of cAMP-dependent RapGEFs. *J Biol Chem*. 2000 Jul 7; 275(27):20829-36.
52. Gloerich M, Bos JL. Regulating Rap small G-proteins in time and space. *Trends Cell Biol*. 2011 Oct; 21(10):615-23.
53. Knox AL, Brown NH. Rap1 GTPase regulation of adherens junction positioning and cell adhesion. *Science*. 2002 Feb 15; 295(5558):1285-8.
54. Crittenden JR, Bergmeier W, Zhang Y, Piffath CL, Liang Y, Wagner DD, Housman DE, Graybiel AM. CalDAG-GEFI integrates signaling for platelet aggregation and thrombus formation. *Nat Med.* 2004 Sep; 10(9):982-6.
55. Duchniewicz M, Zemojtel T, Kolanczyk M, Grossmann S, Scheele JS, Zwartkruis FJ. Rap1A-deficient T and B cells show impaired integrin-mediated cell adhesion. *Mol Cell Biol*. 2006 Jan; 26(2):643-53.
56. Pellis-van Berkel W, Verheijen MH, Cuppen E, Asahina M, de Rooij J, Jansen G, Plasterk RH, Bos JL, Zwartkruis FJ. Requirement of the Caenorhabditis elegans RapGEF pxf-1 and rap-1 for epithelial integrity. *Mol Biol Cell*. 2005 Jan; 16(1):106-16.
57. Raaijmakers JH, Bos JL. Specificity in Ras and Rap signaling. *J Biol Chem*. 2009 Apr 24; 284(17):10995-9.
58. Bos JL. Linking Rap to cell adhesion. *Curr Opin Cell Biol*. 2005 Apr; 17(2):123-8.
59. Branham MT, Bustos MA, De Blas GA, Rehmann H, Zarelli VE, Treviño CL, Darszon A, Mayorga LS, Tomes CN. Epac activates the small G proteins Rap1 and Rab3A to achieve exocytosis. *J Biol Chem*. 2009 Sep 11; 284(37):24825-39.

60. Chepurny OG, Leech CA, Kelley GG, Dzhura I, Dzhura E, Li X, Rindler MJ, Schwede F, Genieser HG, Holz GG. Enhanced Rap1 activation and insulin secretagogue properties of an acetoxymethyl ester of an Epac-selective cyclic AMP analog in rat INS-1 cells: studies with 8-pCPT-2'-O-Me-cAMP-AM. *J Biol Chem*. 2009 Apr 17; 284(16):10728-36.
61. Leech CA, Chepurny OG, Holz GG. Epac2-dependent rap1 activation and the control of islet insulin secretion by glucagon-like peptide-1. *Vitam Horm*. 2010; 84:279-302.
62. Kilpinen S, Autio R, Ojala K, Iljin K, Bucher E, Sara H, Pisto T, Saarela M, Skotheim RI, Björkman M, Mpindi JP, Haapa-Paananen S, Vainio P, Edgren H, Wolf M, Astola J, Nees M, Hautaniemi S, Kallioniemi O. Systematic bioinformatic analysis of expression levels of 17,330 human genes across 9,783 samples from 175 types of healthy and pathological tissues. *Genome Biol*. 2008; 9(9):R139.
63. Ichiba T, Hoshi Y, Eto Y, Tajima N, Kuraishi Y. Characterization of GFR, a novel guanine nucleotide exchange factor for Rap1. *FEBS Lett*. 1999 Aug 20; 457(1):85-9.
64. Rehmann H, Arias-Palomo E, Hadders MA, Schwede F, Llorca O, Bos JL. Structure of Epac2 in complex with a cyclic AMP analogue and RAP1B. *Nature*. 2008 Sep 4; 455(7209):124-7.
65. Rehmann H, Das J, Knipscheer P, Wittinghofer A, Bos JL. Structure of the cyclic-AMP-responsive exchange factor Epac2 in its auto-inhibited state. *Nature*. 2006 Feb 2; 439(7076):625-8.
66. Rehmann H, Wittinghofer A, Bos JL. Capturing cyclic nucleotides in action: snapshots
67. VanSchouwen B, Selvaratnam R, Fogolari F, Melacini G. Role of dynamics in the autoinhibition and activation of the exchange protein directly activated by cyclic AMP (EPAC). *J Biol Chem*. 2011 Dec 9; 286(49):42655-69.
68. Essayan DM. Cyclic nucleotide phosphodiesterases. *J Allergy Clin Immunol*. 2001 Nov; 108(5):671-80.
69. Enserink JM, Christensen AE, de Rooij J, van Triest M, Schwede F, Genieser HG, Døskeland SO, Blank JL, Bos JL. A novel Epac-specific cAMP analogue demonstrates independent regulation of Rap1 and ERK. *Nat Cell Biol*. 2002 Nov; 4(11):901-6.
70. Vliem MJ, Ponsioen B, Schwede F, Pannekoek WJ, Riedl J, Kooistra MR, Jalink K, Genieser HG, Bos JL, Rehmann H. 8-pCPT-2'-O-Me-cAMP-AM: an improved Epac-selective cAMP analogue. *Chembiochem*. 2008 Sep 1; 9(13):2052-4.
71. Rehmann H, Schwede F, Døskeland SO, Wittinghofer A, Bos JL. Ligand-mediated activation of the cAMP-responsive guanine nucleotide exchange factor Epac. *J Biol Chem*. 2003 Oct 3; 278(40):38548-56.
72. Herbst KJ, Coltharp C, Amzel LM, Zhang J. Direct activation of Epac by sulfonylurea is isoform selective. *Chem Biol.* 2011 Feb 25; 18(2):243-51.
73. Baillie GS. Compartmentalized signalling: spatial regulation of cAMP by the action of compartmentalized phosphodiesterases. *FEBS J*. 2009 Apr; 276(7):1790-9.

74. Ponsioen B, Gloerich M, Ritsma L, Rehmann H, Bos JL, Jalink K. Direct spatial control of Epac1 by cyclic AMP. *Mol Cell Biol*. 2009 May; 29(10):2521-31.
75. Consonni SV, Gloerich M, Spanjaard E, Bos JL. cAMP regulates DEP domain-mediated binding of the guanine nucleotide exchange factor Epac1 to phosphatidic acid at the plasma membrane. *Proc Natl Acad Sci U S A.* 2012 Mar 6; 109(10):3814-9.
76. Gloerich M, Ponsioen B, Vliem MJ, Zhang Z, Zhao J, Kooistra MR, Price LS, Ritsma L, Zwartkruis FJ, Rehmann H, Jalink K, Bos JL. Spatial regulation of cyclic AMP-Epac1 signaling in cell adhesion by ERM proteins. *Mol Cell Biol*. 2010 Nov; 30(22):5421-31.
77. Hochbaum D, Barila G, Ribeiro-Neto F, Altschuler DL. Radixin assembles cAMP effectors Epac and PKA into a functional cAMP compartment: role in cAMP-dependent cell proliferation. *J Biol Chem*. 2011 Jan 7; 286(1):859-66.
78. Li Y, Asuri S, Rebhun JF, Castro AF, Paranavitana NC, Quilliam LA. The RAP1 guanine nucleotide exchange factor Epac2 couples cyclic AMP and Ras signals at the plasma membrane. *J Biol Chem*. 2006 Feb 3; 281(5):2506-14.
79. Huston E, Lynch MJ, Mohamed A, Collins DM, Hill EV, MacLeod R, Krause E, Baillie GS, Houslay MD. EPAC and PKA allow cAMP dual control over DNA-PK nuclear translocation. *Proc Natl Acad Sci U S A*. 2008 Sep 2; 105(35):12791-6.
80. Fu D, Wakabayashi Y, Lippincott-Schwartz J, Arias IM. Bile acid stimulates hepatocyte polarization through a cAMP-Epac-MEK-LKB1-AMPK pathway. *Proc Natl Acad Sci U S A*. 2011 Jan 25; 108(4):1403-8.
81. Insel PA, Murray F, Yokoyama U, Romano S, Yun H, Brown L, Snead A, Lu D, Aroonsakool N. cAMP and Epac in the regulation of tissue fibrosis. *Br J Pharmacol*. 2012 May; 166(2):447-56.
82. Bos JL. Epac: a new cAMP target and new avenues in cAMP research. *Nat Rev Mol Cell Biol*. 2003 Sep; 4(9):733-8.
83. Hoque KM, Woodward OM, van Rossum DB, Zachos NC, Chen L, Leung GP, Guggino WB, Guggino SE, Tse CM. Epac1 mediates protein kinase A-independent mechanism of forskolin-activated intestinal chloride secretion. *J Gen Physiol*. 2010 Jan; 135(1):43-58.
84. Rehmann H, Prakash B, Wolf E, Rueppel A, de Rooij J, Bos JL, Wittinghofer A. Structure and regulation of the cAMP-binding domains of Epac2. *Nat Struct Biol*. 2003 Jan; 10(1):26-32.
85. Morris AP, Cunningham SA, Tousson A, Benos DJ, Frizzell RA. Polarization-dependent apical membrane CFTR targeting underlies cAMP-stimulated Cl- secretion in epithelial cells. *Am J Physiol*. 1994 Jan; 266(1 Pt 1):C254-68.
86. Brown D, Stow JL. Protein trafficking and polarity in kidney epithelium: from cell biology to physiology. *Physiol Rev*. 1996 Jan; 76(1):245-97.

87. Mochizuki N, Yamashita S, Kurokawa K, Ohba Y, Nagai T, Miyawaki A, Matsuda M. Spatio-temporal images of growth-factor-induced activation of Ras and Rap1. *Nature*. 2001 Jun 28; 411(6841):1065-8.
88. Zhang J, Ma Y, Taylor SS, Tsien RY. Genetically encoded reporters of protein kinase A activity reveal impact of substrate tethering. *Proc Natl Acad Sci U S A*. 2001 Dec 18; 98(26):14997-5002.
89. Ponsioen B, Zhao J, Riedl J, Zwartkruis F, van der Krogt G, Zaccolo M, Moolenaar WH, Bos JL, Jalink K. Detecting cAMP-induced Epac activation by fluorescence resonance energy transfer: Epac as a novel cAMP indicator. *EMBO Rep*. 2004 Dec; 5(12):1176-80.
90. Hanrahan D. *DNA cloning: a Practical Approach* (Glover, DM., ed). Techniques for transformation of E. Coli. pp. 109-135, IRC Press, Oxford.
91. Ehrhardt C, Collnot EM, Baldes C, Becker U, Laue M, Kim KJ, Lehr CM. Towards an in vitro model of cystic fibrosis small airway epithelium: characterisation of the human bronchial epithelial cell line CFBE41o-. *Cell Tissue Res*. 2006 Mar; 323(3):405-15.
92. Bebok Z, Collawn JF, Wakefield J, Parker W, Li Y, Varga K, Sorscher EJ, Clancy JP. Failure of cAMP agonists to activate rescued deltaF508 CFTR in CFBE41o- airway epithelial monolayers. *J Physiol*. 2005 Dec 1; 569(Pt 2):601-15.
93. Fogh J, Wright WC, Loveless JD. Absence of HeLa cell contamination in 169 cell lines derived from human tumors. *J Natl Cancer Inst.* 1977 Feb; 58(2):209-14.
94. Almaça J, Dahimène S, Appel N, Conrad C, Kunzelmann K, Pepperkok R, Amaral MD. Cystic Fibrosis, *Methods in Molecular Biology.* Springer Science+Business Media. 2011; chapter 15.
95. Graham FL, Smiley J, Russell WC, Nairn R. Characteristics of a human cell line transformed by DNA from human adenovirus type 5. *J Gen Virol*. 1977 Jul; 36(1):59-74.
96. Felgner PL, Gadek TR, Holm M, Roman R, Chan HW, Wenz M, Northrop JP, Ringold GM, Danielsen M. Lipofection: a highly efficient, lipid-mediated DNA-transfection procedure. *Proc Natl Acad Sci U S A.* 1987 Nov; 84(21):7413-7.
97. Franke B, Akkerman JW, Bos JL. Rapid Ca2+-mediated activation of Rap1 in human platelets. *EMBO J.* 1997 Jan 15; 16(2):252-9.
98. Di Benedetto G, Zoccarato A, Lissandron V, Terrin A, Li X, Houslay MD, Baillie GS, Zaccolo M. Protein kinase A type I and type II define distinct intracellular signaling compartments. *Circ Res*. 2008 Oct 10; 103(8):836-44.
99. DiPilato LM, Cheng X, Zhang J. Fluorescent indicators of cAMP and Epac activation reveal differential dynamics of cAMP signaling within discrete subcellular compartments. *Proc Natl Acad Sci U S A*. 2004 Nov 23; 101(47):16513-8.
100. Willoughby D, Cooper DM. Live-cell imaging of cAMP dynamics. *Nat Methods*. 2008 Jan; 5(1):29-36.

101. Berrera M, Dodoni G, Monterisi S, Pertegato V, Zamparo I, Zaccolo M. A toolkit for real-time detection of cAMP: insights into compartmentalized signaling. *Handb Exp Pharmacol.* 2008; (186):285-98.
102. Burdyga A, Conant A, Haynes L, Zhang J, Jalink K, Sutton R, Neoptolemos J, Costello E, Tepikin A. cAMP inhibits migration, ruffling and paxillin accumulation in focal adhesions of pancreatic ductal adenocarcinoma cells: effects of PKA and EPAC. *Biochim Biophys Acta*. 2013 Dec; 1833(12):2664-72.
103. Dunn KW, Kamocka MM, McDonald JH. A practical guide to evaluating colocalization in biological microscopy. *Am J Physiol Cell Physiol*. 2011 Apr; 300(4):C723-42.
104. Costes SV, Daelemans D, Cho EH, Dobbin Z, Pavlakis G, Lockett S. Automatic and quantitative measurement of protein-protein colocalization in live cells. *Biophys J*. 2004 Jun; 86(6):3993-4003.
105. Oheim M, Li D. Quantitative Colocalisation Imaging: Concepts, Measurements, and Pitfalls. Imaging Cellular and Molecular Biological Functions. *Principles and Practice*. 2007; chapter 5.
106. Zinchuk V, Grossenbacher-Zinchuk O. Quantitative colocalization analysis of confocal fluorescence microscopy images. *Curr Protoc Cell Biol*. 2011 Sep; Chapter 4:Unit4.19.
107. Even-Ram S, Artym VV. Extracellular Matrix Protocols. *Methods in Molecular Biology*. Humana Press. 2009; chapter 14.
108. Consonni SV, Gloerich M, Spanjaard E, Bos JL. cAMP regulates DEP domain-mediated binding of the guanine nucleotide exchange factor Epac1 to phosphatidic acid at the plasma membrane. *Proc Natl Acad Sci U S A.* 2012 Mar 6; 109(10):3814-9.
109. Ponsioen B, Gloerich M, Ritsma L, Rehmann H, Bos JL, Jalink K. Direct spatial control of Epac1 by cyclic AMP. *Mol Cell Biol*. 2009 May; 29(10):2521-31.
110. Vliem MJ, Ponsioen B, Schwede F, Pannekoek WJ, Riedl J, Kooistra MR, Jalink K, Genieser HG, Bos JL, Rehmann H. 8-pCPT-2'-O-Me-cAMP-AM: an improved Epac-selective cAMP analogue. *Chembiochem*. 2008 Sep 1; 9(13):2052-4.
111. Wallrabe H, Periasamy A. Imaging protein molecules using FRET and FLIM microscopy. *Curr Opin Biotechnol*. 2005 Feb; 16(1):19-27.
112. Wang Z, Dillon TJ, Pokala V, Mishra S, Labudda K, Hunter B, Stork PJ. Rap1-mediated activation of extracellular signal-regulated kinases by cyclic AMP is dependent on the mode of Rap1 activation. *Mol Cell Biol*. 2006 Mar; 26(6):2130-45.
113. Hancock JF. Ras proteins: different signals from different locations. *Nat Rev Mol Cell Biol.* 2003 May; 4(5):373-84.
114. Ehrhardt A, Ehrhardt GR, Guo X, Schrader JW. Ras and relatives--job sharing and networking keep an old family together. *Exp Hematol.* 2002 Oct; 30(10):1089-106.

115. Albertazzi L, Arosio D, Marchetti L, Ricci F, Beltram F. Quantitative FRET analysis with the EGFP-mCherry fluorescent protein pair. *Photochem Photobiol*. 2009 Jan-Feb; 85(1):287-97.
116. Almahariq M, Tsalkova T, Mei FC, Chen H, Zhou J, Sastry SK, Schwede F, Cheng X. A novel EPAC-specific inhibitor suppresses pancreatic cancer cell migration and invasion. *Mol Pharmacol*. 2013 Jan; 83(1):122-8.
117. Chen H, Wild C, Zhou X, Ye N, Cheng X, Zhou J. Recent advances in the discovery of small molecules targeting exchange proteins directly activated by cAMP (EPAC). *J Med Chem.* 2014 May 8; 57(9):3651-65.
118. Rehmann H. Epac-inhibitors: facts and artefacts. *Sci Rep*. 2013 Oct 23; 3:3032.
119. Bebök Z, Tousson A, Schwiebert LM, Venglarik CJ. Improved oxygenation promotes CFTR maturation and trafficking in MDCK monolayers. *Am J Physiol Cell Physiol*. 2001 Jan; 280(1):C135-45.
120. Voltz JW, Weinman EJ, Shenolikar S. Expanding the role of NHERF, a PDZ-domain containing protein adapter, to growth regulation. *Oncogene.* 2001 Oct 1; 20(44):6309-14.
121. Sun F, Hug MJ, Lewarchik CM, Yun CH, Bradbury NA, Frizzell RA. E3KARP mediates the association of ezrin and protein kinase A with the cystic fibrosis transmembrane conductance regulator in airway cells. *J Biol Chem*. 2000 Sep 22; 275(38):29539-46.
122. Li J, Dai Z, Jana D, Callaway DJ, Bu Z. Ezrin controls the macromolecular complexes formed between an adapter protein Na+/H+ exchanger regulatory factor and the cystic fibrosis transmembrane conductance regulator. *J Biol Chem*. 2005 Nov 11; 280(45):37634-43.
123. Monterisi S, Casavola V, Zaccolo M. Local modulation of cystic fibrosis conductance regulator: cytoskeleton and compartmentalized cAMP signalling. *Br J Pharmacol*. 2013 May; 169(1):1-9.
124. “UniProt.” Available: http://www.uniprot.org.
125. “ScanProsite.” Available: http://prosite.expasy.org/scanprosite/
126. Morales FC, Takahashi Y, Momin S, Adams H, Chen X, Georgescu MM. NHERF1/EBP50 head-to-tail intramolecular interaction masks association with PDZ domain ligands. *Mol Cell Biol*. 2007 Apr; 27(7):2527-37.
127. Tsalkova T, Mei FC, Li S, Chepurny OG, Leech CA, Liu T, Holz GG, Woods VL Jr, Cheng X. Isoform-specific antagonists of exchange proteins directly activated by cAMP. *Proc Natl Acad Sci U S A.* 2012 Nov 6; 109(45):18613-8.
128. Hoque KM, Woodward OM, van Rossum DB, Zachos NC, Chen L, Leung GP, Guggino WB, Guggino SE, Tse CM. Epac1 mediates protein kinase A-independent mechanism of forskolin-activated intestinal chloride secretion. *J Gen Physiol*. 2010 Jan; 135(1):43-58.

129. Martell JD, Deerinck TJ, Sancak Y, Poulos TL, Mootha VK, Sosinsky GE, Ellisman MH, Ting AY. Engineered ascorbate peroxidase as a genetically encoded reporter for electron microscopy. *Nat Biotechnol*. 2012 Nov; 30(11):1143-8.

Appendices

Plasmid maps

pcDNA3.1 (+/-) plasmid map

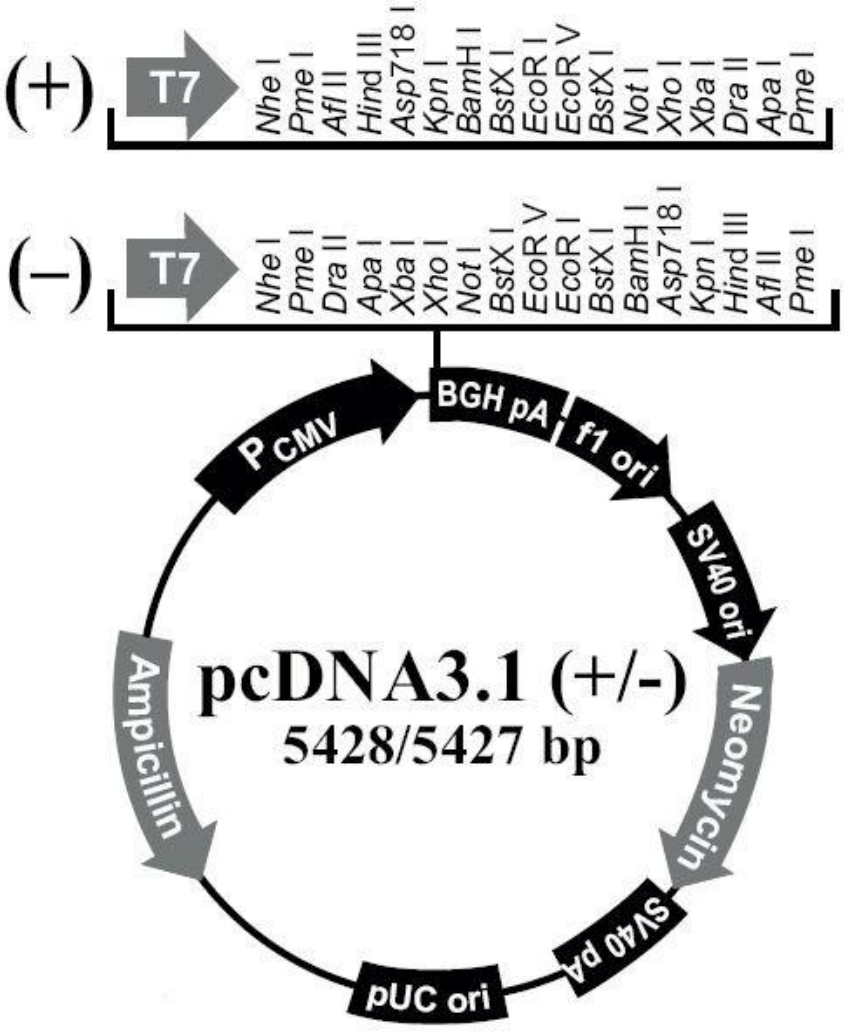

pEGFP-C2 plasmid map

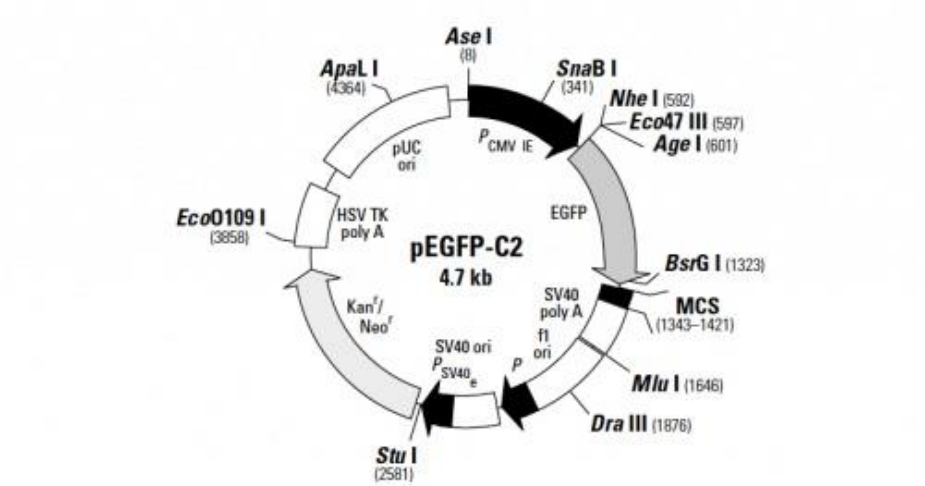

pCAGGS plasmid map

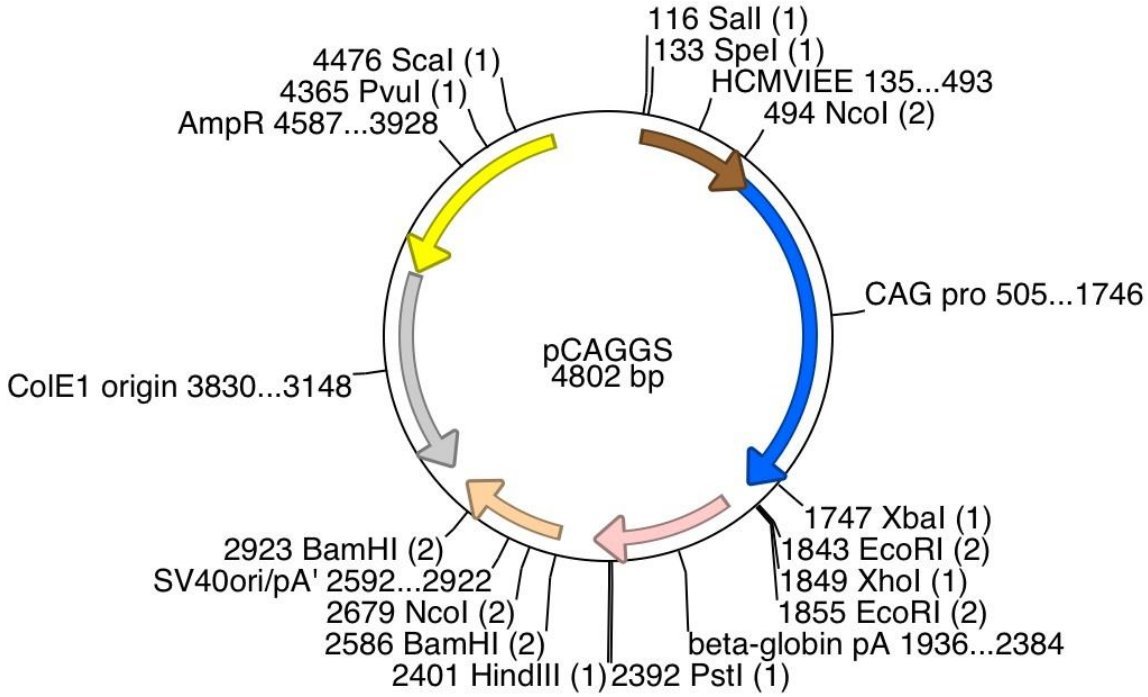

pmCherry-C1 plasmid map

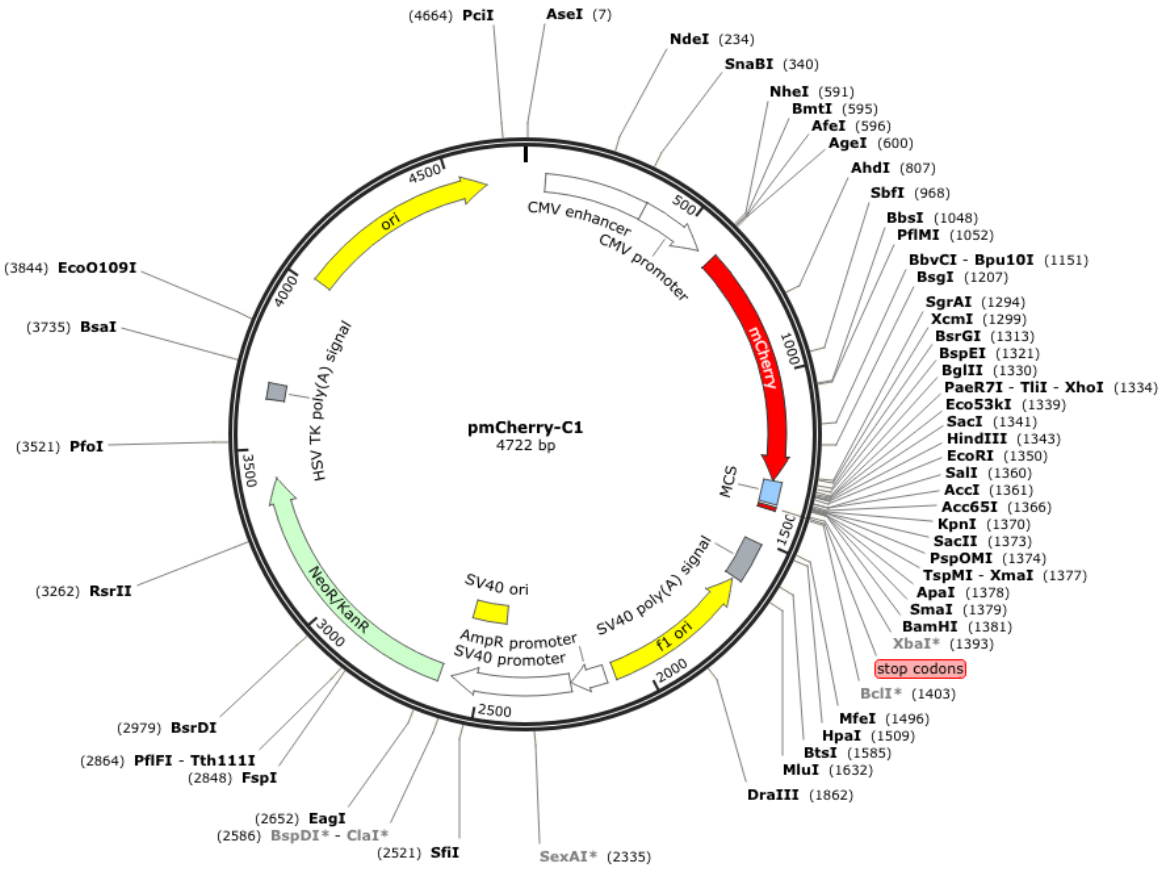

Forskolin standard curve for AKAR4 and camp FRET sensors

To evaluate the dynamic range of AKAR4 and camp FRET sensor, a forskolin standard curve was performed (*Figure 1*).

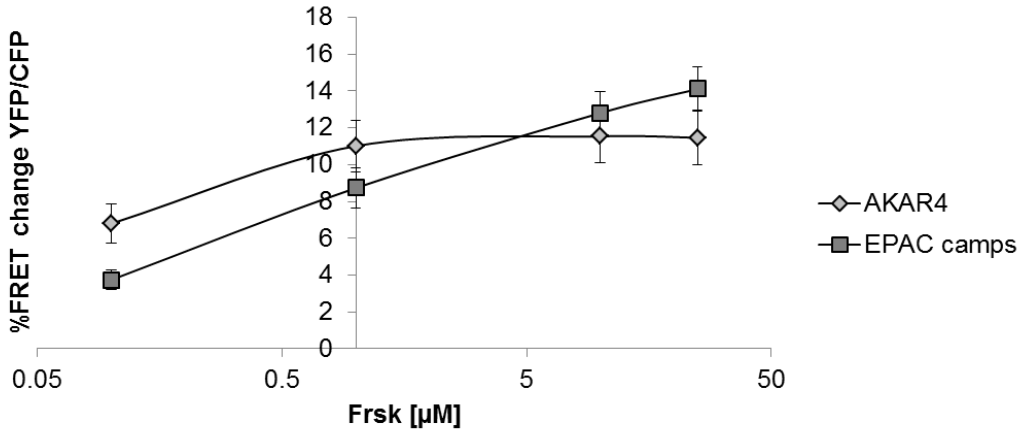

Figure 1: Frsk standard curve for AKAR4 and camp FRET sensors. It was used to evaluate the dynamic range of AKAR4 and camps. Percentage of FRET change is the normalized 545nm/408nm value calculated at each acquisition time point for each Frsk concentration (0.1, 1, 10 and 25µM).

Sequential increases in Frsk caused a rapid increase in FRET and subsequent apparent saturation of the response in the PKA sensor, whereas the EPAC sensor changed more gradually and showed a larger dynamic range. This is in agreement with data already published[89].

Preparation of GST-RalGDS-RBD-coupled beads for Rap1A activity assay

GST-RalGDS-RBD-coupled beads were produced for the Rap1A activity assay. To confirm the expression of the recombinant protein by bacteria transformed with pGEX-GST-RalGDS-RBD-GST, aliquots of bacteria were taken immediately before and after 4h incubation with IPTG, centrifuged at 4000g for 10min and lysed in sample buffer. Extracts were run on an SDS-PAGE gel, which was then stained with Coomassie Blue (*Figure 2*). The appearance of a strong band below the 37kDa marker confirmed the expression of recombinant protein.

However, it was still necessary to know how much glutathione-coupled agarose beads should be added to the bacterial extracts in order to prepare the final beads (GST-RalGDS-RBD-coupled). For this, the amount of recombinant protein recovered was predicted by running simultaneously on the same SDS-PAGE gel increasing amounts of BSA along with an aliquot of the bacterial extract (*Figure 2*).

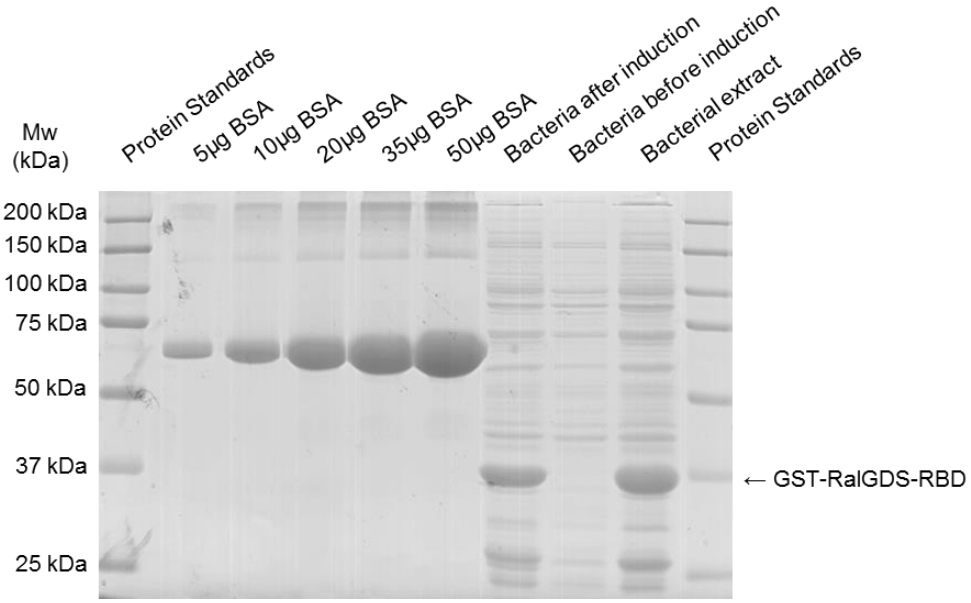

Figure 2: Expression of GST-RalGDS-RBD recombinant protein after induction with IPTG. Coomassie-stained SDS-PAGE gel used to quantify the amount of recombinant protein expressed.

A standard curve was made using BSA bands intensities (*Figure 3*).

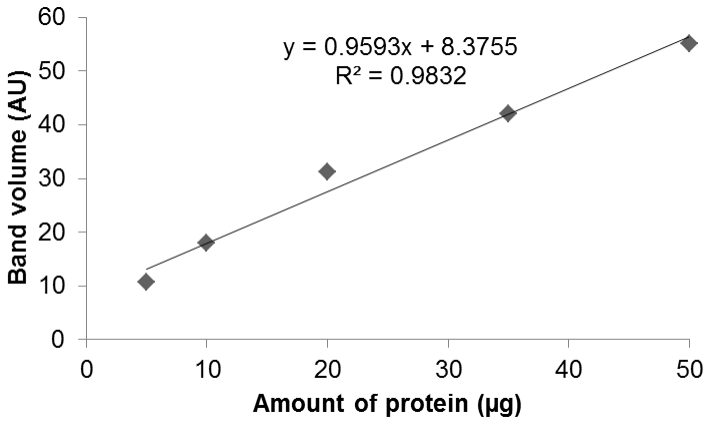

Figure 3: BSA standard curve for the SDS-PAGE gel. It was used to quantify the amount of recombinant protein present in the bacterial extracts. AU, Arbitrary Units.

Lastly, this standard curve was used to determine the amount of protein in the bacterial extracts, yielding a value of 1.106 mg of recombinant protein per mL. 1mL of GSH-beads slurry was added to 6mg of protein (according to the manufacturer's instructions) and for 2h at 4ºC. GST-RalGDS-RBD-coupled beads were then washed and stored at -20ºC. To confirm that the recombinant protein was attached to the beads, several aliquots of beads were run on an SDS-PAGE gel (*Figure 4*).

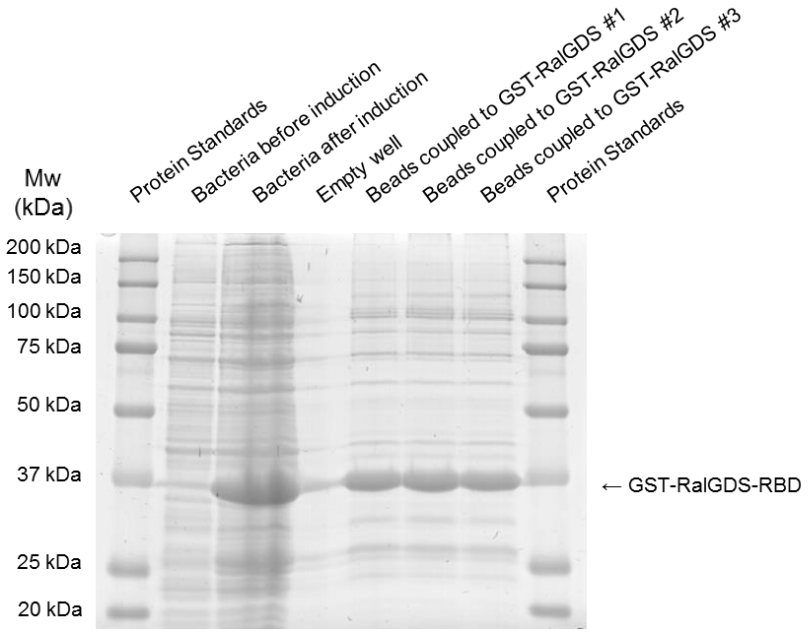

Figure 4: GST-RalGDS-RBD recombinant protein attached to agarose beads. Aliquots of bacteria taken before and after induction were used as negative and positive control, respectively.

GST-RalGDS-RBD-coupled beads were confirmed by the appearance of a strong band near the 37kDa marker.

Fluorescence intensity and number of cells correlation

To ensure that there was a linear correlation between fluorescence intensity and number of cells stained with Hoechst 33342, a standard curve was made for each 96-well plate used (*Figure 5*)

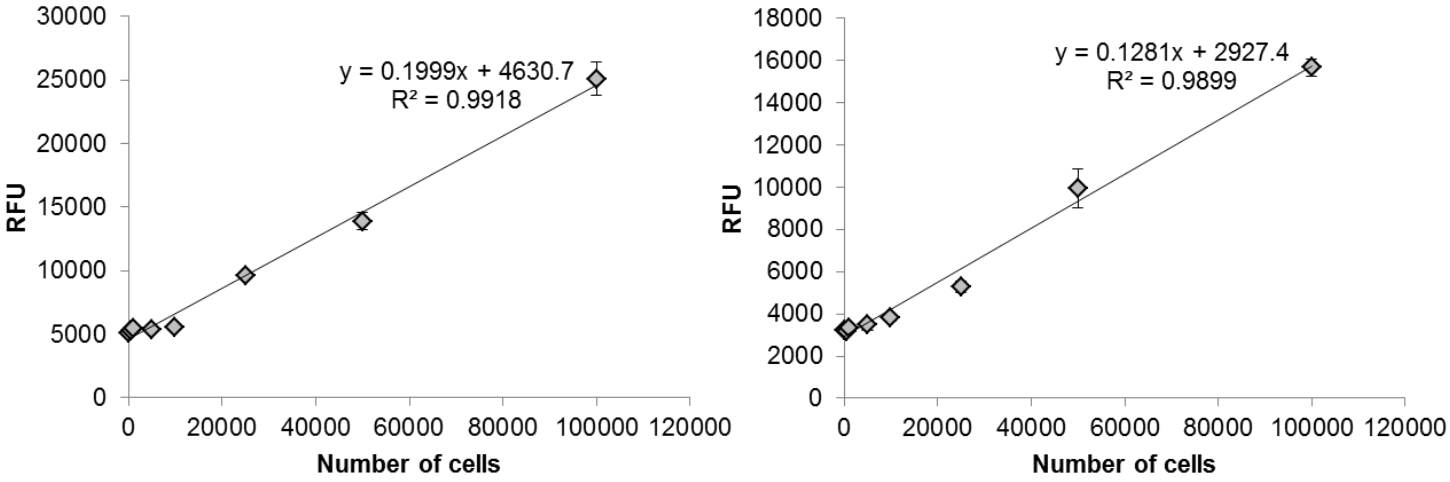

Figure 5: Fluorescence intensity against number of cells. Average of standard curves for CFBE cells stably expressing (A) WT- or (B) F508del-CFTR. Data represent means ± SEM. n = 4/6 (F508del-/WT-CFTR).

A linear correlation between fluorescence intensity and number of cells was confirmed for CFBE cells expressing WT- or F508del-CFTR, confirming the method's robustness.